ORNL-tr--5055

DE84 003447

ORNL-tr-5055

VDI 2230: SYSTEMATIC CALCULATION OF HIGH DUTY BOLTED JOINTS

VDI Society for Design and Development, Committee on Bolted Joints

Translated from the German.* Issued by the Verein Deutscher Ingenieure (VDI), VDI Richtlinien (Düsseldorf), October 1977, 56 pages.

* By LANGUAGE SERVICES, Knoxville, Tennessee

VDI-GUIDELINE VDI 2230: Systematic Calculation of High Duty Bolted Joints

Contents: Page

VDI Society for Design and Development

Division of Design

Committee on Bolted Joints

VDI Design Handbook

Foreword

The present guideline (VDI 2230) is intended to inform practical designers about the very latest findings in the field of the calculation of bolted joints, and, with the recommendation of a systematic calculation process, to offer them aid in the often difficult task of correctly designing bolted joints.

Along with the treatment of the factors in concentrically clamped and concentrically loaded bolted joints normally presented in the literature, solution formulations are developed here for eccentrically clamped and/or eccentrically loaded joints, which occur much more frequently in practice: the formulations have been supported by measurements and recent research. Tables, diagrams and examples facilitate the suggested systematic calculation process.

Due to the great number of possible configurations and interactions, the determination of external forces and moments affecting bolted joints could not be treated in this guideline. On the other hand, the effects which result from the scattering of the initial stress forces when bolted joints are tightened were considered, whereby the given values are based on series of measurements.

The guideline VDI 2230 is the result of many years of collaboration in the Committee on Bolted Joints of the former VDI Design Group (ADKI) and of the Design Division of the present VDI Association for Design and Development. The present second edition represents the revision of the first edition of December 1974 and takes into account the experience and findings acquired in working with the guideline. The leadership of the committee lay in the hands of Dr. G. Junker of Koblenz. To him and the following gentlemen, who made important contributions to the development of this guideline, are due thanks for their voluntary efforts:

Dr. W. Benz, Nürtingen

Mr. H. Dreger, Herborn, Grad. Eng.

Prof. K. Federn, Berlin, D. Eng.

Dr. A. Grotewohl, Wolfsburg

Dr. E. Haibach, Darmstadt-Eberstadt

Dr. K. H. Illgner, Neuss

From the VDI Office:

Mr. P. Selbmann, Düsseldorf, Grad. Eng.

Mr. M. Uhrmann, Düsseldorf, Grad. Eng.

VEREIN DEUTSCHER INGENIEURE

[SOCIETY OF GERMAN ENGINEERS]

1. Scope

The guideline VDI 2230 deals with bolted joints which are to bear static or alternating working loads and which are to be created using high-strength bolts. The guideline should be used above all for joints the failure of which can cause serious damage.

The specifications in this guideline are valid for steel bolts within the temperature range of −40° C to +300° C in which neither embrittlement due to cold nor creep stress of the bolt steels is expected. Above 120° C the adjusted material characteristics must be used for calculations.

Extreme operating stress such as high and low temperatures outside the given limits, corrosion, and non-determinable impact stress are not treated in this guideline.

The following DIN standards, guidelines and special publications can be consulted if necessary:

DIN 105, 6.68: Steel in Building Construction, Calculation and Structural Design;

DIN 120 Bl. 1, 11.36: Calculation Principles for Steel Structural Parts of Cranes and Crane Runways (DIN 15018 in preparation);

DIN 2505, 10.64: Tentative Standard: Calculation of Flange Joints;

DASt-Guidelines 010: Application of High Tensile Bolts in Steel Construction (Published by the Deutscher Ausschuß für Stahlbau, Stahlbau-Verlag GmbH., Cologne: 1974);

AD Bulletin B 7, Jan. 68: Calculation of Pressure Vessels: Bolts;

TRD 309, Technical Rules for Boilers: Bolts (Published by the Vereinigung der Technischen Überwachungsvereine e. V., Essen, Beuth-Vertrieb, Berlin, Cologne);

DV 804 (BE) Ausg. 1960: Service Regulations of the German Railway System: Calculations for Steel Railway Bridges.

2. Calculation

A bolted joint is a separable joint of two or more parts bolted by means of one or more bolts. The bolts and their tensile load must be dimensioned so that the resulting joint fulfills the intended function and withstands the working loads that occur.

Examples:

---In the case of the bolting of the head of a pressure vessel, the clamping force of the bolts is to be established such that the working load caused by the internal pressure is absorbed, and the desired sealing function is attained.

---In big-end bearing cover bolted joints subjected to vibrations in reciprocating engines, the clamping force of the bolts must be set so high that under inertia forces no one-sided lift-off on the interface or slippage occurs. Both would trigger progressive destruction, etc., by automatic unbolting and by fatigue failure of the bolts. Since the clamping forces must also cause the deformation of the stressed bearing bushings until they completely rest on the interface, the clamping forces can be a multiple of the working loads resulting from the inertia forces.

---In the case of front-end bolting of a disk flywheel on an axle, the clamping force of the bolts must be sufficient to produce with certainty friction contact in the interface necessary for the transmission of the resulting moments.

The calculation of a bolted joint is based on the working load F_B which acts externally on the joint. This working load and the elastic deformation of the structural part caused by it bring about at the individual bolting point an axial load F_A, a transverse force F_Q, a bending moment M_B, and sometimes a turning moment (torque) M_T. Due to the variety of designs for structural parts and bolted joints, the difficult and generally complicated load and deformation analysis which leads to the determination of these basic variables cannot be the object of this guideline. This task must be solved using the tools of statics and elastomechanics [22;23;24]. This is especially true for multi-bolted joints. Only in the case of simple, symmetric, and relatively rigid joints can the basic variables be obtained by simple analysis of the working load. The basic variables F_A, F_Q, M_B, and M_T are assumed from now on to be known values.

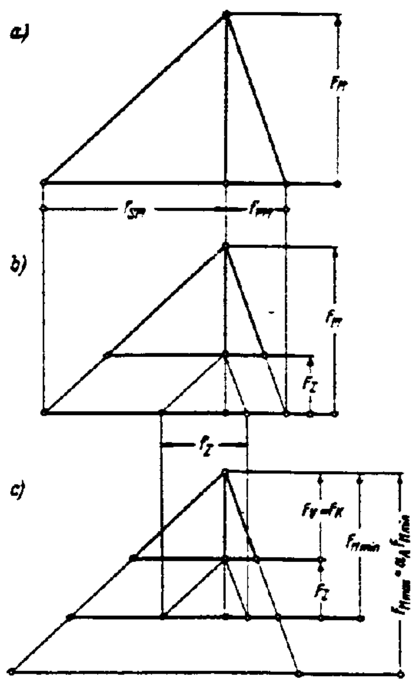

Figure 1: Joint diagrams for a joint without external working load
a) with clamping to an initial preload F_M
b) with loss of preload F_Z due to embedding
c) with deviations of the initial preload due to tightening scatter and loss of preload by embedding

Figure 2: Joint diagram for the general case of any kind of axial working load F_A

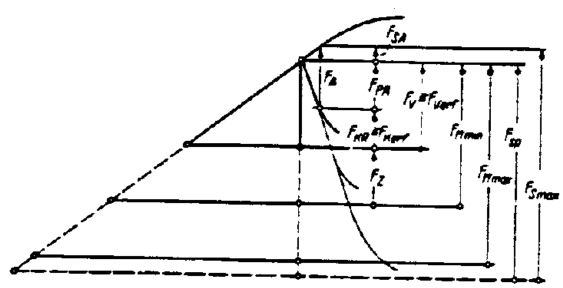

The object of the calculation of the bolted joint is to determine the necessary bolt dimensions by considering the following influencing factors:

---Strength class of the bolt;

---Reduction of the initial clamping load in the interface or parts of the interface by the working load [1,2,3,4];

---Reduction of the initial clamping load by embedding phenomena [1,5];

---Scattering of the preload during tightening [1,6];

---Endurance strength with alternating load [1,2,3,4];

---Compressive stress of clamped parts by bolt head and/or nut [7].

For eccentrically loaded joints no generally valid method of calculation can be given according to the current state of knowledge because the available calculations and measurements of existing joints have not yet been converted into practically applicable methods of computation. For certain joints, however, mathematical formulations which have in part been varified experimentally are described in this guideline under simplified assumptions. If the given conditions are not met or if the simplified assumptions do not hold up to a check in the individual case, then the necessary preload must be determined through experimentation. This can be done by measuring the changes in the bolt force occurring under the working load using wire strain gauges and applying the equations and diagrams contained in this guideline (see Sec.3.2.4.5.). Such measurements can even be done in the development stage using a model or prototype. In such cases a comparison of similarly formed, existing parts can also lead to conclusions. Special cases also can be dealt with using the finite elements method, especially if they can be reduced to two-dimensional problems.

In Sec. 2.1. the calculation process is developed, and in Sec. 2.2.

it is divided into steps for practical application.

The derivation of equations for the different quantities and factors is not taken up until Sec. 3. to provide a better view of the calculation process. References to corresponding subsections, equations and diagrams in this section are made as needed at each calculation step.

2.1. Calculation Process

The calculation process and the development of the dimensioning equations can be illustrated by the joint diagram which is given in its classic form in Figure 1; its modifications for various stress conditions (cf. Figure 2) are more precisely derived and described in Sec. 3.

If a bolt is tightened during assembly to the initial clamping load F_M, then it is elongated by f_{SM}, whereas the bolted parts are shortened by f_{PM}, Figure 1a. After completion of assembly, embedding phenomena appear (especially under the effect of alternating working loads) as a result of the smoothing of technical roughness. The elastic length variation $f_{SM} + f_{PM}$ is reduced by the amount of embedding f_Z. As a result, the initial clamping load F_M decreases by F_Z, Figure 1b (see also Sec. 3.2.2.).

The initial clamping load F_M is subjected during tightening--depending on the method of tightening and the friction conditions--to a scattering of the values between $F_{M\ min}$ and $F_{M\ max}$ (see Sec. 4.6.2.).

A measure of this scattering is the tightening factor α_A, Figure 1c:

$$\alpha_A = F_{M\ max} / F_{M\ min} \qquad (1)$$

If a joint is clamped at the least initial clamping load $F_{M\ min}$ and a drop in the initial clamping load F_Z occurs due to embedding, there remains in the worst case a preload F_V. The efficient clamping force F_K in the interface is equal to the preload F_V.

In operation, the bolted joint loaded with F_V receives additional tension from the axial component F_A of the working load F_B, Figure 2. Thereby the resilience conditions change in general, and with them the pitch and form of the deformation charateristics as compared with Figure 1.

The axial force F_A causes the additional force F_{SA} in the bolt and a reduction of the clamping force F_K at F_{PA} on the residual clamping force F_{KR}. The additional load F_{SA} is proportional to the axial component F_A of the working load. The proportionality factor Φ is called the force ratio and is dependent upon the elastic resilience of the clamping and clamped parts and accordingly on the stress conditions (load introduction, eccentricity of the clamping and loading). Thus the following summations:

$$F_{SA} = \Phi \, F_A \tag{2}$$

$$F_A = F_{SA} + F_{PA} \tag{3}$$

$$F_{PA} = (1-\Phi) \, F_A \tag{4}$$

and $$F_{KR} = F_V - F_{PA} = F_V - (1-\Phi) \, F_A. \tag{5}$$

The bolted joint is designed in such a way that the residual clamping force F_{KR} is at least equal to the required clamping force F_{Kerf} which insures the function of the bolted joint. This force must prevent one-sided lift-off in the interface and must provide sealing requirements or friction contact. Thus:

$$F_{KR} \geq F_{Kerf}. \tag{6}$$

Analogously we can define a required clamping force F_{Verf}. For this:

$$F_{Vert} = F_{Kert} + F_{PA} = F_{Kert} + (1-\Phi)\ F_A \leq F_V. \qquad (7)$$

Thereby the minimum clamping force can be thus computated (see Figure 2):

$$F_{M\ min} = F_{Vert} + F_Z = F_{Kert} + (1-\Phi)\ F_A + F_Z. \qquad (8)$$

Taking into consideration the scattering during tightening, the maximum initial clamping force for which the bolt must be designed is

$$F_{M\ max} = \alpha_A\ F_{M\ min} = \alpha_A\ [F_{Kert} + (1-\Phi)\ F_A + F_Z]. \qquad (9)$$

The required bolt diameter is determined such that, considering the selected strength class and the friction ratios in the threads (see Table 5), the axial clamping force of the bolt F_{sp} is equal to or greater than $F_{M\ max}$. Here F_{sp} signifies the appropriate clamping force for the bolt which has been chosen as the measuring standard. The clamping force, together with the torsional stress occuring during tightening, utilizes the minimum elastic limit to 90% ($\sigma_{red} = 0.9\sigma_{0.2}$; see Sec. 4.6.1.).

Thus:

$$F_{sp} \geq F_{M\ max} \qquad (10)$$

Tables 1 to 4 contain the axial clamping force values for 90% of the elastic limit utilization due to σ_{red}, and indeed for full shank and reduced shank bolts of the strength classes 8.8, 10.9 and 12.9 in the dimension range of M 4 to M 30. [Note: The nominal values for the elastic limit form the basis of Tables 1 to 4 according to ISO/DIS 898 Part (Teil) 1 which supercedes DIN 267 p. (Blatt) 3. The nominal values have a security range from 1.6% to 4% against the minimum values. For the use of the tables, see also Sec. 4.6.2.1.]

The tightening torque M_{sp} belonging to the corresponding F_{sp} can be taken from the same tables. If we must be sure that this torque is not to be exceeded because of the imprecision of the torque wrench, a lower torque must be given as the assembly torque.

In the case of determining the tightening factor α_A, $\pm$10% has been accepted for the partial error for the tightening torque. Therefore the assembly torque M_A can be determined as

$$M_A = 0.9\ M_{sp}. \qquad (11)$$

If such a designed joint, which is clamped at $F_{sp} = F_{M\ max}$, is being loaded for the first time, and if the initial preload is not diminished by embedding procedures, then the maximum bolt strength is

$$F_{S\ max} = F_{sp} + F_{SA} = F_{sp} + \Phi\ F_A. \qquad (12)$$

Since according to the definition the bolt has been loaded to 90% of the elastic limit by F_{sp}, the bolt is not stressed beyond its elastic limit at the initial loading of the joint if the following is true:

$$F_{SA} = \Phi\ F_A \leq 0.1\ \sigma_{0.2}\ A_S. \qquad (13)$$

In the case of reduced shank bolts, A_S is replaced by A_T. If F_{SA} is greater, then the design of the joint must be improved if possible, or a larger dimension, a higher strength class for the bolt or a more precise tightening process must be chosen. If the bolt material is ductile enough and, as in the case of tightening processes which go beyond the elastic limit, if sufficient ductile lenghts are present, a slight over-extension of the elastic limit is permissible in the individual case. Attention should be paid to the consequences described in Sec. 3.2.3.1. and in Figure 15.

If F_A is a load which changes with time and whose dimensions change between the upper force limit F_{Ao} and the lower force limit F_{Au}, then the bolt is alternately stressed by the force:

$$F_{SAa} = \pm\ \Phi\ \frac{F_{Ao} - F_{Au}}{2} \qquad (14)$$

which fluctuates around a mean value:

$$F_{Sm} = F_V + \Phi \frac{F_{Ao} + F_{Au}}{2} \tag{15}$$

In the simplest case of a working load increasing from zero to F_A, the equations are simplified as

$$F_{SAa} = \pm \Phi \frac{F_A}{2} \tag{16}$$

and

$$F_{Sm} = F_V + \Phi \frac{F_A}{2} \tag{17}$$

The endurance strength of a bolt must not be exceeded. We must keep in mind that bending deformations of the bolt can be caused by distorted load-bearing surfaces which can result in additional alternating stress on the bolt (see Sec. 3.2.4.3.).

In order to avoid a preload loss due to creep of the clamped material, the contact pressure under the bolt head or the nut, in its bearing area A_P, must not surpass the limit of contact pressure p_G of the clamped material (see, Sec. 2.2., Calculation Step S 10). Since according to the equations (12) and (13), the elastic limit of the bolt material is not exceeded with the maximum bolt strength $F_{S\ max}$, the calculation is checked with:

$$\frac{F_{S\ max}}{A_P} \leq \frac{F_{Sp} / 0.9}{A_P} \leq p_G \tag{18}$$

Under certain conditions, tightening procedures which reach or exceed the elastic limit can be used for assembly (see Sec. 4.6.). Their introduction leads to a situation in which the bolt is further lengthened plastically by application of the working load (similar to Fig. 15). Therefore, special demands must be placed on the ductility of the material and on the free extension length. In lieu of the check $F_{S\ max} \leq \sigma_{0.2}\, A_S$ according to equations (12) and (13), the test must show how far the bolt is plastically lengthened by the working load and how often reuse can be permitted.

In the case of this tightening process, tne scattering of the preload is produced only from the tolerance of the elastic limit. Since the elastic limit is reached or exceeded by the combined tension and torsional stress σ_{red} caused by the clamping load and the thread torque, only a negligibly small effect of scattering of the friction coefficient appears. The required bolt diameter is then determined without consideration of the tightening factor α_A from $F_{M\ min}$ according to Equation (8).

Since the values in Tables 1 through 4 are designed for an axial clamping force with 90% utilization of the elastic limit, the required bolt dimension can be chosen from these tables, taking into account the selected strength class and the given thread friction coefficients, for:

$$F_{sp}/0.9 \geq F_{M\ min}. \qquad (19)$$

The greatest possible clamping force in such an assembled joint is attained with bolts whose elastic limit lies on the upper end of the standardized tolerance range.

For all considerations concerning surface loading and elastic deformation of clamped parts (e.g., bearing housing deformation), the clamping force for the selected bolt, multiplied by the ratio of maximum to minimum elastic limit, must therefore be the basis of the maximally possible bolt strength $F_{S\,max}$.

$$F_{S\,max} = \frac{\sigma_{0.2\,max}}{\sigma_{0.2}} F_{sp} / 0.9 \qquad (20)$$

2.2. Steps in Calculation

The working load F_B with its components F_A and F_Q at the bolting position must be given as the basic conditions.

The design and assembly conditions are often arbitrary or influenceable; they determine the needed values for embedding and for scattering of the preload. Under observation of the many derivations and comments in Sec. 3., the calculation process can be accomplished as follows in steps S 1 to S 10.

S 1. Rough determination of the bolt diameter d (occasionally with the aid of Table 6), of the clamping length ratio l_K/d, and rough determination of the median bearing stress under the bolt head with

$$p = \frac{F_{sp} / 0.9}{A_P} \leq p_G$$

F_{sp} is found from Tables 1 to 4 for the appropriate bolt dimension and strength class. Recommendations for the allowable bearing stress p_G of several materials are contained in Table 14. If p_G is exceeded, the design conditions must be altered (if need be by means of the placement of a washer of sufficient strength and dimensions). In this case, l_K/d must be determined again, and the rough dimensioning must be checked.

S 2. Determination of the tightening factor α_A, taking into account the chosen tightening procedure and lubrication or surface condition according to Table 17 (is not necessary for any tightening procedures which reach or exceed the elastic limit) (see Sec. 4.6.2.2. and 4.6.2.3.).

S 3. Determination of the required minimum clamping force F_{Kerf}, taking into account the following individual conditions:

Friction contact for taking up any present transverse force component F_Q or for taking up any present moment M_T.

Sealing functions for known pressures and surfaces as well as material characteristics of sealing elements.

No one-sided lift-off with eccentric loading and/or clamping. With simplified assumptions a formulation for F_{Kerf} is possible (see Sec. 3.2.4. with Equation (78)).

The maximum value determined for F_{Kerf} should be put into the dimensioning equations.

S 4. Determination of the embedding amount f_Z from Table 7, and rough determination of the force ratio Φ_K for load introduction under the head from Table 8, and the determination of the elastic resilience δ_P of the clamped parts from Table 9 or Sec. 3.1.2. For other rigidity conditions, as presented in Figure 5, intermediate values can be interpolated.

Thus determination of the preload loss by embedding:

$F_Z = f_Z \frac{\Phi_K}{\delta_P}$ The effect of eccentric clamping and/or loading is hereby neglected.

S 5. Determination of the force ratio Φ.

a) In the simplest cases of concentric clamping and concentric axial loading of the joint it must be assumed that the axial force F_A is introduced in half intensity of the clamped parts. Therefore according to Sec. 3.2.3.2. and Figure 17b and with $n = 1/2$, the force ratio becomes $\Phi = \Phi_n = n\ \Phi_K = 1/2\ \Phi_K$.

b) In the case of axial load application, an assessment of the load introduction zone can be possible or even necessary on the basis of the geometric form of the clamped parts in special cases, Figure 17. If thereby nl_K is the portion of the clamped parts section which is unloaded by the working load, then $\Phi = \Phi_n = n\ \Phi_K$; $(0 < n \leq 1)$ (see Sec. 3.2.3.2.)

c) In the case of eccentric clamping and/or eccentric load application, the following is true:

$$\Phi = \Phi_{en} = n \quad \frac{\delta_P^{**}}{\delta_S + \delta_P^{*}}$$

(see Sec. 3.2.4.1. Equation (68b)).

In the event that an assessment of the situation of the load introduction level is not possible or necessary, then for simplicity $n = 1/2$ can be set likewise.

d) In the case of flange-like parts which are not in contact, the inverse resilience of the flange or of the covering plates (also cylinder head) is to be considered. Thus $\Phi = \Phi_{F1}$ (see Sec. 3.3.1. Equations (104) to (106)).

S 6. Determination of the required bolt dimension.

a) For all tightening procedures in the elastic field of the bolt, the following is valid:

$$F_{M\ max} = \alpha_A\ [F_{Kerf} + (1 - \Phi)\ F_A + F_Z].$$

Seek a bolt (diameter and strength class) from Tables 1 through 4 for which

$$F_{sp} \geq F_{M\ max}$$

If Tables 1 through 4 are not applicable for specially formed bolts (see Example 5.3), then the clamping forces must be calculated according to Equations (114) to (118) and the assembly torque according to Equation (124). Here the friction coefficient is dependent upon the selected lubrication and surface conditions (Table 5). Simultaneously, we can look up in the tables the tightening torque M_{sp} associated with the clamping force F_{sp}. For assembly, the mean tightening torque

$$M_A = 0.9\ M_{sp}$$

is suggested.

b) For tightening procedures which reach or which exceed the elastic limit, the following is valid:

$$F_{M\ min} = F_{Kerf} + (1 + \Phi)\ F_A + F_Z.$$

Seek a bolt (dimensions and strength class) for which

$$F_{sp}\ /\ 0.9 \geq F_{M\ min}$$

Since the scattering of the friction coefficient is negligible, the clamping force values in Table 2 (for a mean friction coefficient μ_G = 0.125) can be used (for comments, see Sec. 4.6.).

S 7 Precise determination of the clamping length ratio $l_K\ /\ d$ and controls of Φ_K and δ_P (Tables 8 and 9) or repetition of Steps S 5 and S 6.

S 8 Test for compliance with allowable bolt strength.

The allowable bolt strength is not exceeded if $\Phi\ F_A < 0.1\ \sigma_{0.2}\ A_S$ ($\sigma_{0.2}\ A_S$ see Tables 11 and 12). For reduced shank bolts, the following is valid accordingly: $\Phi\ F_A \leq 0.1\ \sigma_{0.2}\ A_T$. In the case of tightening procedures which reach or exceed the elastic limit, this test is replaced by another which tests whether an additional plastic lengthening of the bolt by means of the working load can be permitted, how long the bolt is plastically lengthened, and how often it can be reused (see also Sec. 4.6.).

S 9 Determination of the dynamic fatigue stress of the bolt

$$\sigma_a = \Phi\ \frac{F_{AO} - F_{AU}}{2\ A_3} \leq \sigma_A$$

(A_3 core cross section)

In the case of eccentric loading, the bending tension must also be considered (see Sec. 3.2.4.3. Equation (100) for σ_{SAb}).

In the case of increasing working load, this step is simplified to:

$$\sigma_a = \frac{\sigma_{SA}}{2} = \Phi \frac{F_A}{2\,A_S} \leq \sigma_A$$

Optimum values for the allowable stress amplitude σ_A of the endurance strength $\sigma_m \pm \sigma_A$ can be taken from Table 13 (see Sec. 4.5.). If this condition is not fulfilled, then the design must be improved whenever possible by using a bolt of a larger diameter or of greater endurance strength. Greater endurance strength can be achieved, for example, by tempered threading.

S 10. Calculation of the bearing stress under the bolt and nut heads according to Equation (18).

$$p = \frac{F_{SA} / 0.9}{A_P} \leq p_G$$

In the case of determination of the bolt or nut head bearing area A_P, the chamfering in the hole must be considered.

Recommendations concerning the allowable bearing stress p_G of several materials are contained in Table 14.

For tightening procedures which reach or surpass the elastic limit, the following is valid (see Sec. 4.6.2.2.):

$$p = \frac{F_{SA} / 0.9}{A_P} \; \frac{\sigma_{0.2\,max}}{\sigma_{0.2}} \leq p_G$$

3. Load and Deformation Analysis and Derivation of the Principles of Calculation

In this section, the quantities which are used for the development of the dimensioning Equations (8) and (9) in Sec. 2. are derived and their modifications which depend on stress conditions are described. The force and deformation conditions of the bolted joints are investigated; both the elastic and the plastic behavior of the elements used will be considered.

3.1. Elastic Resilience or Spring Constant

The elastic behavior of the elements of a bolted joint is characterized by the elastic resilience δ or by the rigidity C.

In most cases, the elastic deformation f of a body is proportional to the loading force F:

$$f = \delta F. \tag{21}$$

The proportionality factor δ is designated as elastic resilience and is determined by:

$$\delta = f \;/\; F. \tag{22}$$

The reciprocal value of the elastic resilience is called the spring constant:

$$C = 1 \;/\; \delta = F \;/\; f. \tag{23}$$

Depending on the application (series or parallel connection of elastic elements), the usage of δ or C leads to formally simpler and clearer equations. Since in the case of bolted joints tandem connections of elastic elements are most commonly found, preference is given to the elastic resilience δ in the following.

Using Equation (23), however, all equations can easily be converted to the style used particularly in the older literature with the spring constant C.

3.1.1. Resilience of Bolts

The bolt consists of a number of single elements which are easily replaceable by cylindrical shapes of varying length l_i and varying cross section A_i, Figure 3. If E_B is Young's modulus of the bolt material, then the following is valid for the elastic elongation of such a single element under force F:

$$f_i = \frac{l_i\ F}{E_S\ A_i}. \qquad (24)$$

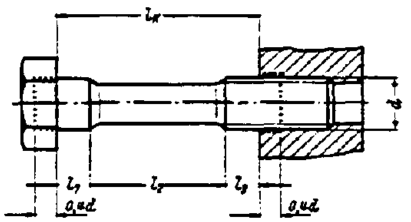

Figure 3: Partition of a bolt into single prismatic elements, for which the resilience δ can be determined.

With the Equations (22) and (24), there follows for the elastic resilience of a cylindrical single element:

$$\delta_i = \frac{f_i}{F} = \frac{l_i}{E_S\ A_i}. \qquad (25)$$

In the case of the bolt, the cylindrical elements are connected one after the other so that the total elastic resilience δ_S is obtained by addition of the resiliencies of the single cylindrical elements:

$$\delta_S = \delta_K + \delta_1 + \delta_2 + \ldots\ldots\ldots + \delta_G. \qquad (26)$$

Here δ_K is the elastic resilience of the head and δ_G is the elastic resilience of t'e screwed-in threaded part including the nut, Figure 3. The resilience of non-screwed-in threaded parts is determined by using the core cross section A_3. Based on experience, the elastic resilience of the head of standardized hexagonal and hexagonal recess bolts and that of the screwed-in thread which participates in the deformation is approximately as great as that of cylinders of an external thread diameter d and of a length 0.4 d. Therefore these elastic resiliencies are obtained as:

$$\delta_K = \delta_G = \frac{0.4\ d}{E_S\ A_N}. \qquad (27)$$

In Equation (27) $A_N = d^2\pi/4$ is the nominal cross section of the bolt.

Greater or smaller head and thread resiliencies than those of standard bolts must be considered by a correspondingly modified factor ($\neq$0.4).

3.1.2. Resilience of Directly-stacked, Clamped Plates

3.1.2.1. Cross Sectional Areas Of Substitutional Pressure Bodies in Sleeves and Plates

For the determination of the elastic resilience of sleeves with an external diameter D_A which is less or equal to the diameter of the head bearing area d_K, the cross sectional area

$$A_P = \pi/4\ (D_A^2 - D_B^2) \qquad (28)$$

and Young's modulus E_P of the sleeve material must be inserted into Equation (25).

The resilience of plates where $D_A > d_K$, Figure 4, cannot be precisely calculated in a simple fashion even in the case of concentric loading. On massive bodies and firmly stacked parts, various authors [8 to 13] have measured the deformations under conditions of concentric loading. Thereby resiliencies resulted which approximately correspond to those of cylindrical substitutional pressure bodies, the cross sectional areas A_{ers} of which can be calculated for two fields from D_A / d_K to a clamping length l_K = 8 d with a high degree of precision in the following way, Figure 5 :

—For sleeves with an external diameter D_A between d_K and 3 d_K:

$$A_{ers} = \pi/4\ (d_K^2 - D_B^2) + \pi/8 \left(\frac{D_A}{d_K} - 1\right) \left(\frac{d_K l_K}{5} + \frac{l_K^2}{100}\right) \qquad (29)$$

—For plates with a radial expansion $D_A > 3\ d_K$:

$$A_{ers} = \pi/4 \left[\left(d_K + \frac{l_K}{10}\right)^2 - D_B^2\right] \qquad (30)$$

3.1.2.2. Resilience with Concentric Bolt Arrangement and with Concentric Load Introduction

The elastic resilience δ_P of the concentrically clamped parts is produced from the relation

$$\delta_P = \frac{l_K}{A_{ers}\ E_P}. \qquad (31)$$

The condition of the deformation of massive bodies as a prerequisite for the validity of this derivation is generally only valid for firmly stacked parts and not for thin layers of greater number which are not completely level. In this case the longitudinal resilience δ_P increases and can be experimentally determined, if necessary, depending upon the load.

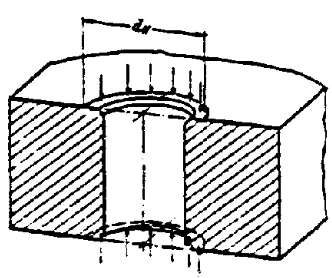

Figure 4: Plate compressed on the hole edge as if by bolt head or nut.

3.1.2.3. Resilience with Eccentric Bolt Arrangement and Concentric or Eccentric Load Introduction in the Bolted Joint

An eccentric load application on a bolted joint causes, along with the longitudinal deformation of the substitutional pressure body, a bending deformation of the clamped parts which produces an additional longitudinal deformation and thus increases the longitudinal resilience of eccentrically clamped plates and sleeves as opposed to concentrically clamped ones. In order to demonstrate the tendencies, formulations are made under the following conditions and simplified assumptions:

---The clamped parts form a prismatic body.

---The clamped parts form a "bending body" in the interface cross section in which the interface pressure on the stressed bending side is greater than zero.

---All cross sections of this prismatic body remain plane under loading. A distribution of tension takes place in them.

---The bending rigidity of the bolt is much less than that of the substitutional bending body and is neglected.

These simplified assumptions are generally only allowable for bending bodies whose cross dimensions lie within the diameter $d_K + h_{min}$ of the interface area.

The bending body is depicted in Figure 6. It can be a section from a multi-bolted joint. The lateral distance b is then given by the bolt arrangement or by $d_K + h_{min}$.

There are investigations concerning the distribution of the interface pressure in eccentrically clamped joints [4]. According to these, calculations can be made on the stressed bending side of the bending body with interface pressure, if the external contour in the area of the interface is not more than $(d_K + h_{min}) / 2$ away from the bolt axis S-S. Here h_{min} signifies the thickness of the thinner of two clamped plates. The interface area A_B of the bending body depicted in Figure 6 is under interface pressure if the bending body is preloaded by the bolt eccentrically arranged around s at its axis of gyration O–O with a preload F_V. The area A_B can be presented and calculated as a rectangle $b \cdot c$ minus the bolt hole. The axis of gyration at the area A_B is O–O. The area A_B with the appropriate moment of inertia $I_B = k_B^2 A_B$ is needed in Sec. 3.2.4.2. for the calculation of the clamping force F_{Kerf} which is required for the prevention of one-sided lift-off. [Note: With the use of A_B, the bending resilience of the bolt is neglected.]

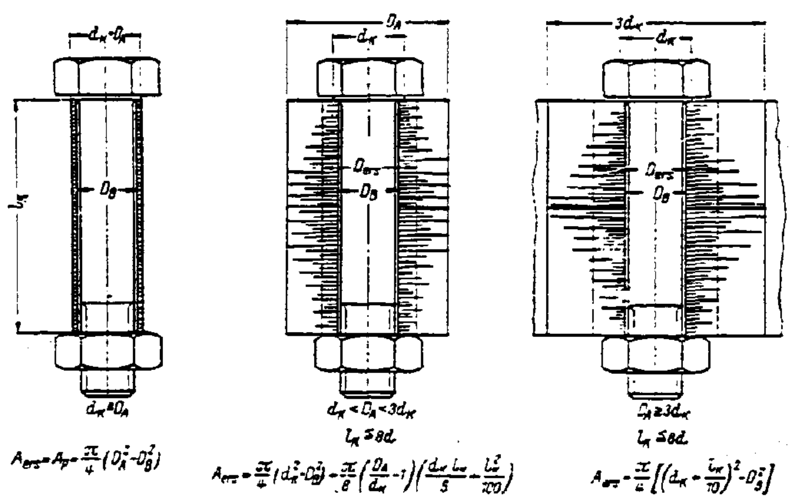

Figure 5: Substitutional compression body for calculation of the elastic resilience of clamped sleeves and plates.

Given these assumptions, we get the following resiliencies which usually are valid for the deformation in the bolt axis S–S. These resiliencies are for the loading situation depicted in Figure 7:

a) In the case of concentric configuration of the bolts (distance of the bolt axis S–S from the axis of gyration O–O of the bending body $s = 0$) and, simultaneously, concentric load introduction (distance of the load point of application from the axis of gyration $a = 0$) corresponding to Equation (31):

$$\delta_P = \frac{f}{F} = \frac{l_K}{A_{ers}\ E_P}.$$

b) In the case of eccentric bolt configuration in the distance s form the axis of gyration O–O of the bending body and load introduction in the eccentrically lying bolt axis S–S, thus $a = s$:

$$\delta_P^* = \delta_P \left(1 + \frac{s^2}{k_B^2\ A_B\ /\ A_{ers}}\right) \tag{32}$$

With the introduction of a length ratio λ for the eccentrically clamped, unloaded joint

$$\lambda = \frac{s\ /\ k_B}{\sqrt{A_B\ /\ A_{ers}}}, \tag{33}$$

Equation (32) is simplified to

$$\delta_P^* = \delta_P\ (1 + \lambda^2) \tag{34}$$

c) In the case of eccentric bolt configuration in the distance s from the axis of gyration O–O of the bending body and of a load introduction in the distance a from the axis of gyration as the most general case:

$$\delta_P^{**} = \delta_P \left(1 + \frac{a\ s}{k_B^2\ A_B\ /\ A_{ers}}\right) \tag{35}$$

where, δ_P^{**} is the quotient of the plate deformation f_{PA} in the bolt axis and from the external force F_A being applied in the distance a.

With the introduction of λ according to Equation (33) this becomes

$$\delta_P^{**} = \delta_P\ (1 + a/s\ \ \lambda^2). \tag{36}$$

Here the distance a must always be put in as positive.

The distance s is to be put in as positive if the bolt axis S–S and the load point of application A–A lie on the same side of the axis of gyration O–O and negative if the load point of application and bolt axis are located on opposite sides of the axis of gyration.

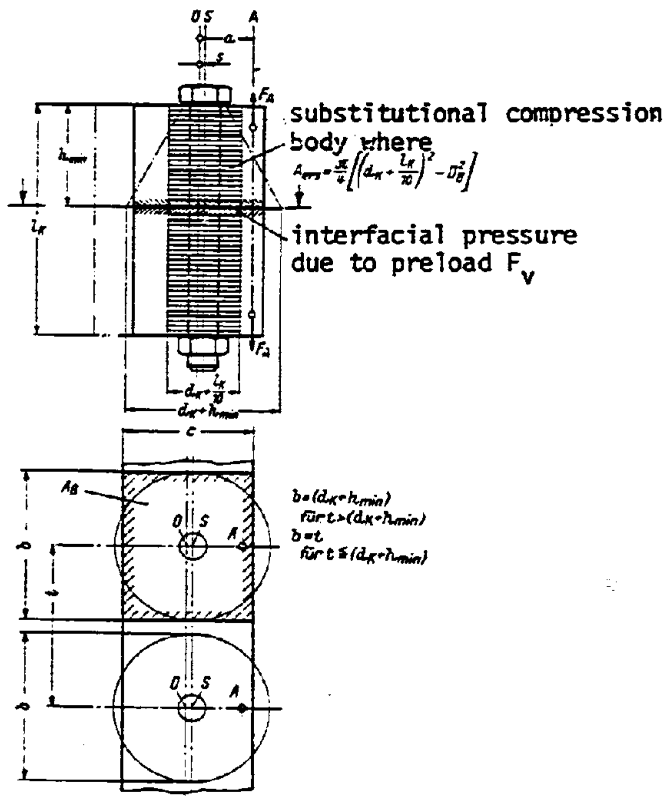

Figure 6: Bending solids and interfaces under interfacial pressure with eccentric clamping and loading.

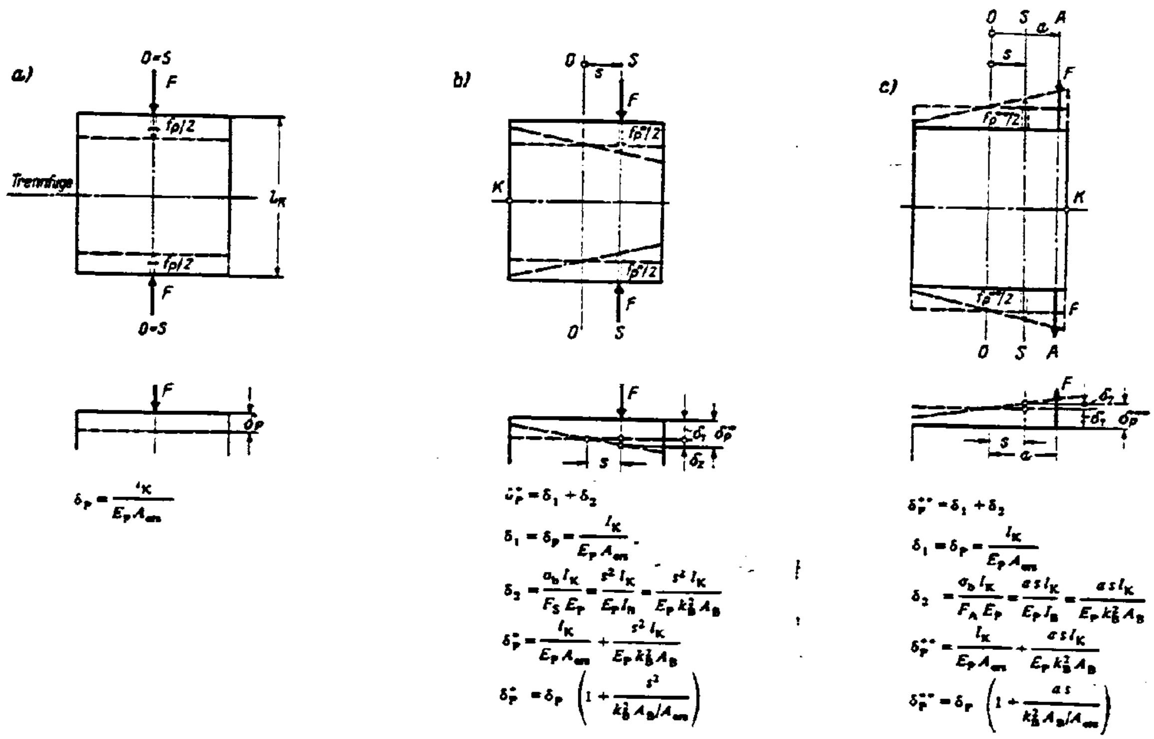

a) concentrically compressed in the bolt axis

b) compressed in eccentrical bolt axis

c) eccentically loaded

Figure 7: Influence of the line of force on the elastic deformation of a "bending solid" according to Figure 6.

One must keep in mind that with unfavorable cross section conditions small eccentricities of the load introduction cause considerable lateral tilt due to which the resilience of the clamped parts constantly increases.

If by the eccentricity of the preload F_V and of axial bolt strength F_A the unloading in the interface on the stressed side becomes greater than the pressure preload, then a one-sided lift-off begins, whereby the elastic resilience of the clamped parts progressively increases. This condition is not considered in the case of the calculation of resilience and that of the force ratio derived from it because it is the purpose of this guideline to recommend the prevention of one-sided lift-off by the introduction of a sufficient minimum clamping force. The determination of the differential force F_{SA} and of the force ratio Φ_e is of interest then only in the area of one-sided lift-off.

The calculation can be considerably improved by consideration of local resilience of the surfaces of the interface under pressure and of the contact resilience in the sense of leveling of microgeomtrical roughness of these surfaces. These effects are of essential importance in the case of bolted joints which form a closed statically indeterminate structure with the parts to be joined, since the local resiliencies in the interface correct, in the favorable sense, the position of the appropriate point of zero moment—and with it the distance *a*. The one-sided lift-off occurs earlier in opposition hereto by the contact resilience in the interface. A calculation which takes these effects into consideration is basically possible; however, the calculation can be very complex.

3.1.3. Resilience of Bent Plates and Sleeves

In Figure 8 a symmetric plate under bending forces is depicted. Forces are acting on points A, P and S.

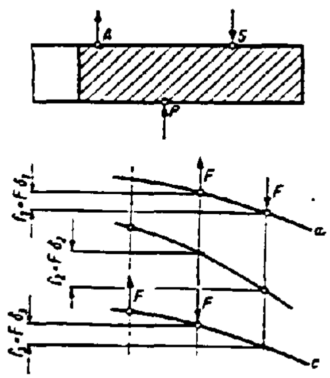

Figure 8: Stressed symmetric plates.

Case	Forces F being applied in the Points	Relative Shift of Point S opposite Point P caused by the Forces F	Definition of the Elastic Resilience
a	P and S	$f_1 = F\ \delta_1$	$\delta_1 = f_1 / F$
b	A and S	$f_2 = F\ \delta_2$	$\delta_2 = f_2 / F$
c	A and P	$f_3 = F\ \delta_3$	$\delta_3 = f_3 / F$

The resiliencies δ_1, δ_2 and δ_3 are defined according to Figure 8. They are necessary for the calculation of the force ratio (see Sec. 3.3.1.). The calculation of the δ-values is very complicated. For definite forms there are experimentally established approximate solutions to which we will refer in the following:

The circular flange, Figure 9, is being loaded by forces F which can also be thought of as working in circles around the flange axis.

The elastic thickness variation of the flange is much less than the deformation as a result of inversion and can therefore be neglected. The elastic resilience of the flange can be described by a single quantity ψ which is designated as inverse resilience. In the case of the loading of the flange by the force pairs FF, Figure 9, the cross section experiences inclinations at the angle γ. With $\gamma = f / a_F$ it becomes

$$\psi = \frac{\gamma}{W} = \frac{\gamma}{F a_F} = \frac{f}{F a_F^2} \qquad (37)$$

From Equation (23) of the specifications DIN 2505 (Tentative Standard, pub. Oct. 1964) the inverse resilience can be derived as

$$\psi = \frac{d_a + d_i}{4 \pi E h W} \qquad (38)$$

whereby according to Equation (27) in DIN 2505 for the loose flange

$$W = 1/12 \, (d_a - d_i - 2d'_L) \, h_F^2 \qquad (39)$$

and $h = h_F$.

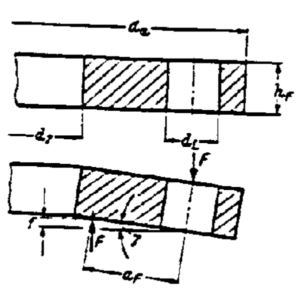

Figure 9: Circular loose flange.

For the firmly prewelded flange, Figure 10, Equation (38) can be used as well; however, W is to be calculated with

$$W = 1/12 \, (d_i + s_F) \, s_F^2 + 1/12 \, (d_a - d_i - 2 \, d'_L) \, h_F^2 \qquad (40)$$

and $h = h_A$ is to be put in (see DIN 2505 [Tentative Standard, pub. Oct. 1964] Equations (24) to (26)).

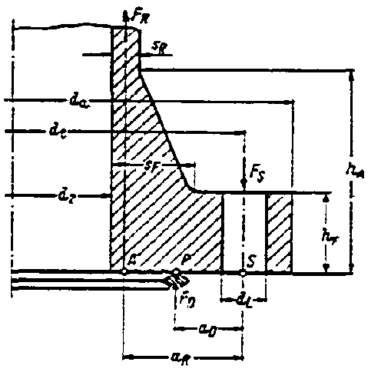

Figure 10: Firm prewelded flange

Thereby for the nominal distances

$$NM > 500 : d_L' = d_L / 2 \qquad (41a)$$

$$NM < 500 : d_L' = \left(1 - \frac{NW}{1000}\right) d_L \qquad (41b)$$

[Note: All quantities in mm.]

Since the bolt strength variation essential for the clamping ratios is conditioned by the relative shift between points P and S from Figure 10, the following is produced for this case

$$\gamma = f / a_D,$$

and in connection with the Equations (37) to (40) the elastic resiliencies can now be calculated as (see also Figure 8):

$$\delta_1 = a_D\, a_D\, \gamma = a_D^2\, \gamma \qquad (42a)$$

where $M_1 = F_1\, a_D$,

$$\delta_2 = a_R\, a_D\, \gamma \qquad (42b)$$

where $M_2 = F_2\, a_R$, and

$$\delta_3 = (a_R - a_D)\, a_D\, \gamma \qquad (42c)$$

where $M_3 = F_3\, (a_R - a_D)$.

(Further tips on calculation in [14]).

3.2. Load and Deformation Conditions in Directly-stacked Parts

In this section the quantities given in Sec. 2 for the dimensioning equations and for the various calculations will be derived from the elastic resiliencies of elements involved in a bolted joint for diverse loading conditions. Also the effect of plastic deformations will be observed in dependence of the resilience of the joint.

The joints discussed consist of plates, sleeves or other parts which in level interfaces (the preload in all the participating bolts in the joint has just been applied) lie directly on one another and have metallic contact.

3.2.1. Conditions in the Assembly Stage

In the case of a bolted joint the clamped parts are pressed together by the clamping parts. Thereby the bolt preload force F_V is equal to the preload force in the clamped parts but is directed oppositely. In the assembly stage without external loading, the clamping preload force in the bolt is identical with the bolt strength F_S, and the clamping preload force in the clamped parts is identical with the clamping force F_K.

In the simple case (without working load), Figure 11, the bolt is merely the clamping part while the plates with their full thickness represent the clamped parts. During tightening, the bolt is lengthened elastically by the preload force F_M by

$$f_{SM} = \delta_S \, F_M \qquad (43)$$

while the clamped parts are pressed together

$$f_{PM} = \delta_P \, F_M. \qquad (44)$$

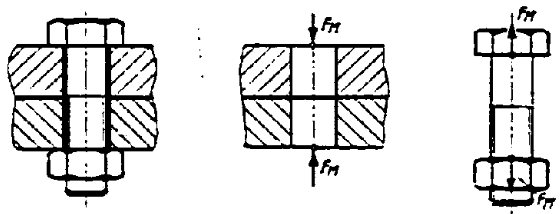

Figure 11: Simple bolted joint following assembly: traction force in the bolt F_M (← →) = pressure force in the clamped parts F_M (← →).

In Sec. 2.1. we have already seen in the joint diagram a graphic representation of these conditions for the preload force F_M, in which embedding procedures are not considered (see Figure 1a).

For the general case the sum of the deformations in the bolted joint under preload force F_M becomes:

$$f_{SM} + f_{PM} = (\delta_S + \delta_P)\ F_M. \qquad (45)$$

In the joint diagram, the increases of the deformation lines are inversely proportional to the resiliencies.

3.2.2. Variation in the Initial Clamping Force Resulting from Remaining Deformation by Embedding

In addition to the elastic deformations, embedding phenomena occur in a bolted joint. These phenomena are primarily caused by the leveling of surface roughness. These post-assembly embedding phenomena which can be designated by the embedding amounts f_Z (see also Sec. 4.4.) reduce the elastic deformations so that a new state of equilibrium is established. Thereby the preload force F_M is reduced by the preload force loss F_Z as a result of embedding.

The connection between the preload force loss F_Z and the embedding amount f_Z is obtained from relations between similar triangles, according to Figure 1b, as

$$\frac{F_Z}{F_M} = \frac{f_Z}{f_{SM} + f_{PM}} = \frac{f_Z}{\delta_S F_M + \delta_P F_M} \qquad (46)$$

From this it follows that:

$$F_Z = \frac{f_Z}{\delta_S + \delta_P} \qquad (47)$$

or--anticipating Equation (53)--:

$$F_Z = \frac{f_Z \Phi_K}{\delta_P} \qquad (48)$$

Φ_K can be taken for the various dimensions of bolted joints from the nomogram in Table 8; δ_P can be taken from the nomogram in Table 9.

If greater plastic deformations of the clamping and clamped parts appear under the working load, then there is also in this case a preload loss which can be determined according to Sec. 3.2.3.1.

3.2.3. Effects Caused by Type of Load Introduction

External forces are generally introduced into the joint through the clamped parts. The resilience conditions change with the situation of the load introduction level in which we can imagine the load introduction.

3.2.3.1. Application of Force on the Bolt Head and Nut Bearing Areas

The introduction of the axial force F_A (axial working load or axial components of a working load in any direction) in levels by means of the bolt head or or nut bearing areas is only theoretically conceivable (see Figure 17a). However, this case is suited for the derivation of basic relationships between forces and deformations.

Under such external loading, the bolt and the clamped parts become longer, as compared with the assembly condition, by the same amount $f_{SA} = f_{PA}$, Figure 12. The bolt must take up the entire force F_S, which is F_{SA} greater than the preload force F_V. The clamping force in the clamped parts is simultaneously reduced by the amount F_{PA}, so that the residual clamping force $F_{KR} = F_V - F_{PA}$ still remains.

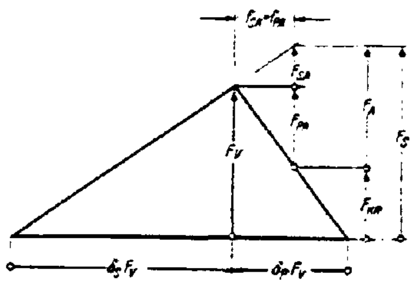

Figure 12: Joint diagram for for the theoretical case of concentric introduction of an axial traction force at the bolt head and nut bearing area.

The differential forces F_{SA} in the bolt and F_{PA} in the clamped parts which occur in loading of the joint cause the variations in length:

$f_{SA} = \delta_S \; F_{SA}$ and $f_{PA} = \delta_P \; F_{PA}$. (49)

Equating them provides the relation:

$$\delta_S \; F_{SA} - \delta_P \; F_{PA} = 0. \qquad (50)$$

Furthermore the following is valid (see Equation (3)):

$$F_A = F_{SA} + F_{PA}.$$

From Equations (3) and (50) follow:

$$F_{SA} = \frac{\delta_P}{\delta_S + \delta_P} F_A = \Phi_K \; F_A \qquad (51)$$

and

$$F_{PA} = \frac{\delta_S}{\delta_P + \delta_S} F_A = (1 - \Phi_K) \; F_A \qquad (52)$$

Thus the force ratio introduced in Sec. 2.1., Equation (2), for the theoretical case of load introduction in the bolt head and nut is referred back to the elastic resiliencies with:

$$\Phi_K = \frac{\delta_P}{\delta_S + \delta_P} \tag{53}$$

Further, there follows for the case of complete lift-off $F_{PA} = F_V$ and therefore $(1 - \Phi_K)\ F_A = F_V$.

Thus the axial force which leads to lift-off amounts to:

$$F_{Aab} = \frac{1}{1 - \Phi_K}\ F_V \tag{54}$$

If F_A is a concentrically acting compressive force, then it should be put into the equation with a negative sign. F_{SA} and F_{PA} are then negative; that means that the loading of the bolt decreases and that the clamped parts are additionally compressed.

Figure 12 shows the joint diagram for F_A as a tension force, Figure 13 the joint diagram for F_A as a compressive force. F_A is in both cases put between the two deformation lines--proceeding from the deformation lines for the clamped parts.

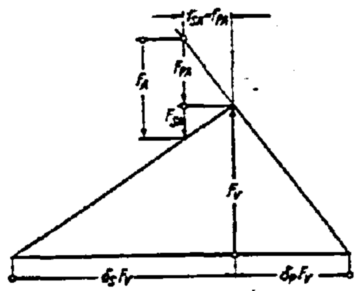

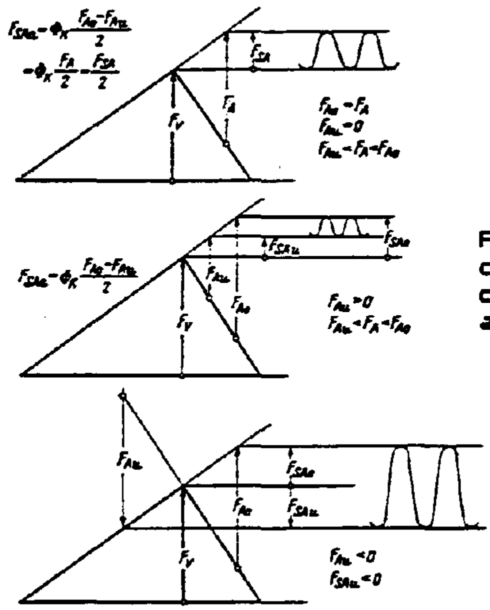

Figure 13: Joint diagram for the theoretical case of concentric introduction of an axial compressive load in planes through the bolt and nut bearing areas.

Figure 14: Possible cases of alternating stress of a bolted joint.

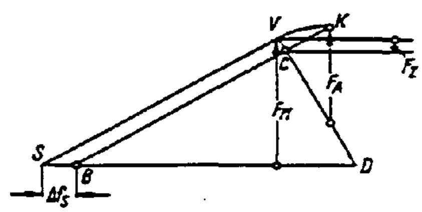

Figure 15: Joint diagram for the case of stress on the clamping parts by the working load into the plastic area.

In the case of bolted joints which are undergoing an alternating working load, Figure 14, the bolt also experiences an alternating stress. From the values for F_A as well as the upper limit force F_{Ao} and the lower limit force F_{Au}, we obtain the force amplitude in the bolt according to Equation (51) as

$$F_{SA} = \Phi_K \frac{(F_{Ao} - F_{Au})}{2} \tag{55}$$

and the accompanying mean force as

$$F_{SM} = F_V + \Phi_K \frac{(F_{Ao} + F_{Au})}{2} \qquad (56)$$

Since the continually bearable tension amplitude of the bolt, calculated from F_{SA} and from the core cross section A_S of the thread, is small (see Table 13), we must strive to keep the load portion assigned to the bolt as small as possible. This can be accomplished, among other things, by great elastic resilience δ_S of the bolt and by slight elastic resilience δ_P of the clamped parts (see also Table 15).

The joint diagrams express the same thing. The flatter the deformation line of the bolt and the steeper that of the clamped parts run, the smaller F_{SA} becomes.

If the bolt is plastically deformed by the tension force F_A, then its deformation line runs as a curve as per Figure 15 to point K. The deformation in the case of unloading runs along the line KB and cuts off the plastic deformation Δf_S on the base line. For the subsequent equal-sized or smaller loadings F_A, the joint diagram DBCK is applicable, in which the preload force is reduced by F_Z as compared with the assembly state . Analogous conditions exist if the clamped parts are plastically deformed by a pressure force F_A, Figure 16. From Figures 15 and 16 we obtain the preload reduction that occurs as a result of plastic deformation, as in Sec. 3.2.2.,

as

$$F_Z = \frac{\Delta f_S}{\delta_S + \delta_P} \quad \text{or} \qquad (57)$$

$$F_Z = \frac{\Delta f_P}{\delta_S + \delta_P}. \qquad (58)$$

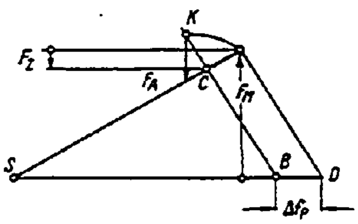

Figure 16: Joint diagram for the case of the stressing of the clamped parts by the working load into the plastic area.

3.2.3.2. Load Introduction within the Clamped Parts

The general case of load introduction through the clamped parts is depicted in Figure 17b. The assumed load introduction levels are thereby 2-2 and 3-3. F_A causes an unloading of the parts lying between load introduction levels 2-2 and 3-3 of F_{PA}, while, due to F_A, the remaining parts, which lie in the force flux of the bolt between the two load introduction levels, are additionally loaded by F_{SA}. These are the parts of the clamped plates between the levels 1-1 and 2-2, 3-3 and 4-4 as well as the bolt between the levels 1-1 and 4-4.

Given the simplified assumption of Sec. 3.1.2.1., the elastic resilience of the parts between the load application levels 2-2 and 3-3 can be assumed as $n\delta_P$ as a part of δ_P, whereby $n < 1$. For the parts between levels 1-1 and 2-2, as well as 3-3 and 4-4, the elastic resilience remains.

$\delta_P - n\delta_P = (1 - n)\ \delta_P.$

With these elastic resiliencies, F_{SA} causes the following deformation between the load introduction levels 2-2 and 3-3:

$$f_{SAn} = F_{SA}\ [\delta_S + (1 - n)\ \delta_P] \qquad (59)$$

and F_{PA} causes the deformation:

$$f_{PAn} = F_{PA}\, n\delta_P. \tag{60}$$

As long as no lift-off occurs, both deformations must be equal to one another. This leads to the relation:

$$F_{SA}\,[\delta_S + (1 - n)\ \delta_P] - F_{PA}\, n\delta_P = 0 \tag{61}$$

(Equation (61) is analogous to Equation (50) in Sec. 3.2.3.1.).

In addition the following equilibrium condition appears (see Equation (3)):

$$F_A = F_{SA} + F_{PA}.$$

The desired forces are obtained as:

$$F_{SA} = \frac{n\delta_P}{\delta_S + \delta_P}\, F_A = n\ \Phi_K\ F_A = \Phi_n\ F_A \tag{62}$$

$$F_{PA} = \frac{\delta_S + (1 - n)\ \delta_P}{\delta_S + \delta_P}\, F_A =$$

$$= (1 - n\ \Phi_K)\ F_A = (1 - \Phi_n)\ F_A \tag{63}$$

In Equations (62) and (63)

$$\Phi_n = n\ \Phi_K = n\ \frac{\delta_P}{\delta_S + \delta_P} \tag{64}$$

In place of the bolt resilience δ_S in Sec. 3.2.3.1. the resilience $\delta_S + (1 - n)\ \delta_P$ has appeared. This is the elastic resilience of all the parts between intended load introduction levels 2-2 and 3-3 on the bolt side, which are to be considered as clamping. In place of δ_P, $n\delta_P$ appears . This is the elastic resilience of portions of the clamped parts lying between the intended load application levels 2-2 and 3-3. Figure 17 also contains, along with the general form of the load introduction within the clamped parts, Figure 17b, the two theoretically conceivable bounding cases, Figures 17a and 17c.

Depending on the situation of the load introduction levels, the differential force F_{SA} can lie between 0 and $\Phi_K F_A$ in the case of a bolted joint according to Figure 17 with loading by F_A.

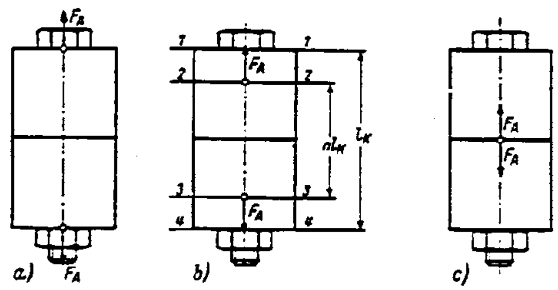

Figure 17: Load introduction in the bolted joint.

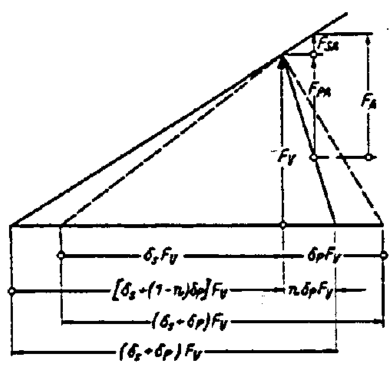

Figure 18: Joint diagram for a working load introduced inside of the clamped parts.

In Figure 18 the force and deformation conditions in the joint diagram are depicted for the case of load introduction within the clamped parts. The case for the assembly stage is shown by dotted lines.

3.2.4. Eccentric Clamping and Loading

The case of a concentrically clamped and concentrically loaded bolted joint treated in Sec. 3.2.3. is realized in design only very rarely. In most cases, the line of contact of the axial force F_A will not lie in the bolt axis, and the bolt axis itself will not fall together with the axis of gyration of the clamped parts (to be exact, of the bending body, Figure 6). Due to eccentricities, a resulting bending moment is produced in the bolted joint. Along with the tensions produced by the forces F_V and F_{SA}, bending tensions become effective in the bolt cross section which must be considered when testing for endurance strength. Over and above this, eccentrically loaded bolted joints tend toward one-sided lift-off at the interface if the axial force F_A exceeds a value dependent upon the preload F_V and the eccentricities of both forces. One-sided lift-off causes a sharp increase in bolt tensions from axial force and bending. The requirement to avoid one-sided lift-off and its detrimental consequences for the security of the joint determines decidedly the quantity of the preload F_V to be applied and therefore also influences the dimensions of the bolt, for which endurance strength is to be demonstrated with alternating working loads.

In the case of eccentrically clamped and eccentrically loaded bolted joints, elastomechanical problems involving a considerable amount of calculation, due to the design multiplicity, for a mathematical treatment.

The following derivation of the calculation equations is based on the elastic resiliencies which were given in Sec. 3.1.2.3. and is subject to the simplified assumptions made there. The user of these equations must check the dependability of the simplifications in each case and, if necessary, must make additional calculations (in this regard, cf. [4]). The consideration of eccentric load applications will lead to a greater accuracy of goal with the measurement of bolts than the use of simple equations for concentric clamping and concentric loading.

3.2.4.1. Forces and Deformations up to the Lift-Off Limit

An eccentrically clamped and also eccentrically loaded bolted joint is depicted in Figure 19. During assembly, the bolt was tightened to the preload force F_V. For this joint the conditions and assumptions of Sec. 3.1.2.3. will suffice, i.e., it can be defined as a bending body with the axis of gyration O-O. The bolt axis S-S lies eccentrically to the axis of gyration O-O by the amount $x = s$. The line of force A-A of the axial force F_A which is being externally applied has the distance $x = a$ from the axis of gyration O-O.

As given in Figure 19, the axis of gyration O-O fixes the zero point of the x-axis. Moreover, the value $x = a$ should always be positive, as for Equation (36). The value $x = s$ is then likewise positive if the bolt axis S-S and the load line of application A-A lie on the same side eccentrically to the axis of gyration O-O. If they are located on opposite sides of the axis of gyration, then $x = s$ is negative. It is further stipulated that in practice $a > s$ always.

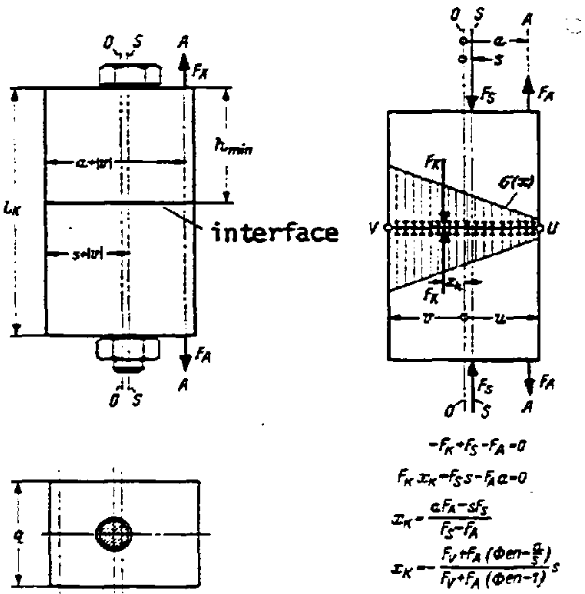

Figure 19: Eccentric clamping and eccentric loading of a bolted joint ("bending body" according to Figure 6).

If the bolted joint, which has been preloaded with F_V by eccentrically arranged bolts depicted in Figure 19, is additionally loaded with the eccentrically functioning force F_A, then the bolt load increases by F_{SA}.

Since the elongation of the bolt f_{SA} is equal to the elongation of the clamped parts f_{PA}, then:

$$f_{SA} = f_{PA}$$

$$\delta_S \cdot F_{SA} = \delta_P \cdot F_{PA}$$

$$\delta_S \cdot F_{SA} = \delta_P \; (F_A - F_{SA})$$

$$\delta_S \cdot F_{SA} = \delta_P \cdot F_A - \delta_P \cdot F_{SA}$$

This equation is valid primarily in general cases. For the case of eccentrically loaded and eccentrically clamped bolted joints this equation goes over into:

$$\delta_S \cdot F_{SA} = \delta_P^{**} \cdot F_A - \delta_P^{*} \cdot F_{SA} \qquad (65)$$

because δ_P^{**} can be set for the resilience in the eccentric force line of application A–A, and δ_P^{*} for the resilience in the eccentric bolt axis S–S.

In the case of load introduction in bolt heads and nuts, we obtan, solved according to F_{SA},

$$(\delta_S + \delta_P^*)\ F_{SA} = \delta_P^{**} \cdot F_A$$

and from that:

$$F_{SA} = F_A \frac{\delta_P^{**}}{\delta_S + \delta_P^*} = F_A \cdot \Phi_{eK} \tag{66}$$

By substituting δ_P^* and δ_P^{**} according to Equations (34) and (36), we get the force ratio Φ_{eK} for the eccentrically clamped and eccentrically loaded joint with the load introduction in the levels of the bolt head and nut:

$$\Phi_{eK} = \frac{\delta_P^{**}}{\delta_S + \delta_P^*} = \frac{\delta_P\ (1 + a/s\ \lambda^2)}{\delta_S + \delta_P\ (1 + \lambda^2)}. \tag{67}$$

In the case of an introduction of the forces F_A, F_{SA} and F_{PA} within the clamped parts at the height of levels 2-2 and 3-3 at a distance nl_K, according to Figure 17b, Equation (65) should be written as follows, as in Sec. 3.2.3.2.:

$$[\delta_S + (1 - n)\ \delta_P^*]\ F_{SA} = n\delta_P^{**}\ F_A - n\delta_P^*\ F_{SA}. \tag{68a}$$

From this follows that

$$[\delta_S + \delta_P^*]\ F_{SA} = n\delta_P^{**}\ F_A$$

where

$$\Phi_{en} = F_{SA}\ /\ F_A$$

$$\Phi_{en} = n\ \frac{\delta_P^{**}}{\delta_S + \delta_P^*} = n\ \frac{\delta_P\ (1 + a/s\ \lambda^2)}{\delta_S + \delta_P\ (1 + \lambda^2)} = n\ \Phi_{eK} \tag{68b}$$

Equation (68b) can thus be also purely formally derived from Equation (67) by replacing δ_P^{**} by $n\delta_P^{**}$.

According to Equation (3) there follows, using Equation (63):

$$F_{PA} = F_A - F_{SA} = (1 - \Phi_{en})\ F_A. \tag{69}$$

In the case of the force ratio Φ_{en} according to Equation (68), the longitudinal forces of an eccentrically clamped and eccentrically loaded bolted joint, under observation of the sign rule for s according to Sec. 3.1.2.3., can be calculated analogously to those of a concentrically clamped and loaded one, as long as one-sided lift-off in the interface is prevented by a sufficiently great preload.

3.2.4.2. Forces and Deformations at the Lift-off Limit

If the axial force F_A in an eccentrically loaded bolted joint surpasses a limit value F_{Aab} dependent upon a preload, then the clamped parts unilaterally lift off in the interface beginning at the position $x = u$, Figure 19. The one-sided lift-off begins when the resulting pressure tension in the interface becomes zero at the position $x = u$.

In the case of the bending body observed here, Figure 19, the tension distribution in the interface is approximately:

$$\sigma(x) = -\frac{F}{A_B} + \frac{M_B}{I_B}\, x \tag{70}$$

where:

$$F = F_V - (1 - \Phi_{en}) - F_A \tag{71}$$

and

$$M_B = F_A\,(a - \Phi_{en}\, s) - F_V \cdot s. \tag{72}$$

Therefore

$$\sigma(x) = -\frac{F_V - (1 - \Phi_{en})\, F_A}{A_B} + \frac{F_A\,(a - \Phi_{en}\, s) - F_V\, s}{I_B}\, x \tag{73}$$

or

$$\sigma(x) = \frac{1}{A_B}\left[F_A\,(1 - \Phi_{en}) - F_V + \frac{F_A\,(a - \Phi_{en}\, s)\, F_V\, s}{k_B^2}\, x\right] \tag{74}$$

Lift-off begins in the edge fiber $x = u$ if the tension there becomes $\sigma(u) = 0$. If F_A is a tension force and $a > s$, then the lift-off begins in the edge fiber next to the force line of application A–A (Point U in Figure 19). In this case the edge fiber distance u can be put in as a positive value for x. If $a < s$, then the lift-off begins in Point V. The edge fiber distance v can be then put in as a negative value. In the case of a pressure force F_A which acts at a sufficiently great distance a and which can be put in as negative, the lift-off begins likewise on the opposite side of the cross section (Point V in Figure 19). This is taken into account if the edge fiber distance to Point V is put in as a negative value v in the place of u in the otherwise unaltered equations.

By substitution of $x = u$ in Equation (70), the condition $\sigma(u) = 0$ leads to the lift-off-causing axial force F_{Aab} as a function of the applied preload F_V:

$$F_{Aab} = \frac{F_V}{\left(1 + \frac{au}{k_B^2}\right) : \left(1 + \frac{su}{k_B^2}\right) - \Phi_{en}} \tag{75}$$

For a given axial force F_A, we get conversely that very preload F_{Vab}, at which one-sided lift-off occurs:

$$F_{Vab} = \frac{(a - s)\ u}{k_B^2 + s\ u} F_A + (1 - \Phi_{en})\ F_A \tag{76}$$

Thus the clamping force present at the lift-off limit is:

$$F_{Kab} = \frac{(a - s)\ u}{k_B^2 + s\ u} F_A \tag{77}$$

If it is to be confirmed that no one-sided lift-off occurs under the eccentrically acting axial force F_A, then a required clamping force F_{Kerf} must be inserted into the dimensioning equations (8) or (9) which is at least equal to the clamping force F_{Kab} present at the lift-off limit, i.e.,

$$F_{Kerf} = \frac{(a - s)\ u\ F_A}{k_B^2 + s\ u} \tag{78}$$

The dimensioning equations (8) and (9) for the determination of the bolt sizes are applicable to the eccentrically loaded bolted joint under the restrictions given in Sec. 3.2.4. if the force ratio Φ_{en} according to Equation (68) as well as a required clamping force according to Equation (78) are substituted. If this value of the clamping force F_{Kerf} is not sufficient to take over the required friction contact or the required sealing functions, then we must reckon on the highest value F_{Kerf} required in Equation (8) or (9).

Special Cases

a) Bolt strength and external force work eccentrically on the clamped parts. The clamped parts are prismatic; however, they are so thin that the interface area A_B becomes more or less equal to A_{ers} F_{Kerf}, however

$$\Phi_{en} = n \frac{\delta_P \ (1 + sa/k_B^2)}{\delta_S + \delta_P \ (1 + s^2/k_B^2)} \tag{79}$$

b) The bolt is concentrically arranged ($s = 0$); the external force works eccentrically ($a \neq 0$). For the rest, the general case with the conditions described in Secs. 3.1.2.2. and 3.2.4.1. is valid. The force ratio according to Equation (68) is reduced as a result of $s = 0$ to:

$$\Phi_{en} = n \frac{\delta_P}{\delta_S + \delta_P} = \Phi_n$$

and this does not differ from the case of the concentric joint; but the eccentrically loaded bolt experiences an additional bending stress. For the prevention of one-sided lift-off, a minimum clamping force F_{Kerf} is needed which can be calculated as follows:

$$F_{Kerf} = \frac{a \ u \ F_A}{k_B^2} \tag{80}$$

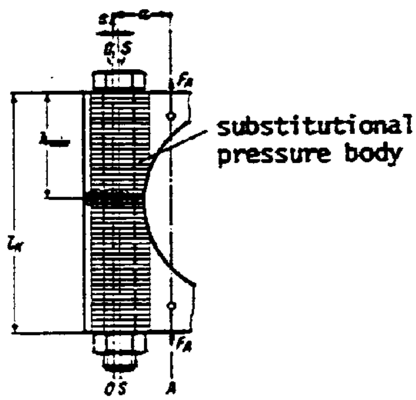

Figure 20: Special case of a "bending body."

c) In the case of a pure moment loading, the force variable Φ_m and the minimum clamping force can be derived for a bolted joint under the conditions defined in Secs. 3.1.2.2. and 3.2.4.1. From Equations (66) and (67) this becomes:

$$F_{SA} = \frac{\delta_P \lambda^2}{\delta_S + \delta_P (1 + \lambda^2)} \cdot \frac{M_B}{s} \qquad (81)$$

or for the purpose of definition of a dimensionless force ratio:

$$\Phi_m = \frac{\delta_P \lambda^2}{[\delta_S + \delta_P (1 + \lambda^2)] \, s/k_B} \qquad (82)$$

and therefore:

$$F_{SA} = \Phi_m \frac{M_B}{k_B} \qquad (83)$$

The minimum clamping force for the prevention of one-sided lift-off is produced in the same way from Equation (78) as:

$$F_{Kmb} = \frac{u}{k_B^2 + s\, u} M_B \qquad (84)$$

Here we must note that for the case of a pure moment loading where $a\, F_A \rightarrow M_B$ and $1/a \rightarrow 0$, $F_A \rightarrow 0$.

Therefore we obtain from Equation (3) the equation:

$$F_{PA} = -F_{SA} = \frac{-\Phi_m M_B}{k_B} \tag{85}$$

in place of the otherwise generally valid Equation (4) and thus:

$$F_{Vab} = F_{Kab} + F_{PA} = \frac{u}{k_B^2 + s\,u} M_B - \Phi_m \frac{M_B}{k_B} \tag{86}$$

with Φ_m in accordance with Equation (82). In the case of given F_V, we can calculate from this M_{Bab} as the limit value of the external moment which leads directly to one-sided lift-off.

For the special case $s = 0$ we obtain with $\lambda^2 = 0$ according to Equation (33) and with $\Phi_m = 0$ according to Equation (82):

$$F_{SA} = -F_{PA} = 0$$

according to Equations (83) and (85) and therefore also $F_V = F_K$.

For a rectangular cross section where $k_B^2 = u/3$ we obtain:

$$M_{Bab} = u/3\ F_V, \tag{87}$$

i.e., lift-off occurs as soon as the clamping force F_K in the interface, shifted to the left by the external moment M_B in the sense of Figure 19, emerges from the core area of the interface cross section.

3.2.4.3. Moments, Angle Deformations and Bolt Stress

The bending moment acting additionally on the clamped parts due to eccentric loading amounts to:

$$M_b = F_A\,a - F_{SA}\,s = \left(1 - \frac{s}{a}\Phi_{en}\right) a\,F_A \tag{88}$$

Analogous to the longitudinal resilience δ for the calculation of longitudinal deformation f, a bending resilience β can be defined for the calculation of the bending deformation γ. It can be determined like the longitudinal resilience (see Equation (31)) for the case of the simply observed bending body (as long as no lift-off occurs) as:

$$\beta_P = \frac{l_K}{I_B\,E_P} = \frac{l_K}{k_B^2\,A_B\,E_P} \tag{89}$$

Analogous to the longitudinal resilience (see Equation (26)), but with the simplification that the bolt is not treated in a strict fashion as a bent tension member, the following is produced for the bolt as the sum of the partial resiliences $\beta_i = l_i / I_i E_s$:

$$\beta_s = \beta_K + \beta_1 + \beta_2 + \ldots + \beta_G \tag{90}$$

The sum can also be written in the form

$$\beta_s = \frac{l_{ers}}{I_3 E_s} \tag{91}$$

From this follows that

$$l_{ers} = \beta_s I_3 E_s. \tag{92}$$

The angle of inclination of the clamped prisms under the portion M_{Pb} of the bending moment M_b taken up by the prisms is obtained from

$$\gamma_P = \beta_P M_{Pb} \tag{93}$$

and the angle deformation of the bolt under the portion M_{Sb} of the bending moment taken up by the bolt as

$$\gamma_S = \beta_S M_{Sb}. \tag{94}$$

Since $\gamma_S = \gamma_P$ and $M_b = M_{Sb} + M_{Pb}$ must be the case, then

$$M_{Pb} = \frac{\beta_S}{\beta_P} M_{Sb} \tag{95}$$

$$M_{Sb} = M_b - M_{Pb} = M_b - \frac{\beta_S}{\beta_P} M_{Sb} \tag{96}$$

or

$$M_{Sb} = \frac{M_b}{1 + \beta_S/\beta_P} \tag{97}$$

Since in general $\beta_S >> \beta_P$, β_S/β_P is much greater than 1, so that the moment which is to be taken up by the bolt can be written approximately as:

$$M_{Sb} \approx \frac{\beta_P}{\beta_S} M_b.$$

With Equation (88) this becomes:

$$M_{Sb} \approx \frac{\beta_P}{\beta_S} \left(1 - \frac{s}{a} \Phi_{en}\right) a F_A \tag{98}$$

For the endurance strength of the bolt in an eccentrically loaded joint, the nominal tension σ_{SAb} to be calculated from the longitudinal force F_{SA} and the moment M_{Sb} for the highest stessed mantle fiber of the core cross section at the first load-bearing thread proves to be the determining factor. It is calculated from:

$$\sigma_{SAb} = \sigma_{SA} + \sigma_{b} = \frac{F_{SA}}{A_3} + \frac{M_{Sb}}{W_3} =$$

$$= \Phi_{en} \frac{F_A}{A_3} + \frac{\beta_P}{\beta_S} \quad 1 - \frac{s}{a} \Phi_{er} \quad \frac{a\, F_A}{W_3} \qquad (99)$$

and can be changed with the formulas of the circular cross section $A_3 = \pi d_3^2/4$ and $I_3 \;/\; W_3 = d_3/2$ into the relation:

$$\sigma_{SAb} = \left[1 + \left(\frac{1}{\Phi_{en}} - \frac{s}{a}\right) \frac{I_K}{I_{ers}} \quad \frac{E_S}{E_P} \, \frac{a\, \pi\, d_3^3}{8\, A_D\, k_D^2}\right] \frac{\Phi_{en}\, F_A}{A_3} \qquad (100)$$

Here the expression to the right next to the brackets is the tension alone from the differential force F_{SA}, and the bracketed expression is its increase due to the additional bending tension.

3.2.4.4. Presentation of the Forces, Deformations and Tensions in Joint Diagrams

Even for the general case of eccentrically clamped and eccentrically loaded bolted joints we can depict a joint diagram. Figure 21 shows the joint diagram for the case of loading by an axial force F_A at the lift-off limit (F_A is thus slightly less than F_{Aab}). Under the preload F_V, which in this case is equal to the preload F_{Verf} required for the prevention of lift-off, the bolt is elongated by the amount of SO = $\delta_S\, F_V$, while the prisms are compacted at the position $x = s$, where the bolt head and nut of the bolt make contact by the amount of OP = $\delta_P^*\, F_V$ (δ_P^* according to Equation (34)).

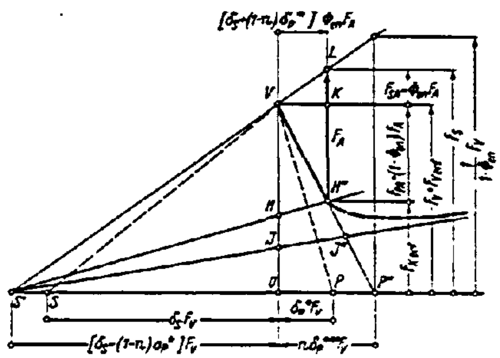

Figure 21: Joint diagram for eccentric clamping and eccentric loading.

With that we can draw the force deformation diagram SOPV for the condition of preload.

Furthermore, the joint diagram for the loaded condition should be formed in such a way that we can determine the load portions F_{SA} and F_{PA} between two deformation lines with the insertion of F_A.

For this purpose, one of the deformation lines should be the characteristic of the clamping parts. This characteristic is not identical with the bolt characteristic in the case of load introduction over the clamped parts. It is determined in this case similarly to Figure 18 by the Points S' and V.

The deformation line valid for the bolt strength (F_V + F_{SA}) through the Points S', V and L must designate a angle of inclination whose cotangent is equal to the resilience between the points of force application in the bolt axis during loading in the bolt axis. In the case of load application in the levels beneath the bolt head and nut this would be δ_S; however, in the case of load application within the clamped parts at a distance of $n\ l_K$ according to Figure 17b, this resilience changes according to Equation (68a) into (δ_s + (1 − n) $\delta_p{}^*$). Therefore

$$\overline{S'O} = [\delta_s + (1 - n)\ \delta_p{}^*]\ F_v$$

with $\delta_p{}^*$ in accordance with Equation (34).

The reciprocal negative inclination scale of the deformation lines falling to the right through Point V which are valid for the additional plate force between the force application levels 2–2 and 3–3, as per Figure 17b, is designated, as in Figure 7c, as $n\ \delta_p{}^{***}$. It is not necessarily assignable, since the line of application of the additional plate force F_{pA} is not known at first. Its distance q from the middle line O–O of the prismatic joint which is to be used in the place of a, results, however, from the following equilibrium conditions:

$$F_A = F_{SA} + F_{pA},$$

$$F_A\ a = F_{SA}\ s + F_{pA}\ q.$$

Therefore

$$F_A\ a = \Phi_{en}\ F_A\ s + (1 - \Phi_{en})\ F_A\ q$$

and

$$\frac{q}{s} = \frac{a/s - \Phi_{en}}{1 - \Phi_{en}}$$

where

$$\Phi_{en} = n\ \frac{\delta_p{}^{**}}{\delta_s + \delta_p{}^*}$$

according to Equation (68b).

With the substitution of a by q in Equation (36) and accordingly the substitution of $\delta_p{}^{**}$ by $\delta_p{}^{***}$ we obtain:

$$n\delta_p{}^{***} = n\delta_p \left(1 + \frac{q}{s}\,\lambda^2\right) =$$

$$= n\delta_p \left(1 + \lambda^2\ \frac{a/s - \Phi_{en}}{1 - \Phi_{en}}\right)$$

and after short intermediate calculation where:

$$\delta_P \left(1 + \frac{a}{s} \lambda^2\right) = \delta_P^{**}$$

according to Equation (36) and δ_P $(1 + \lambda^2) = \delta_P^{*}$ according to Equation (34),

$$n\delta_P^{***} = \left[\delta_S + \delta_P^{*} - n\delta_P^{*}\right] \frac{\Phi_{en}}{1 - \Phi_{en}}.$$

The deformation line thus falls from V towards P", whereby:

$$\overline{OP''} = n\delta_P^{***} F_V = [\delta_S + (1 - n)\ \delta_P^{*}] \frac{\Phi_{en}}{1 - \Phi_{en}} F_V$$

as has to be the case on the basis of the similarity relation

$$\overline{H''K}:\overline{KL}=\overline{S'O}:\overline{OP''} = (1 - \Phi_{en}) : \Phi_{en}$$

If the joint is preloaded at $F_V = F_{Verf}$ to prevent lift-off of the joint under the working load F_A, then the joint would lift off at Point H" if F_{Aab} were to be exceeded.

After lift-off, stress bearing appears in the borderline case. For reasons of equilibrium (see Figure 19)

$$F_A\ (a + |v|) = F_S\ (s + |v|). \qquad (101)$$

The relation is satisfied by all points of the lines S'JJ" if:

$$\overline{VJ}\ /\ \overline{VO} = \frac{s + |v|}{a + |v|}$$

In the case of loading surpassing the lift-off point, the characteristic VH" will continue more of less like the broken line and will tend toward the line S'JJ". The exact course is of little interest since the lift-off limit given by Point H should not be exceeded.

3.3. Force and Deformation Conditions in the Case of Non-directly Clamped Plates

As in the previous section, the quantities given in Sec. 2. will refer to the elastic resiliencies. The joints treated in this section will consist of flanges and flange-like plates which are not in direct contact even after application of the preload.

3.3.1. Load Ratio for Flanges and Flange-like Joints

In the symmetrical bolted joint in Figure 22, the parts PP, which are clamped with the preload F_V by means of a plate with the bolts S, are clamped to a base object said to be inflexible. The bolts are elongated at f_S; the flanges are bent at 2 f_1.

We are investigating force variations F_{SA} in both bolts S, and F_{PA} in the clamped parts PP if the joint is loaded by the external force F_A.

F_{SA} and F_{PA} cause the following deformations shown in Figure 22 (δ-values see Sec. 3.1.3.).

---Length alteration per bolt by loading
with F_{SA} $\qquad f_{SA} = \delta_S\ F_{SA}$

---Deformation of the plate
(Shifting of the Point S with
respect to Point P)
by the force pair
F_{SA}--F_{SA} $\qquad f_2 = \delta_2\ F_{SA}$
by the force pair
F_{PA}--F_{PA} $\qquad f_3 = \delta_3\ F_{PA}$

---Deformation of clamped parts
by loading with F_{PA} $\qquad f_{PA} = \delta_P\ F_{PA}$.

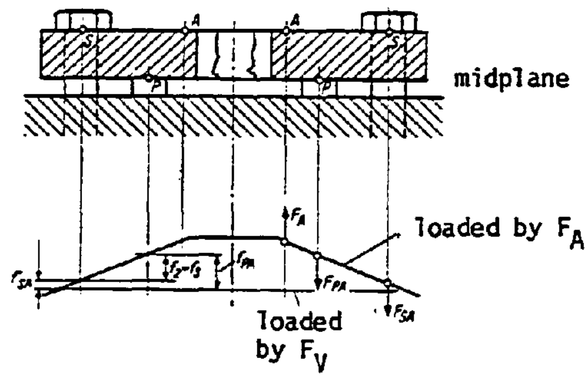

Figure 22: Forces and deformations of clamped, non-directly stacked plates.

As long as the parts do not lift off from one another, the following is true according to Figure 22:

$$f_Z + f_S + f_{SA} = f_{PA} \qquad (102)$$

or according to a transformation:

$$F_{SA}\ (\delta_S + \delta_Z) = F_{PA}\ (\delta_P - \delta_Z). \qquad (103)$$

From the Equations (2) and (103) there follows for the force ratio:

$$\Phi_{F1} = \frac{F_{SA}}{F_A} = \frac{F_{SA}}{F_{SA} + F_{PA}} = \frac{1}{1 + \frac{F_{PA}}{F_{SA}}} = \frac{1}{1 + \frac{\delta_S + \delta_Z}{\delta_P - \delta_Z}} \qquad (104)$$

and similar to Equation (4):

$$F_{PA} = (1 - \Phi_{F1})\ F_A. \qquad (105)$$

As per the quantity of the δ-values, F_{SA} can be positive as well as negative. The bolt load no longer increases with negative F_{SA} in spite of tension force on the joint, but even decreases. In the case of the symmetrical flange joint with m bolts according to Figure 23, we should observe that two flanges take part in the deformation. However, in the case of two equal flanges:

$$\Phi_{F1} = \frac{F_{SA}}{F_A} = \frac{1}{1 + \frac{\frac{1}{m}\delta_S + 2\,\delta_2}{\delta_P - 2\,\delta_3}} = \frac{\delta_P - 2\,\delta_3}{\frac{\delta_S}{m} + \delta_P + 2\,\delta_2 - 2\,\delta_3} \qquad (106)$$

(δ_2 or δ_3 is the appropriate deformation on the flange) and, as above:

$$F_{PA} = (1 - \Phi_{F1})\, F_A$$

After the insertion of δ_2 and δ_3 from the Equations (42b) and (42c) into Equation (106) we get an expression corresponding to Equation (31) in DIN 2505.

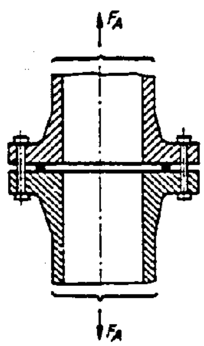

Figure 23: Flange joint with m bolts.

3.3.2. Joint Diagrams for Flange Joints

3.3.2.1. Joint Diagram with Linear Deformation Lines

Each bolt in Figure 23 is preloaded with $1/m\ F_V$ and thereby elongates at $1/m\ \delta_S\ F_V$. Both flanges bend under F_V at $2\ \delta_1\ F_V$ while the clamped parts are compressed at $\delta_P\ F_V$. This is depicted by the triangle SPV in the joint diagram, Figure 24. The diagram will be set up from now on in such a way that the deformation line VP also serves as one of the two characteristic lines in the case of additional loading by F_V. A second characteristic line—in the case of linear characteristics the line VM—must still be determined. V is the point of these lines for which $F_A = F_V$ and $F_{SA} = 0$.

For the determination of the point M (in the case with unpressured seal) the following is valid according to Figure 24:

$$\overline{PN} \sim F_{PA} = F_V. \qquad (107)$$

If we substitute Equation (107) into Equation (105), then we get:

$$\overline{PM} \sim F_A = \frac{F_V}{1 - \Phi_{F1}} \qquad (108)$$

From Equation (104) there follows then:

$$\overline{NM} \sim F_{SA} = \Phi_{F1}\, F_A = F_V \frac{\Phi_{F1}}{1 - \Phi_{F1}} \qquad (109)$$

With $\overline{PM}$ from Equation (108) or $\overline{NM}$ from Equation (109), Point M can be drawn into the diagram.

F_{SA} and F_{PA} for any F_A are found by inserting $F_A \sim$ HK. F_A is separated into both partial forces F_{SA} and F_{PA} by the line $\overline{VN}$ (// OP).

Figure 25 shows the force deformation diagram for negative F_{SA} or for the falling characteristic line $\overline{VM}$.

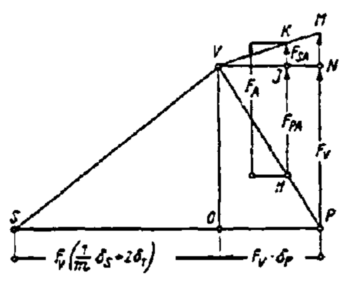

Figure 24: Joint diagram for a flange joint according to Figure 23 (F_{SA} as a positive or rising sealing characteristic).

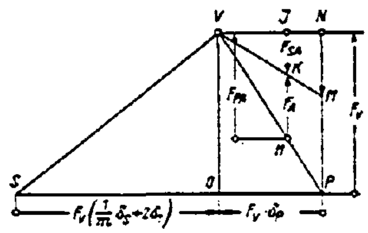

Figure 25: Joint diagram for a flange joint according to Figure 23 (F_{SA} as a negative or falling sealing characteristic).

3.3.2.2. Joint Diagram with Non-linear Deformation Characteristic Lines.

In the case of clamped parts with a non-linear characteristic, e.g., in the case of seals, the experimentally determined unloading characteristic line of the seal appears in the place of the deformation line VHP.

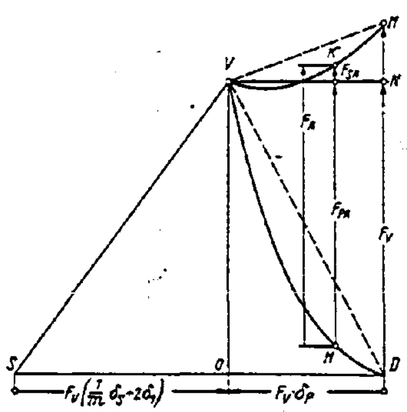

Figure 26: Joint diagram for a flange joint according to Figure 23 with clamped sealing and a non-linear characteristic.

When determining the appropriate curved line VKM in Figure 26, we must return to Equation (102). After initiation of deformations due to F_{SA} this reads for two flanges:

$$F_{SA}\left(\frac{1}{n}\,\delta_S + 2\,\delta_Z\right) = f_P - 2\,\delta_Z\,F_{PA} \qquad (110)$$

From this follows:

$$F_{SA} = \frac{f_P - 2\,\delta_Z\,F_{PA}}{2\,\delta_Z + \frac{1}{n}\,\delta_S} \qquad (111)$$

The two characteristic lines are determined point by point. For an accepted f_P, F_{PA} is taken from the seal characteristic line (example: $\overline{JH}$) and with it F_{SA} is calculated according to Equation (111) and plotted in the diagram (Point K).

4. Influencing Factors

Besides the function quantities (treated in Sec. 3), which essentially depend upon the design configuration of the building part and the bolted joint, there is an entire series of effects to be considered which are dependent either upon material and the surface design of the clamping parts and of the clamped areas, upon the shape designs of the selected bolts and nuts, or on the assembly conditions. The multiplicity of these effects will be treated in this section.

4.1. Strength Classes

Strength and elastic limit greatly influence the bolt dimensions. The strength classes have been standardized in DIN 267, p. [Blatt] 3, pub. 1967, and correspond to DIN/ISO 898. Decisive for the dimensioning is the elastic limit; it should not be exceeded by the nominal tension when tightening the bolt and under loading of the bolted joint in general. Only under special prerequisites, e.g., during angle controlled tightening (see Sec. 4.6.2.2.), may the elastic limit be exceeded. The rupturing elongation, the tenacity of the bolt head, the notch-impact toughness, and, to a lesser extent, the ratio of the elastic limit for the tensile strength are criteria for the toughness of the bolt material. Therefore, toughness in the case of bolts plays a significant role because the threads are notches and local deformations must be taken up for the prevention of breakage due to brittleness in these notches, despite anti-yielding measures, in order to be able to utilize the bolt fully.

High-duty bolts (beginning with quality class 8.8) can be manufactured to be lighter and generally less expensive, even if the external material dimensions cannot be reduced.

4.2. Minimum Engagement Depth; Strength of Bolt-Nut Combination

A bolted joint should be so arranged that the threads can take up the full strength of the bolt without destroying the interacting threading. In the case of overloading, the breakage should occur in the free threading or in the shaft. The appropriate strength arrangement of the bolt and nut is given, according to DIN 267, pp. [Blatt] 3 and 4 (in accordance with DIN/ISO 898), when the code for the strength class of the nut corresponds to the first code in the strength class of the bolt (example: Nut 10 for Bolt 10.9).

For blind hole bolts Table 16 gives the minimum engagement depth for several mechanical materials. Fine threads require greater engagement depths or greater strengths of the nut threading. They are more sensitive to damage and contamination. In the case of frequent tightening they are more inclined to binding; however, they have advantages with respect to security and can support somewhat greater loads, with the choice of the correct engagement depth, than the bolts with standard threads.

4.3. Bearing Stress on Bolt Head and Nut Surfaces

In the bearing surfaces between the bolt head or nut on one side and the clamped parts on the other, no bearing stresses which cause creepage processes due to either preload or to maximum force should be allowed. The bearing stress calculated from the maximum force should therefore not exceed the compressive yield point of the clamped material.

If the bearing head of the bolt or the nut is smaller than that of the clamped material, then greater bearing stress can conditionally be allowed. Experimentally determined bearing stress limits are given for several mechanical materials in Table 14. In the case that washers are used for the reduction of the bearing stress, sufficient strength and thickness must be considered.

4.4. Embedding

The assembly embedding amounts f_z occuring after assembly (see Sec. 3.2.2.), which cause the reduction of preload force, are smaller than the surface roughness of the clamped interfaces leads us to expect, since during the tightening process an extensive leveling is already taking place and even in the case of alternating working loads, the contact alterations in the interfaces remain relatively small. From this we can explain the results of measurements which show that the surface roughness of the interfaces in the case of the application of usual preparation methods has little effect on the degree of the embedding amount following assembly. On the contrary, the embedding amount decreases per interface with an increasing number of interfaces and increases with growing resilience of the clamped parts. Both phenomena are explained by the fact that embedding is a process comparable to relaxation: with a smaller number of interfaces the pressure decreases more quickly in the interfaces, and in the case of greater resilience more slowly.

If no embedding amounts are present which are determined in the prototype, the values given in Table 7 can be used as optimum values. These have been determined in massive joints with varying degrees of hardness of the clamped parts and differentiating degrees of surface roughness of the interface in which there was full area contact in the interfaces under applied preload. These optimum values are valid for the case that the values given in Table 14 for the contact pressure limit are not exceeded. Otherwise creepage of the clamped material in the bolt head and/or nut bearing surface appears and the embedding amounts can become uncontrollably larger.

According to Sec. 3.1.2.1., as opposed to clamped plate stacks, the resilience can be essentially greater than in the case of massive joints of equal clamping lengths so that experimental detemination of the embedding amounts is recommended in such cases.

4.5. Fatigue Strength

The fatigue strength of a bolted joint is dependent upon the following two main effects:

a) the dimension of the alternating axial force amount acting on the bolt which is dependent upon the design configuration of the joint. Design measures, which reduce this amount and thereby raise the endurance strength of the joint, are listed in Table 15 under 1.

b) the fatigue strength of the bolts in connection with the mated nut threads. Measures for the improvement of the endurance strength are contained in Table 15 under 2 to 5. For standardized bolts, like, for example, bolts according to DIN 931, DIN 933, DIN 912, the threading determines the fatigue strength. For such bolts, the values given in Table 13 can be inserted.

4.6. Tightening the Bolted Joints

The tightening procedure influences the required dimension of the bolt because, in addition to the axial force, torque must by taken up by the bolt. However, the effect which comes from the variability of the preload force in various tightening procedures is especially strong.

If, for example, the bolt dimension M10 is sufficient for a bolted joint with a determined loading, in the case that the bolt is tightened according to the procedure directed by the angle of rotation, then the dimension M18 would have to be selected in keeping with the same strength class of the bolt if the bolt is to be tightened automatically with a power wrench. The tightening procedure should therefore be carefully selected. Here the number of assembly pieces should be especially considered. We must take care that the tightening procedure established by calculation is used in assembly.

4.6.1. Bolt Stress in Tightening

During tightening the bolt is stressed by the preload force F_M in tension and by the torque M_{GA} acting in the threads additionally in torsion. Decisive for the calculation is the combined stress σ_{red}. From the laws of mechanics for inclined planes we can derive:

$$M_{GA} = F_M \frac{d_2}{2} \tan(\varphi + \rho') \qquad (112)$$

where

$$\tan\varphi = \frac{P}{\pi d_2}, \quad \tan\rho' = \mu'_G = \frac{\mu_G}{\cos\frac{\alpha}{2}}$$

In the case of threads with an angle of pressure $\alpha = 60°$, we get $\mu'_G = 1.155\ \mu_G$.

In the case of the normally small angles φ and ρ' we can write the following instead of Equation (112):

$$M_{GA} = F_M \frac{d_2}{2} \left(\frac{P}{\pi d_2} + 1.155\ \mu_G\right) \tag{113}$$

If d_0 is the diameter of the smallest core section A_0 of the bolt and W_P its resistance torque, then the stress ratio becomes:

$$\frac{\tau}{\sigma_M} = \frac{M_{GA}\ A_0}{W_P\ F_M} = \frac{2\ d_2}{d_0} \left(\frac{P}{\pi d_2} + 1.155\ \mu_G\right) \tag{114}$$

The beginning of the yielding of the threaded bolt and the retention of tension during tightening are influenced by the simultaneously acting tension and torsion stress.

With the combined tension:

$$\sigma_{red} = \sqrt{\sigma_M^2 + 3\ \tau^2} \tag{115}$$

there follows for the case that for this comparative tension σ_{red}, 90% of the minimum elastic limit $\sigma_{0.2}$ of the bolt is allowed:

$$\frac{\sigma_{red}}{\sigma_M} = \sqrt{1 + 3\left(\frac{\tau}{\sigma_M}\right)^2} = 0.9\ \frac{\sigma_{0.2}}{\sigma_M} \tag{116}$$

and

$$\sigma_M = \frac{0.9\ \sigma_{0.2}}{\sqrt{1 + 3\left[\frac{2\ d_2}{d_0}\left(\frac{P}{\pi\ d_2} + 1.155\ \mu_G\right)\right]^2}} \tag{117}$$

In the case of the reduced shank bolts with a reduced shank diameter d_T, which is smaller that the minor thread diameter d_3, the weakest cross section lies in the non-grooved shaft so that, for the calculation of the tension loads F_{sp}, the normal tension σ_M can be inserted with $d_0 = d_T$ according to Equation (117):

$$F_{sp} = \sigma_M\ A_T = \sigma_M\ \pi/4\ d_T^2\ . \tag{118}$$

The tension load value F_{sp} for reduced shank bolts in Tables 1 to 4 were calculated with $d_T = 0.9\ d_3$ in this way.

As soon as the reduced shank diameter becomes larger than the diameter $d_s = (d_2 + d_3)/2$ belonging to the tension cross section, then the weak point in steel bolts usually lies in the reduced shank so that yielding begins here. Since the thread of the bolt is a grooved part, a multiaxial stress develops in this area with stresses of different levels—σ_1, σ_2, σ_3—which cannont be readily calculated. Experiments have proved, however, that we can calculate the intended edge thread at the distance $d_s/2$ from the axis with the comparable tension σ_{red} according to Equation (115) and with the diameter d_s as a reference quantity for the determination of w_p.

Therefore, for full shank schrews and thin shank screws where $d > d_3$, σ_M becomes

$$\sigma_M = \frac{0.9\,\sigma_{0.2}}{\sqrt{1 + 3\left[\frac{4}{1 + d_3/d_2}\left(\frac{P}{\pi d_2} + 1.155\,\mu_G\right)\right]^2}} \qquad (119)$$

and the tension force:

$F_{sp} = \sigma_M\,A_s$.

Here the tension cross section A_S was based on the values standardized in DIN 13 P. [Blatt] 28 (pub. August 1975). They are based on the nominal values for the pitch diameter d_2 and core diameter d_3 and thus correspond to the maximum of the tolerance position h.

Also, for the calculation of the reduced shank cross section, the maximum core diameter where $d_T = 0.9 \cdot \bar{d_3}$ was inserted for the tolerance position h according to DIN 13 P [Blatt] 28.

The tension forces determined in this way were rounded off in Tables 1 to 4 so that the rounding error amounts to no more than 1%.

4.6.2. Scattering of the Initial Clamping Load in Tightening

By means of the tightening factor $\alpha_A = F_{M\,max} / F_{M\,min}$, the error of the preload force desired when tightening is considered in the dimensioning Equation (9) as opposed to the required minimum preload force.

This tightening factor is calculated as:

$$\alpha_A = \frac{1 + \Delta F_V / F_{Vm}}{1 - \Delta F_V / F_{Vm}} \qquad (121)$$

Here ΔF_V for the various tightening techniques is composed of single errors, which can be added according to the law of error propagation for random errors.

Table 17 gives optimal values for the tightening factor α_A for the various tightening procedures. Information concerning the particulars of the most common tightening procedures are contained in [6]. For the most important procedures, only such data will be given in the following which are necessary for the use of this guideline.

4.6.2.1. Torque-Controlled Tightening

Under torque-controlled tightening we understand generally tightening with indicating or signalling torque wrenches. In principle, however, powered tightening with automatic wrenches falls under this category since a compressed air wrench produces a measurable and adjustable torque.

The total tightening torque is a combination of the thread tightening torque and the head and nut friction torque:

$$M_A = M_{GA} + M_K \qquad (122)$$

$$M_A = F_M \left[\frac{d_2}{2} \tan(\varphi + \rho') + \frac{D_{Km}}{2} \tan \rho \right] \qquad (123)$$

Given the condition = 60°, this equation can be simplified as:

$$M_A = F_M \, [0.16\, P + \mu_G\, 0.58\, d_2 + \frac{D_{Km}}{2}/2\, \mu_K] \qquad (124)$$

The tension torques M_{sp} in Tables 1 to 4 are calculated with $M_{sp} = M_A$ and F_{sp} according to Equations (119) and (120).

Here the simplified assumption $\mu_G = \mu_K = \mu_{ges}$ has no longer been made—deviating from the first edition of the guideling VDI 2230 (pub. Dec. 1974), as well as from the older literature. More recent investigations with separate grasping by the bolt head and thread friction had shown that the grasping of the total friction condition by a ficticious friction coefficient μ_{ges} is too imprecise, especially when the friction coefficients μ_G and μ_K are very different, as can be the case for modern self-securing joint elements.

The free combination of all possible friction coefficients μ_G with all possible friction coefficients μ_K would lead, however, to exceedingly extensive tabulation for the tension torque M_{sp}. For the plotting of the Table 1 to 4 there has been therefore a simplification by which the tabulation remains limited to four tables. For this reason we must take into account a maximum error of about 10%, which is small, however, in relation to the expected estimated error for the friction coefficients μ_G and μ_K. The simplification is obtained from Figure 27.

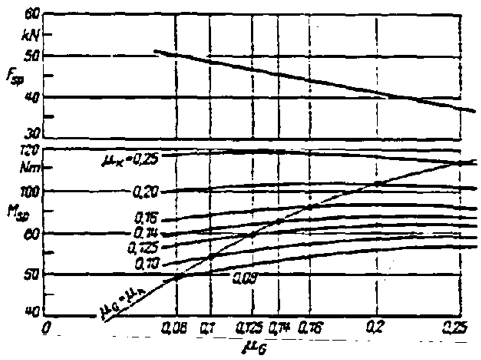

Figure 27: Tightening torque M_{sp} and clamping force F_{sp} (90% yield load) as a function of thread friction μ_G

If we plot the required tightening torques M_{sp} for the various bolt head friction coefficients μ_K above the thread coefficient μ_G for the tension forces F_{sp} determined by σ_{red} according to Equations (119) and (120), then the curves run approximately horizontal, i. e., the tightening torques M_{sp} are almost totally dependent upon the bolt head friction coefficient μ_K in the case of 90% elastic limit utilization due to σ_{red}.

The tightening torques M_{sp} given in Tables 1 to 4 are consequently calculated for a constant thread friction coefficient and particularly for μ_G = 0.125.

When using Tables 1 to 4 we should proceed as follows:

---Determination of the necessay bolt dimension and strength class for the calculated required tension force F_{sp} and for the thread friction coefficient μ_G according to Table 5 from the appropriate left part of Tables 1 to 4; followed by

---Location of the tightening torque M_{sp} which belongs with this bolt dimension and strength class, and specifically from that line of the right side of Tables 1 to 4 which corresponds to the bolt head friction coefficient μ_K estimated according to Table 5.

The calculation of M_{sp} in Tables 1 to 4 according to Equation (124) is based on the nominal size of the pitch diameter and friction radii $D_{Km}/2$ of the bolt head area corresponding to the head dimension of hexagonal recess bolts according to DIN 912 or Draft Standard DIN/ISO 4762 (pub. Dec. 1975) in accordance with those of hexagonal bolts according to Draft Standard DIN/ISO 4014 (pub. Dec. 1975) a bolt hole m according to DIN 69 (pub. Aug. 1971). The values in the Tables are rounded off in such a way that the rounding error is less than 2%.

An even more exact understanding of the different friction coefficients μ_G and μ_K, particularly in the case of very high thread friction coefficients, is possible if in Equation (124) we replace the term found in the brackets with $k \cdot d$ and also express P and d_2 like $D_{KM}/2$ as a function of d, and insert the mean values for the diameter group M4–M30 with the previously given basic dimensions.

Thus

for standard threads $K = 0.0222 + 0.528\ \mu_G + 0.668\ \mu_K$

for fine threads $K = 0.0151 + 0.545\ \mu_G + 0.668\ \mu_K$.

By this way we get the K values for any pairing of μ_G with μ_K according to Table 18 with which the tightening torque M_A for any initial preload F_M or also the tightening torque M_{sp} for the clamping force F_{sp} can be determined according to the Equations:

$$M_A = F_M \cdot K \cdot d \tag{125a}$$

$$M_{sp} = F_{sp} \cdot K \cdot d. \tag{125b}$$

In Equation (125b) the yield load F_{sp} for 90% elastic limit utilization taken from Tables 1 to 4 would have to be inserted.

Figure 28 shows the conditions in the case of tightening to the initial preload F_M with the consideration of the scattering of the friction coefficient μ_G and of the scattering of the applied tightening torque M_A. Additionally, F_M is plotted as dependent upon the thread torque M_{GA} for both values $\mu_{G\ max}$ and $\mu_{G\ min}$. Furthermore, lines of equal, reduced tension $\sigma_{red} = 0.9\ \sigma_{0.2}$ and $\sigma_{0.2}$ are included. The maximum initial preload $F_{M\ max}$ is present in Point X in the case of $M_{GA\ max}$ and $\mu_{G\ min}$; the least force $F_{M\ min}$ is present in Point Y in the case of $M_{GA\ min}$ and $\mu_{G\ max}$.

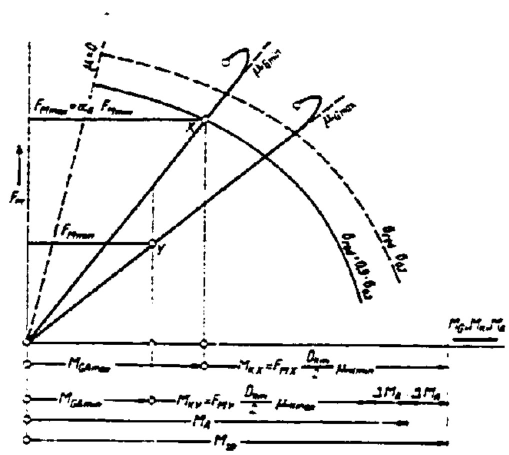

Figure 28: Tightening torque/preload diagram (with friction scattering and tightening torque scattering).

During assembly according to instruction, σ_{red} should not exceed the amount 0.9 $\sigma_{0.2}$ in the case of torque-controlled tightening.

In the case of torque-controlled tightening with a torque wrench, the total error is composed of the following partial errors:

---Error in the estimation of the friction coefficient; with the estimated friction coefficient the maximum tightening torque M_{sp} is determined from either Equation (123) or (124) or from the Tables.

---Scattering of the friction coefficient within a bolt of material lot including the tolerances which affect the friction radii.

---Imprecision of the tightening device including errors in use and reading.

The estimation error for the friction coefficient can be restricted if the designated torque on the original part is determined by elongation measurements on the bolt.

From the results of experimentation and experience up to the present, partial errors result for tightening with torque wrenches which when combined correspond to a tightening factor α_A in Table 17.

In the case of "torque-controlled" wrenches we must must differentiate between:

A) stationary wrenches which can be adjusted within a certain range by regulating the pressure,

B) wrenches with automatic clutches on which the clutch releases at a set torque,

C) precision wrenches with dynamic torque measuring, which is usually done over the wrench support.

All wrenches should be adjusted only in bolt experiments on the original part, whereby the adjustment of the wrenches like a) and b) can either be done via retightening torque or the exact lengthening measurement on the bolt.

The retightening torque is the torque which is specifically required to turn the bolt further after tightening is completed. It differs from the designated tightening torque for torque tightening by the retightening factor, which, according to the type of wrench and the friction and elasticity conditions, can vary between 0.85 and 1.32 [6].

The following partial errors arise:

Adjustment by Way of Retightening Torque

---Errors when estimating the friction coefficient for the determination of the designated tightening torque for torque tightening.

---Errors when estimating the retightening factor by which the tightening torque differs for the designated tightening torque.

---Tool and reading erros when measuring the retightening torque.

---Errors from faulty accuracy of mean value in the case of adjustment attempts: the greater the number of adjustment attempts, the smaller the errors.

Adjustment by Way of Elongation Measurement

---Errors from elongation measuring (tool errors, reading errors, dimension and Young's modulus variations of the bolt).

---Scattering of the preload force when adjusting powered wrenches.

The adjustment of the wrench as described in c) should also be done on the original part, whereby in a sufficient number of bolting experiments the given torque can be measured either in the wrench itself or by torque measuring devices placed on the wrench.

The most precise type of adjustment here is also the determination of the designated tightening torque by way of elongation measurement of the bolt. Less precise is the determination of the designated tightening torque by mutual clamping of piezoelectric ergostat units or even the estimation of the friction coefficient and tabular or mathematical determination of the designated tightening torque.

For determining the partial errors for bolts as described in c), the same is logically valid as previously stated for the tightening done with a torque wrench.

The empirical values available to date [6] allow the recommendation of optimum values for torque-controlled tightening with wrenches according to Table 17.

4.6.2.2. Elastic Limit-Controlled Tightening Procedures

Elastic limit-controlled tightening methods are based on the fact that when the elastic limit of the bolt material has been reached, the tightening torque no longer increases linearly with the angle of rotation, i.e., the $d M_A / d\vartheta \neq$ constant or $d^2 M_A / d\vartheta^2 = 0$. This principle is realized in the following way in the case of the prototypes of bolts developed currently:

An air-driven torque wrench with an electric control unit first tightens the joint to a "setting torque" in order to bring all interfaces firmly into contact. Beginning at this point, the appropriate differential quotient is computed and stored by way of an adjustable length of chord of the M_A,ϑ-curve, Figure 29. As soon as this differential quotient falls on a firmly set fraction of the maximum value $(\Delta M_A / \Delta\vartheta)_{max}$ when the elastic limit of the bolt material is reached, the wrench is disengaged by a quick release valve. In this way the desire preload in the case of assembly of a bolt and material lot is largely independent of the friction effects and influenced solely by the scattering of the elastic limit of the bolt material in a lot (upper and lower F_V-curve in Figure 29). The plastic elongations, which the bolts experience thereby, lie in the order of magnitude of the values with which the $\sigma_{0.2}$-limit for materials with the unspecified yield strength is defined (0.2%) so that the reusability of "elastic limit-controlled" tightened bolts is not practically impaired.

A tightening factor α_A is not needed for this procedure (see Sec. 2.1) since the bolts are dimensioned according to $F_{M\ min}$. For comparison of the precision with other procedures, $\alpha_A = 1$ is given in parentheses in Table 17.

<u>4.6.2.3. Tightening Procedures which Exceed the Elastic Limit (Angle-of-Rotation-Controlled)</u>

Angle-of-rotation control of the tightening procedure is also used today for power tightening in the practice of mass production. Control by way of the angle of rotation is indirectly control by elongation measurement. Since in the case of angle-of-rotation-controlled tightening, plastic deformations of the clamped parts are also measured, Figure 30, this process attains its greatest precision only when the joint is first clamped with a "setting torque" at an intermediate preload force F_{MT}, and from that is further clamped at a certain angle ϑ in the plastic area of the bolt, Figure 30. As in the case of elastic-limit-controlled tightening, a slight effect of friction is produced by the fact that the combined stress

$$\sigma_{red} = \sqrt{\sigma_M{}^2 + 3\tau^2}$$

exceeds the elastic limit in the case of lower preload force values if the thread torque, and therefore τ likewise, increases as a result of greater thread friction.

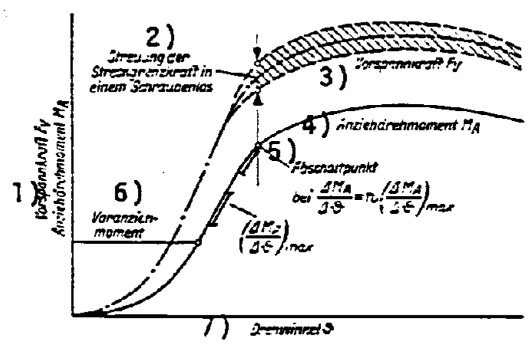

1. scattering of the elastic limit force in a bolt lot
2. preload F_v, tightening torque M_A
3. preload F_v
4. tightening torque M_A
5. disengagement point at ... [see equation]
6. pre-tightening moment
7. angle of rotation ϑ

Figure 29: Elastic-limit-controlled tightening (powered).

For normal friction coefficient scattering this effect is negligible. Since the elastic limit is always reached or surpassed, variations are produced in the specified initial preload F_M as in the case of elastic limit controlled tightening only from the tolerance of the elastic limit.

The essential difference between this and elastic-limit-controlled tightening consists in the fact that the greatest precision is specified only in the case that the elastic limit of the bolt material is exceeded and, due to this, greater plastic deformations of the bolt must be accepted. Due to this, the reusability of the bolts is restricted, and the process can only be used for bolts with sufficiently ductile material as well as with sufficiently large extension length (also with free thread lengths).

For the specification of a tightening factor α_A the same is valid as for elastic limit controlled tightening.

4.6.2.4. Impulse-Controlled Tightening (Impact Wrenches)

Impact wrenches transmit energy through impulse; therefore, a given torque is hardly measurable.

The adjustment of impact wrenches must be done, as in the case of torque wrenches, on the original bolting part. It is more precise by elongation measurement on the bolt, and less precise by tightening torque. The consideration of errors is logically the same as in the case of torque wrench types a) and b). From [6] as well as other empirical values, the tightening factors in Table 17 must applied. The tightening factors are so high that this tightening procedure cannot be recommended for high duty bolted joints.

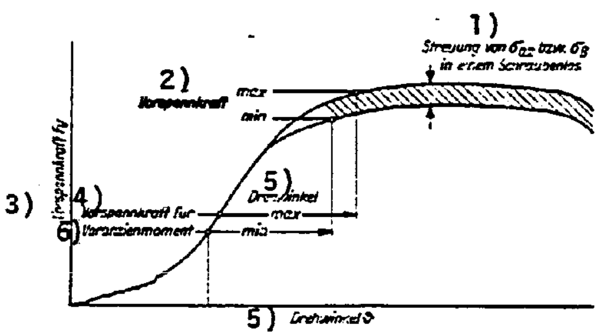

1. scattering of $\sigma_{0.2}$ or σ_B in a bolt lot
2. preload
3. preload F_V
4. preload for ...
5. angle of rotation
6. pre-tightening torque

Figure 30: Angle of rotation-controlled tightening (past yield).

5. Calculation Examples

5.1. Calculation of a Bolted Joint between Piston and Piston Rod in a Hydraulic Cylinder as an Example of Concentric Clamping and Concentric Loading

5.1.1. Basic Conditions

According to Figure 31, the bolted joint is calculated as a concentrically clamped and concentrically loaded joint. In the case of an internal pressure of 5.5 N/mm^2 and a pressure-bearing surface of 4536 mm^2, the axial force is produced at:

$F_A = 24.9 \cdot 10^3$ N.

The cylinder is part of a press with 300 working strokes per hour. The axial force is accordingly considered as a dynamic working load.

The residual clamping force should amount to at least $F_{KR} = 10^3$ N for security reasons because of the sealing function of the bolt in the case of unloading by the working load.

The piston material is C45V.

The joint should be tightened with a gauged torque wrench.

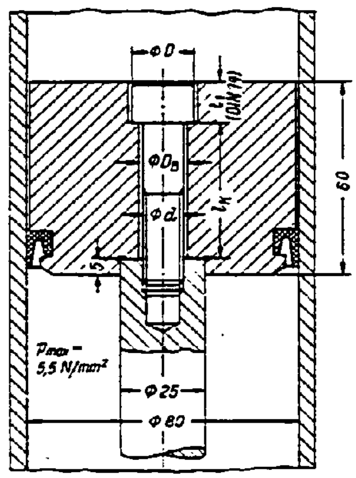

Figure 31: Hydraulic cylinder with central bolted joint between the the piston and piston rod.

5.1.2. Calculation Process

The joint is calculated following the calculation steps S 1 to S 2 given in Sec. 2.2.

S 1. Rough determination of the bolt diameter and of the clamping length ratio l_K / d, as well as the bearing stress under the bolt head.

With the aid of Table 6, we can assess a required preload of $63 \cdot 10^3$ N for a concentrically acting dynamic working load in the bolt of $F_A = 24.9 \cdot 10^3$. From the possible diameter/strength combinations, a bolt M 12 X 60 DIN 912 – 12.9 is chosen.

This amounts to the clamping length ratio

$l_K / d = 42 / 12 = 3.5$

(l_K = 55 mm – t_1).

The bearing stress under the bolt head is

$$p = \frac{F_{Sp} / 0.9}{A_p} = 741 \text{ N/mm}^2$$

(from Table 1 for $\mu_G = 0.125$: $F_{Sp} = 67,000$ N; (Equation (28)): $A_p = 100.5 \text{ mm}^2$).

The allowable bearing stress for C 45 V according to Table 14 amounts to:

$$p_G = 900 \text{ N/mm}^2$$

Thus:

$$p < p_G.$$

S 2. Determinatic.. of the tightening factor α_A.

The bolt should be tightened with a gauged torque wrench. From Table 17 follows: $\alpha_A = 1.6$.

S 3. Determination of the required minimum clamping force F_{Kerf}.

The required minimum clamping force must at least be equal to smallest residual preload intended for the problem ($F_{Kerf} = F_{KR}$). Thus it is:

$$F_{Kerf} = 10^3 \text{ N}.$$

S 4. Determination of the preload force loss F_Z as a result of embedding.

According to Table 7, a total embedding amount of $f_Z = 6\ \mu m$ is produced for three interfaces (incl. threads) and the clamping length ratio 3.5.

The rough determination of the force ratio according to Table 8 is: $\Phi_K = 0.24$.

The rough determination of the elastic resilience of the clamped parts according to Table 9 is:

$$\delta_P = 0.76 \cdot 10^{-3}\ \mu m / N.$$

The preload force loss therefore becomes (Equation (48)):

$$F_Z = f_Z \frac{\Phi_K}{\delta_P} = 1.9 \cdot 10^3 \text{ N.}$$

S 5. Determination of the force ratio Φ.

Corresponding to Figure 17b, we estimate that the load introduction levels lie at the distance $nI_K = 0.3\ I_K$. Thus:

$$\Phi = \Phi_n = 0.3\ \Phi_K = 0.072.$$

S 6. Determination of the required bolt size.

According to Equation (9):

$$F_{M\ max} = \alpha_A\ [F_{Kerf} + (1-\Phi)\ F_A + F_Z] = 41.6 \cdot 10^3 \text{ N.}$$

From Table 1 (full shank bolt) $\mu_G = 0.125$, a required bolt M10 DIN 912 - 12.9 with a tension force of $F_{sp} = 46 \cdot 10^3$ N is obtained for the condition $F_{sp} > F_{M\ max}$.

S 7. Precise determination of the clamping length ratio $I_K\ /\ d$ and control of Φ_K and δ_P.

With the dimensions of the new bolt this becomes:

$\Phi = 0.22$ from Table 8 for $I_K\ /\ d = 44/10 = 4.4$

$\delta_P = 1.0 \cdot 10^{-3}\ \mu m\ /\ N$ from Table 9

and therefore

$$F_Z = f_Z \frac{\Phi_K}{\delta_P} = 1.3 \cdot 10^3 \text{ N}$$

$$\Phi = \Phi_n = n\ \Phi_K = 0.3 \cdot 0.26 = 0.066$$

$$F_{M\ max} = \alpha_A\ [F_{Kerf} + (1-\Phi)\ F_A + F_Z] = 40.9 \cdot 10^3 \text{ N.}$$

Since $F_{sp} = 46 \cdot 10^3 \text{ N} > F_{M\ max}$, we select bolt M10 X 60 DIN 912 - 12.9.

The corresponding maximum tension torque amounts to the following: for $\mu_{K\ min} = 0.10$ according to Table 1, for $M_{sp} = 72$ Nm according to Table 5.

According to Equation (11) a tightening torque of

$M_A = 0.9\ M_{sp} = 65$ Nm

must be provided.

S 8. Test for compliance with the allowable bolt load.

According to Equation (13) there must be:

$\Phi\ F_A < 0.1\ \sigma_{0.2}\ A_s$.

This relation reads with number values:

$0.066 \cdot 24.9 \cdot 10^3$ N $< 0.1 \cdot 63 \cdot 10^3$ N

(see also Table 11).

The condition according to Equation (13) is fulfilled, i.e., the maximum bolt load is not surpassed.

S 9. Determination of the dynamic fatigue stress of the bolt.

It is

$$\sigma_a = + \frac{\sigma_{SA}}{2} = + \frac{\Phi_n\ F_A}{2\ A_S}\quad \sigma_A$$

$\sigma_A = \pm 55$ N/mm^2

(from Table 13 on the dotted auxiliary line plotted for torque-controlled tightening)

$A_S = 52.3$ mm^2

$$\sigma_a = \pm \frac{0.066 \cdot 24.9 \cdot 10^3}{2 \cdot 52.3} \text{ N/mm}^2 = 15.7 \text{ N/mm}^2 < \sigma_A$$

S 10. Calculation of the bearing stress under the head bearing area.

$$p = \frac{F_{sp}\ /\ 0.9}{A_p} \leq p_G$$

$A_p = 106$mm^2 (according to Equation (28))

$$p = \frac{46 \cdot 10^3\ /\ 0.9}{106} = 482 \text{ N/mm}^2$$

The allowable bearing stress for C 45 V according to Table 14 amounts to

$p_G = 900\ N/mm^2$.

With that it is

$p < p_G$.

5.2. Calculation of Bolts of a Positive-acting Clutch as an Example of Bolt Loading with Transverse Force

5.2.1. Basic Conditions

The joint on a disc clutch, Figure 32, is to be measured. The torque which securely transmits the coupling effect (in both directions of rotation) amounts to

$M_{t\ max} = 13 \cdot 10^3$ Nm.

Both clutch halves are composed of cast iron 20 and are connected with $i = 12$ hexagonal bolts according to DIN 931. As adhesive friction coefficient of the material combination cast iron/cast iron, we have accepted $\mu_o = 0.15$.

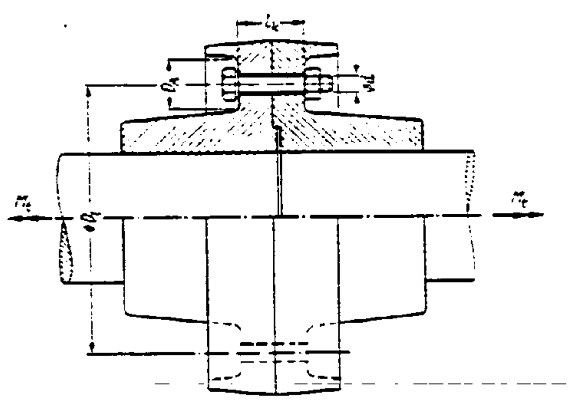

Figure 32: Bolted joint on a plate clutch.

The diameter of the bolted part amounts to

$D_t = 258$ mm.

Therefore we obtain a circumferential force per bolt of:

$$F_Q = \frac{2M_{t\ max}}{i \cdot D_t} = 8.4 \cdot 10^3 \text{ N}$$

and a clamping force of

$$F_{Kerf} = \frac{F_Q}{\mu_0} = 56 \cdot 10^3 \text{ N}$$

The clamping length (see Figure 32) amounts to $l_K = 60$ mm.

5.2.2. Calculation Process

S 1. Rough determination of the bolt diamete d with the aid of Table 6.

$F_Q = 8.4 \cdot 10^3$ N dynamic.

The bolts are tightened with a torque wrench.

Consequently we obtain by way of

A with 10,000 N as the next greater comparative force

B with four steps for dynamic transverse force F_Q

finally $F_{M\ min} = 63{,}000$ N

C with one step for tightening with a torque wrench

$F_{M\ max} = 100{,}000$ N

D according to this from Column 1 of Table 6 a bolt size M16

if we choose the strength class 10.9.

With the clamping length $l_K = 60$ mm the clamping ratio amounts to

$$\frac{l_K}{d} = \frac{60}{16.} = 3.75$$

A hexagonal bolt 16 X 80 DIN 931 – 10.9 is chosen with

d_K = 24 mm diameter

$D_B = d_2$ = 17 mm diameter

I_1 = 53 mm

I_2 = 7 mm.

Testing of the bearing stress under the bolt head:

$$p = \frac{F_{Sp} / 0.9}{A_P} \leq p_G;$$

$F_{Sp} = 105 \cdot 10^3$ N in the case of $\mu_G = 0.125$ from Table 1

$A_P = \pi / 4 \; d_K^2 - (D_B + 2 \cdot 0.5)^2 = 198 \text{ mm}^2$

(0.5 mm hole thread!)

$p = 590 \text{ N/mm}^2 < p_G = 750 \text{ N/mm}^2$ according to Table 14.

S 2. Determination of the tightening factor α.

From Table 17 we get the following for tightening with a torque wrench

$\alpha_A = 1.6$.

S 3. Determination of the required minimum clamping force F_{Kerf} for given friction contact joint for the taking up of a defined dynamic transverse force F_Q.

$F_{Kerf} = 56 \cdot 10^3$ N (see Sec. 5.2.1.).

S 4. Determination of the preload force loss due to embedding.

There are four interfaces including the threads.

$I_K / d = 3.75$

from Table 7:

$f_Z = 4 \cdot 1.25 = 5.0 \; \mu m$,

from Table 8 and Figure 32

with $D_A \approx 50$ mm diameter $\frac{D_A}{d_K} = \frac{50}{24} = 2.08 \approx 2$

this becomes $\Phi_K = 0.416$ (GG)

from Table 9

$\delta_P = 1.4 \cdot 10^{-3}\ \mu m/N$

$F_Z = f_Z \frac{\Phi_K}{\delta_P} = 1.48 \cdot 10^3$ N

S 5. [Is not necessary, since the working load appears here as a transverse force.]

S 6. Determination of the required bolt size.

The maximum initial preload force is determined with:

$F_{M\ max} = \alpha_A\ [F_{Kerf} + (1-\Phi_K)\ F_A + F_Z]$

Since $F_A = 0$, then

$F_{M\ max} = \alpha_A\ [F_{Kerf} + F_Z]$

$F_{M\ max} = 9.2 \cdot 10^3\ N < F_{sp} = 105 \cdot 10^3\ N.$

S 7. [Is not necessary.]

S 8. [Is not necessary.]

S 9. [Is not necessary.]

S 10. Proof is already rendered by S 1.

Thus the measuring task is completed.

The maximum tightening torque belonging with $F_{sp} = 105 \cdot 10^3$ N in the case of $\mu_G = 0.125$ according to Table 1 amounts to

$M_{sp} = 260$ Nm

for $\mu_{K\ min} = 0.10$ according to Table 5.

According to Equation (11) a tightening torque of

$M_A = 0.9 \cdot M_{sp} = 0.9 \cdot 260 = 234$ Nm

is to be applied.

5.3. Calculation of a Flywheel Fastening Using a Central Bolt as an Example of Bolt Loading with Torsion Shearing

5.3.1. Basic Conditions

The bolted joint should transmit securely a maximum torque of 110 Nm.

Taken strictly, the torque introduction occurs from the crank shaft to the flywheel in two ways:

—directly from the crank shaft to the flywheel,

—through the rotationally elastic hollow bolt and plate to the flywheel.

Since as a result of the rotational elasticity of the hollow bolt only a decreasingly small portion flows in the second way, the full torque is introduced in the first way for calculation for security reasons.

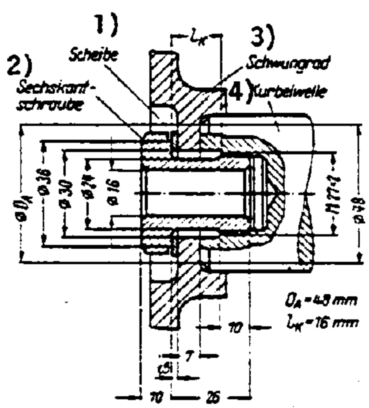

1. plate
2. hexagonal bolt
3. flywheel
4. crankshaft

Figure 33: Fly-wheel fastening by means of a central bolt.

As a result of the rotationally symmetrical form of the clamping and clamped parts, the fastening of a flywheel with a central bolt is an example of a concentrically clamped bolted joint. For design reasons the bolt must be designed as a hollow bolt.

5.3.2. Calculation Process

The designed joint is calculated on the basis of the Calculation Steps S 1 to S 10 given in Sec. 2.2.

S 1. Rough determination of the bolt diameter and of the clamping length ratio l_K / d.

For design reasons a hexagonal bolt with the thread M 27 X 2 of the strength class 8.8 was chosen (without regard to Table 6).

The clamping length ratio l_K / d amounts to (see Figure 33): 16/27 = 0.59.

Rough determination of the area surface pressure under the bolt head.

In this case it can drop out since the clamping force of the hollow bolt is relatively low, and therefore the contact pressure under the head probably lies within the dependable contact pressure value.

Precise calculation is produced in Step 10.

S 2. Determination of the tightening factor α_A.

The bolt should be tightened with a gauged torque wrench.

Tightening factor α_A = 1.6 according to Table 17.

R 3. Determination of the required minimum clamping force F_{Kerf}.

Known torque M_T = 110 Nm.

Mean effective friction radius

$$\frac{D_{Km}}{2} = \frac{1}{3}\ \frac{D_a^3 - D_i^3}{D_a^2 - D_i^2} = 19.7 \cdot 10^{-3} \mathrm{m}.$$

Friction coefficient in the interface μ_{Tr} is accepted at 0.125.

For the production of the friction contact this becomes:

$$F_{Kerf} = \frac{M_T}{\mu_{Tr}\ \frac{D_{Km}}{2.}} = 44.4 \cdot 10^3\ \mathrm{N}$$

S 4. Determination of the embedding amount f_Z.

For four interfaces (incl. the thread) an embedding amount of f_Z = 3 μm.

<u>§ 5.</u> Determination of the force ratio Φ.

Since this is the case of a hollow bolt, Tables 8 and 9 cannot be used for the determination of the elastic resilience of the clamping and clamped parts and of the force ratio Φ. The elastic resilience of the bolt is determined according to Equation (26) (see Sec. 3.1.1.)

$\delta_S = \delta_K + \delta_1 + \delta_G$.

With l_1 = 16 mm, A_1 = 252 mm^2 and $E = 21 \cdot 10^4$ N/mm^2 it becomes:

$$\delta_1 = \frac{l_1}{E\ A_1} = 0.30 \cdot 10^{-3}\ \mu\text{m/N}$$

The elastic resilience of the bolt head and of the screwed-in threads produces, under support of Equation (27) with

A_N = 371 mm^2, the following:

$\delta_K = \delta_G = 0.14 \cdot 10^{-3}\ \mu$m/N.

[Note: There was no correction of the factor 0.4 because the greater resilience of the head and the smaller resilience of the threads mutually cancel one another.]

Therefore the following is obtained:

$\delta_S = 0.58 \cdot 10^{-3}\ \mu$m/N.

The elastic resilience of the clamped parts is obtained from Equation (31) (see Sec. 3.1.2.1.) where

l_K = 16 mm and A_{ers} = 324 mm^2 according to Equation (29) as

$$\delta_P = \frac{l_K}{A_{ers}\ E_P} = 0.24 \cdot 10^{-3}\ \mu\text{m/N}.$$

When the load introduction is accepted under the bolt head or at the transfer of bolt shaft/thread, a force ratio is obtained according to Equation (53) as

$$\Phi = \Phi_K = \frac{\delta_P}{\delta_S + \delta_P} = 0.29$$

and therefore a preload force loss as a result of embedding of

$$F_Z = f_Z \frac{\Phi_K}{\delta_P} = 3.6 \cdot 10^3 \text{ N.}$$

S 6. Calculation of the design-established bolt measurements.

With Equation (9) (see Sec. 2.1.) and

$F_A = 0$ as well as $F_{Kerf} = 44.4 \cdot 10^3$ N then

$F_{M\ max} = \alpha_A\ [F_{Kerf} + (1-\Phi)\ F_A + F_Z] = 76.8 \cdot 10^3$ N.

Since Tables 1 to 4 are not applicable for the hollow bolt treated in this example, the dependable clamping force must be calculated. The following is produced by logical application of Equations (115) through (118) (see Sec. 4.6.1.):

$F_{Sp} = 133 \cdot 10^3$ N (> $F_{M\ max}$) in the case of $\mu_{G\ min} = 0.125$.

The bolt measurements are thus sufficient.

The required torque can be calculated with $\mu_{G\ min} = 0.125$ and $\mu_{K\ min} = 0.10$ (Table 5) according to Table 18 with $K = 0.15$:

$M_A = 485$ Nm.

S 7. [The control calculation for l_K / d and Φ_K can drop out.]

S 8. [Since the axial force is $F_A = 0$, the test for compliance with the allowable bolt force is not necessary.]

S 9. [Due to the lack of the axial force F_A, the determination of the dynamic fatigue stress also is not necessary.]

S 10. Calculation of the bearing stress.

The bearing stress between the bolt head and the hard washer amounts to:

with $A_p = 310\ mm^2$

$p_{max} = \frac{F_{sp}}{A_p} = 430\ N/mm^2.$

The allowable bearing stress according to Table 14 amounts to for steel 50

$p_G = 500\ N/mm^2 > p_{max}.$

5.4. Calculation of a Big-end Bearing Cover Joint as an Example of Eccentric Clamping and Eccentric Loading

5.4.1. Basic Conditions

The big-end bearing cover joint according to Figure 34 is for an automobile motor and is calculated as an eccentrically clamped and eccentrically loaded bolted joint. From a design standpoint, the bolts are of the strength class 12.9 with the thread measurements M 9 X 1 and the nuts of the strength class 12. The bolts are tightened with a precision torque wrench. C 45 was chosen as the material for the clamped parts. In the case of a nominal rpm-rate (n = 4000 rpm) the following basic quantities are produced:

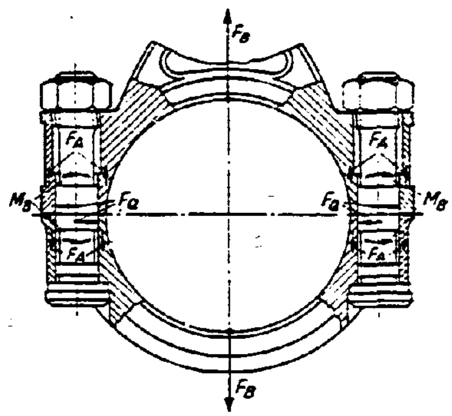

Figure 34: Action forces in the interface of a big-end bearing cover joint.

axial force in the interface:

$F_A = 3.7 \cdot 10^3$ N,

bending moment in the interface [Note: Determined according to [19]]:

$M_B = 30$ Nm,

transverse force in the interface [Note: Determined according to [19]].

$F_Q = 420$ N.

From the bending moment M_B and the axial force F_A, the lever arm of the eccentric load application can be determined as

$$a = \frac{M_B}{F_A} = 8.2 \text{ mm}$$

whereby it was accepted in a simplified fashion that the bending moment is constant over the clamping length ratio l_K.

5.4.2. Calculation Process

The calculation is produced according to the Steps S 1 to S 10 given in Sec. 2.2.

S 1. Rough determination of the bolt diameter d and of the clamping length ratio l_K / d.

The bolt diameter is given from the design plan with 9 mm, Figure 37. The clamping length ratio amounts to $lK / d = 41.5 / 9 = 4.6$.

Rough determination of the bearing stress under the bolt head.

$$p = \frac{F_{Mp} / 0.9}{A_p} \leq p_G$$

$F_{Mp} = 40 \cdot 10^3$ N in the case of $\mu_G = 0.125$ by interpolation from Table 3.

With $A_p = 65$ mm^2 this becomes

$$p = \frac{40 \cdot 10^3}{0.9 \cdot 65} = 682 \text{ N/mm}^2 < p_G = 900 \text{ N/mm}^2$$

Allowable bearing stress according to Table 14.

S 2. Determination of the tightening factor α_A.

The bolt is tightened with a precision torque wrench with adjustment of the bolt over the elongation measure of the bolt (according to previous calibration of the bolt as a force measuring instrument).

Tightening factor α_A =1.6 according to Table 17 (for large angles of rotation, fine threads, resilient joint).

S 3. Determination of the required minimum clamping force F_{Kerf}.

a) Friction contact requirement in the interface ($\mu_{Tr} = 0.125$)

$$F_{Kerf} = \frac{F_Q}{\mu_{Tr}} = 3.4 \cdot 10^3 \text{ N.}$$

b) In order to avoid one-sided lift-off during the nominal rpm of the motor, F_{Kerf} is calculated in accordance with Equation (78) (see Sec. 3.2.4.2.) with the measurements from Figure 35 as

$$F_{Kerf} = \frac{(a - s)\ u}{k_B^2 + su} F_A = 9.94 \cdot 10^3\ \mathrm{N}.$$

A

Abmessungen der Schraube in mm

E Stelle	l_i	d_i
1	2,5	9,7
2	3	9,2
3	6,5	9
4	10	9,2
5	15,8	8,35
6	8,5	

B

Gewindeabmessungen in mm

d_2	8,27
d_3	7,63
d	9
P	1
A_3	47,5 mm²

C Kennwerte der Trennfugenfläche:

$I_B = 2465\ \mathrm{mm}^4$

$A_B = 171\ \mathrm{mm}^2$

$k_B^2 = \frac{I_B}{A_B} = 14\ \mathrm{mm}^2$

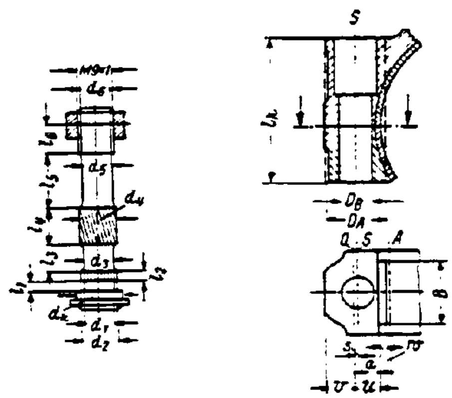

D

Abmessungen der verspannten Teile in mm

d_h	13
D_A	15,5
D_B	9,25
l_k	41,5
s	0,3
a	8,2
r	5,3
v	6,8
w	1,4
B	17,6

Figure 35: Dimensions of the clamping and clamped parts of the big-end bearing cover joint.

A dimensions of the bolt in mm
B thread dimensions in mm
C interface coefficients
D dimensions of clamped parts in mm
E location

S 4. Determination of the embedding amount f_Z of the elastic resilience of the clamping and the clamped parts and of the force ratio Φ. (see Sec. 3.1.1. and 3.1.2.)

Embedding amounts according to Table 7:

$f_Z = 5\ \mu\mathrm{m}$ for four interfaces (incl. threads).

Because of the fact that the bolt used is non-standard, the resiliencies of the clamped parts and the force ratio cannot be determined directly according to Tables 8 and 9, but rather are to be calculated individually.

Resilience of the bolt according to Equations (25), (26) and (27)

$\delta_S = 3.7 \cdot 10^{-3}\ \mu\mathrm{m/N}.$

Resilience of the clamped parts:

In the case of the determination of the resilience of the clamped parts, the slight eccentricity of the bolt (s = 0.3) is not considered, thus not δ_P^*, but rather δ_P is determined. The initial preload force which conditions the embedding acts concentrically.

With A_{ers} according to Equation (29) this becomes with Equation (31)

$\delta_P = 2.6 \cdot 10^{-3}$ $\mu m/N$.

Force ratio Φ according to Equation (53):

$$\Phi = \frac{\delta_P}{\delta_P + \delta_S} = 0.41.$$

With that the preload force loss as a result of embedding becomes

$$F_Z = f_Z \frac{\Phi_K}{\delta_P} = 0.79 \cdot 10^3 \text{ N}.$$

<u>S 5.</u> Determination of the force ratio Φ.

The transmission of bending moments and normal forces in the interface leads to a bolted joint with eccentric load application. Besides this, the load introduction does not take place under the bolt head and the nut but rather within the clamped parts. Since the largest part of the bolt pipe of the small-end hole can be considered as a clamping sleeve, n = 1/3 is estimated here.

Corresponding to Equation (68) this becomes with

s = 0.3 mm, a = 8.2 mm, A_D = 171 mm^2 and $A_{ers} \approx$ 75 mm^2:

$$\Phi_{en} = n \frac{\delta_P (1 + a/s \ \lambda^2)}{\delta_S + \delta_P (1 + \lambda^2)} = 0.15$$

<u>S 6.</u> Determination of the required bolt size.

According to Equation (9) (see Sec. 2.1.) the maximum initial preload amounts to

$$F_{M\,max} = \alpha_A \left[F_{Kerf} + (1 - \Phi_{en}) F_A + F_Z\right] = \alpha_A F_{M\,min}.$$

For the case of bearing cover bolting, $F_{M\ min}$ must still be increased at the amount F_L which is required for the elastic and plastic deformation of the bearing bushings in order to overcome the bearing excess.

For overcoming the bearing excess, an axial force of $6.2 \cdot 10^3$ N per bolt is necessary according to *Roemer* [20].

Thus valid for this case is:

$F_{M\ max} = \alpha_A\ [F_{Kerf} + (1 - \Phi_{en})\ F_A + F_Z + F_L]$

$= 1.6\ (9.94 + 3.15 + 0.79 + 6.2) \cdot 10^3$ N $= 32.1 \cdot 10^3$ N.

If we accept a friction coefficient $\mu_{G\ min} = 0.125$ according to Table 5, we obtain for the bolt M9 X 1 of the strength class 12.9 according to Equation (118) a tension force of

$F_{sp} = 45.1 \cdot 10^3\ N > F_{M\ max}$

and a tension moment according to Equation (124) where $\mu_{K\ min} = 0.125$ of $M_{sp} = 68$ Nm.

For the assembly, then, the mean tightening torque is obtained:

$M_A = 0.9 \cdot M_{sp}$

$M_A = 61$ Nm.

Thus the bolt is correctly dimensioned.

S 7. [The check for I_K / d can be eliminated since these values were already accurately determined.]

S 8. Test for compliance with the maximum allowable bolt force.

$\Phi_{en}\ F_A \leq 0.1\ \sigma_{0.2}\ A_T$

$0.15 \cdot 3.7 \cdot 10^3 < 0.1 \cdot 1062 \cdot 54.8$

$555 < 5800.$

S 9. Determination of the dynamic fatigue stress of the bolt.

The bolt is stressed due to eccentric clamping and loading by tension and bending.

According to Equation (100) (see Sec. 3.2.4.3.):

$$\sigma_{SAb} = \left[1 + \left(\frac{1}{\Phi_{en}} - \frac{s}{a}\right)\frac{I_K}{I_{ers}}\frac{E_S}{E_P}\frac{a\ \pi\ d_S^3}{8\ A_S\ k_S^2}\right]\frac{\Phi_{en}\ F_A}{A_S}$$

follows with the measurements from Figure 35 and

$\Phi_{en} = 0.15$, $I_K / I_{ers} = 1$, $A_S = 171\ mm^2$

$F_A = 3.7 \cdot 10^3\ N$, $E_S / E_P = 1$, $I_S = 2465\ mm^4$

and $k_S^2 = 14\ mm^2$

on the tension side:

$\sigma_{SAb} = (1 + 3.96)\ 12.1\ N/mm^2 = 12.1\ N/mm^2 + 47.9\ N/mm^2 = 60\ N/mm^2$.

With extention measuring markings which were placed on the bolt shaft in the vicinity of the interface, a tension variation was measured in the case of a minimum preload $F_{Verf} = 13.1 \cdot 10^3$ N after application of the axial force $F_A = 3.7 \cdot 10^3$ on the tension side as opposed to the preload of 52 N/mm^2, and on the pressure side there was a preload of −32 N/mm^2 measured. From this there is a tension clamping portion of 10 N/mm^2 produced (12.1 N/mm^2 was calculated), and a bending clamping portion of 42 N/mm^2 (47.9 N/mm^2 was calculated).

Figure 36 shows the comparison of calculated and measured tension distribution in the interface plane of the bolt.

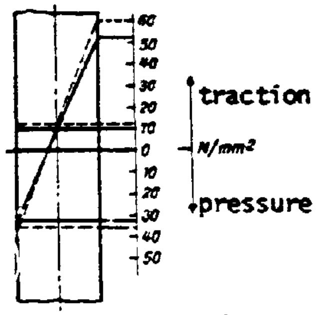

Figure 36: Tension distribution in the interface planes of the bolt.

The dynamic stress fatigue of the bolt on the tension side amounts to

$$\sigma_a = \frac{\sigma_{SAG}}{2} = \pm\ 30\ N/mm^2$$

From Table 13 we can obtain an endurance strength on the dotted auxiliary line plotted for torque controlled tightening of at least:

$\sigma_A = \pm\ 55\ N/mm^2$.

Therefore:

$\sigma_a < \sigma_A$.

S 10. Calculation of the contact pressure under head and nut.

$$p = \frac{F_{Mp}\ /\ 0.9}{A_p} = 772\ N/mm^2$$

$p < p_G = 900\ N/mm^2$ according to Table 14.

5.5. Calculation of a Cylinder Cover Bolting as an Example of Eccentric Clamping and Loading

5.5.1. Basic Conditions

The bolted joint between a cover and a hydraulic cylinder which is internally pressurized is to be dimensioned. The cylinder is constructed out of steel 50, the cover out of C 45 V. The greatest internal pressure amounts to

$p_{max} = 20\ N/mm^2$.

It can decrease in the course of functioning to

$p_{min} = 6\ N/mm^2$.

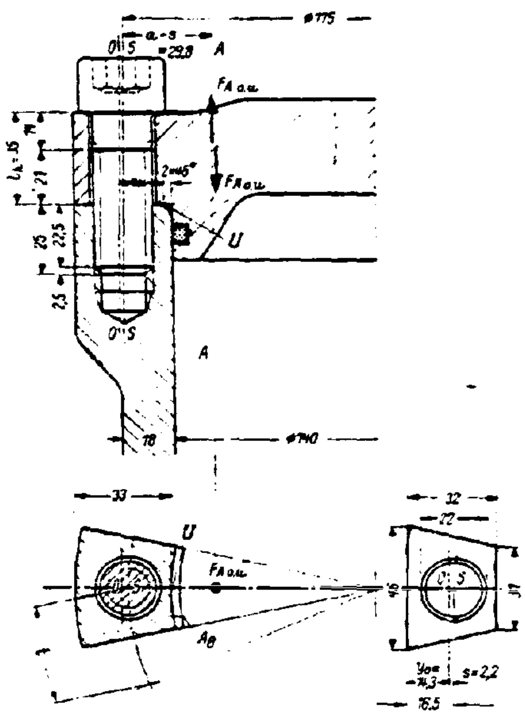

Figure 37: Bolt arrangement for the cylinder joint.

The following quantities are based on a primary design (see Figure 37):

Internal cylinder diameter $D_i = 140$ mm

External cylinder diameter in the area of the cover bolting $D_a = 210$ mm

Number of bolts $i = 15$.

In the case of maximum pressure, the residual clamping force per bolt amounts to at least

$F_{KR} = 3000$ N.

The bolts should be tightened with a gauged torque wrench.

With that we are able to calculate:

---external diameter of the clamped sleeves

$D_A = 1/2\ (D_a - D_i) = 35$ mm;

---the greatest axial pressure force in the cylinder

$F_{max} = \pi/4\ D_i^2\ p_{max} = 308 \cdot 10^3$ N;

---the smallest axial pressure force in the cylinder

$F_{min} = \pi/4\ D_i^2\ p_{min} = 92.4 \cdot 10^3$ N;

---working loads on a bolt

$$F_{B\ max} = F_{Ao} = \frac{F_{max}}{i} = 20.5 \cdot 10^3 \text{ N}$$

$$F_{B\ min} = F_{Au} = \frac{F_{min}}{i} = 6.16 \cdot 10^3 \text{ N}$$

5.5.2. Calculation Process

S 1. Rough determination of the bolt diameter d and the clamping length ratio l_K / d.

We are dealing with an eccentrically loaded bolted joint produced by the perimeter moment of the bending of the circular plate of the cover. The dimensioning of the bolts is selected under the assumption of a bending-resilient cover which is firmly clamped in the bolt plate (the system line of the end cylinder). The cover is a circular plate with constant plate thickness. Local contact resiliencies and the bending resilience of the cylinder in the since of the theory of circular cylinder bearings are neglected. Additionally, we can consider an eccentric clamping due to the differentiating situation of the axses of rotation of the collaborating pressure body and the bending body. Given these assumptions we are on the safe side when dimensioning the bolts.

The following bolt sizes are produced for $F_A = F_{AO}$ with the aid of Table 6 for dynamically and eccentrically loaded bolts in the direction of the axis and for tightening with a gauged torque wrench:

A with 25,000 N the next greatest bolt strength
F_A = 25000 N > 20,500 N,

B with two steps for a dynamic and eccentrically acting
working force $F_{M\ min}$ = 63,000,

C with one step for tightening with a torque wrench now
$F_{M\ max}$ = 100,000 N,

D with $F_{M\ max}$ = 100,000 N from column 1 a bolt
size of M20 DIN 912 - 8.8

where

d_K = 30 mm and

D_B = 22 mm according to DIN 69

d_a = 22.4 mm according to DIN 912.

Determination of the clamping length and the clamping length ratio:

I_1 = 21 mm

I_2 = 14 mm

$I_K = I_1 + I_2$ = 35 mm

$I_{K/d}$ = 1.75.

Calculation of the contact pressure under the bolt head:

$$p = \frac{F_{sp} / 0.9}{A_p} \leq p_G$$

$F_{sp} = 117 \cdot 10^3$ N in the case of $\mu_G = 0.125$ from Table 1

$A_p = \pi/4\ [d_K^2 - d_a^2] = 312.7\ mm^2$

$p = 415.7\ N/mm^2 < p_G = 900\ N/mm^2$ according to Table 14.

S 2. Determination of the tightening factor α_A.

$\alpha_A = 1.6$.

S 3. Determination of the required minimum clamping force.

The minimum clamping force is determined on the one hand by the required residual clamping force established in the problem:

$F_{Kerf1} = 3000$ N

and on the other hand by the clamping force which in the case of eccentric clamping and loading directly prevents one-sided lift-off in the interface, namely according to Equation (78)

$$F_{Kerf2} = \frac{(a - s)\ u}{k_B^2 + s \cdot u.} \cdot F_A$$

With the division

$$t = \frac{D_i + D_A}{i} \cdot \pi = 36.7\ mm$$

we obtain according to [18]

$$a - s = \frac{p_{max}\ D_i^2 \left[2 - \left(\frac{D_i}{D_A + D_i}\right)^2\right] t}{32 \cdot F_{AO}} = 29.8\ mm$$

In order to keep the amount of calculation effort as small as possible, the annulus sector is replaced by a plane-like suspension frame (see Figure 37).

With the measurements of this suspension frame we get:

$y_o = 14.3$ mm

$s = 16.5 - 14.3 = 2.2$ mm

$A_B = 852$ mm²

$I_B = 89.744 \cdot 10^3$ mm⁴

$k_B^2 = \frac{I_B}{A_B} = 105.33$ mm²

$a = (a - s) + s = 29.8 + 2.2 = 32$ mm

$u = 17.5 - 2 + 2.2 = 17.7$ mm

Therefore

$F_{Kerf2} = 75.8 \cdot 10^3$ N.

S 4. Determination of the preload force loss.

$F_Z = f_Z \frac{\Phi_K}{\delta_P}.$

According to Table 7, we obtain for three interfaces (including the threads) and a clamping length ratio $l_K / d = 1.75$

$F_Z = 4.5$ µm.

According to Table 8, Φ_K is determined as

$\Phi_K = 0.324$

(interpolated for $D_A / d_K = 1.167$)

and according to Table 9

$\delta_P = 0.437 \cdot 10^{-3}$ µm/N

(interpolated for the parameter $d = 20$ mm, $l_K / d = 1.75$ and $D_A / d_K = 1.167$).

Therefore $F_Z = 3.34 \cdot 10^3$ N.

S 5. Determination of the force ratio.

$$\Phi_{en} = n \frac{\delta_P (1 + a / s \lambda^2)}{\delta_S + \delta_P (1 + \lambda^2)}$$

with $n = 0.5$ and

$\delta_s = \delta_k + \delta_1 + \delta_2 + \delta_a = 0.83 \cdot 10^{-3}\ \mu m/N$

as well as

$\lambda = 0.14$ according to Equation (33), then

$\Phi_{en} = 0.22$.

S 6. Determination of the required bolt size.

First the maximum initial prelaod is determ ined as

$F_{M\ max} = \alpha_A\ [F_{Kerf} + (1 - \Phi_{en})\ F_{Ao} + F_Z] = 152 \cdot 10^3$ N.

According to Table 1 in the case of $\mu_G\ _{min} = 0.125$,

M 20 DIN 912 - 10.9

is selected as the proper bolt with $F_{sp} = 164 \cdot 10^3\ N > F_{M\ max}$.

Therefore the clamping moment for $\mu_{K\ min} = 0.10$ (Table 5) according to Table 1 becomes $M_{sp} = 600$ Nm, and the tightening torque becomes $M_A = 0.9 \cdot M_{sp} = 540$ Nm.

S 7. The exact determination of the clamping length ratio and the control of Φ_K and δ_P can be eliminated since the bolt size does not deviate from the one originally selected.

S 8. Test for compliance with the maximum allowable bolt strength.

According to the relation,

$\Phi_{en} \cdot F_{Ao} \leqq 0.1 \cdot \sigma_{0.2} \cdot A_s$

then

$0.22 \cdot 20.5 \cdot 10^3 < 0.1 \cdot 220 \cdot 10^3$

$4.51 \cdot 10^3 < 22 \cdot 10^3$.

This condition is fulfilled.

S 9. Determination of the dynamic fatigue stress of the bolt.

In the case of given eccentric loading with raised tension amplitude due to the effect of bending, the following must be calculated according to Equation (100):

$$\sigma_{SAb} = \left[1 + \left(\frac{1}{\Phi_{en}} - \frac{s}{a}\right)\frac{l_K}{l_{ers}}\frac{E_S}{E_P}\,8\,\frac{a\ \pi\ d_3^3}{A_D\ k_B^2}\right] \cdot$$

$$\cdot\ \Phi_{en}\ \frac{(F_{Ao} - F_{Au})}{A_3}.$$

Where

d_3 = 16.93 mm

A_3 = 225 mm^2

l_1 = 14 mm

l_2 = 21 mm and

l_{ers} = 36.42 mm from Equation (91) becomes

σ_{SAb} = 59.8 N/mm^2

σ_a = 0.5 $\cdot$ σ_{SAb} = 29.9 N/mm^2 < σ_A = 44 N/mm^2

according to Table 13 on the dotted line plotted for torque controlled tightening.

S 10. Calculation of the bearing stress under the bolt head.

$\sigma_{0.2} \cdot A_S = 220 \cdot 10^3$ N according to Table 11

$A_P = \pi/4\ [d_K^2 - (D_B + 2 \cdot 0.2)^2] = 312.6\ mm^2$

$p = 704\ N/mm^2 < p_G = 900\ N/mm^2$.

5.6. Calculation of a Flange Joint as an Example for Bolt Calculation in the Case of Non-directly Stacked Plates

Here we are calculating a pipe flange joint NW 200/ND 40, Figure 38, under the following conditions:

	Forces	Means of Pressure
a)	free of axial force	water
b)	with additional axial force	water
c)	free of axial force	steam (300° C)

Standard prewelded flanges of the pressure level ND 40 according to DIN 2635, which are being used here, have the following dimensions:

d_i = 200 mm

d_a = 375 mm

d_L = 30 mm

m = 12 holes

h_F = 34 mm

d_3 = 240 mm

k = 320 mm

In this case the calculations are performed to determine

---whether the stress can be taken up,

---whether the sought sealing property is suited,

---which bolt force is needed for assembly.

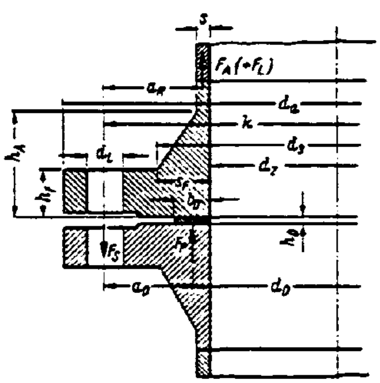

Figure 38: Dimensions on a pipe flange joint with flanges according to DIN 2635 (bolt removed!).

These calculations are not strictly schematically feasible according to the calculation steps in Sec. 2.2.

5.6.1. Basic Conditions

As a seal, It-material is considered in all three cases. With consideration of conditions c), a good quality is selected. The following are the dimensions (Figure 38):

h_D = 2 mm

b_D = 20 mm

and therefore

d_D = 220 mm and

a_D = 50 mm.

The sealing characteristics are obtained according to DIN 2505 for water as

$k_o\ K_D = 1.5\ b_D = 30$ kp/mm 300 N/mm;

for gases and steam at

$k_o \cdot K_D = 20\ \sqrt{b_D/h_D} = 63$ kp/mm $\approx$ 630 N/mm

as well as

$k_1 = b_D = 20$ mm for water or

$k_1 = 1.3\ b_D = 26$ mm for steam.

The decisive forces are obtained as

---working load $F_A = \dfrac{\pi d_D^2}{4} \cdot p = 152 \cdot 10^3$ N

---minimum sealing force $F_{D\ min} = \pi d_D\ k_1\ p\ S$

$F_{D\ min} = 83 \cdot 10^3$ N for water or

$F_{D\ min} = 108 \cdot 10^3$ N for steam

(in the case of a safety factor $S = 1.5$ according to DIN 2505).

---minimum initial compression force of the sealing property:

$F_{V\ min} = \pi d_D\ k_o\ K_D$

$F_{V\ min} = 207 \cdot 10^3$ N for water or

$F_{V\ min} = 435 \cdot 10^3$ N for steam.

The additional axial force is set with $F_L = 500 \cdot 10^3$ N; the tightening factor at $\alpha_A = 1.7$ (tightening with torque wrench [see Table 17]); the embedding amount $f_z = 0.1$ mm for water and $f_z = 0.2$ mm for steam (see also DIN 2505). The friction coefficient in the threads is $\mu_G = 0.14$.

The bolt dimensions are consistant through the normal flange with M 27. A reduced shank bolt is chosen according to Figure 39.

5.6.2. Determination of the Elastic Resiliencies

The elastic resiliencies of the participating elements are produced as follows:

For reduced shank bolts M 27 (Figure 39) with the dimensions

$d_K = 27$ mm

$d_T = 21$ mm

$l_1 = 5$ mm

$l_2 = 55$ mm

$l_3 = 10$ mm

the following cross sections are obtained

$$A_N = A_1 = \frac{k_k^2 \pi}{4} = 573 \text{ mm}^2$$

$$A_2 = \frac{d_T^2 \pi}{4} = 376 \text{ mm}^2$$

$A_S = 459$ mm^2 (tension cross section) and accordingly

$$\delta_S = \frac{1}{E}\left(\frac{l_1}{A_1} + \frac{l_2}{A_2} + \frac{l_3}{A_S} + \frac{2 \cdot 0.4\ d}{A_N}\right)$$

$\delta_S = 1.10 \cdot 10^{-6}$ mm/N for 20° C or

δ_S $1.10 \cdot \frac{2.1}{1.8} \cdot 10^{-6}$ mm/N $= 1.28 \cdot 10^{-6}$ mm/N for 300° C.

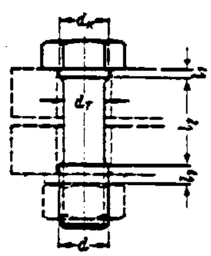

Figure 39: Dimensions of the reduced shank bolt for the pipe flange joint.

For the flange, the resistance moment with Equation (40) becomes

$$W = \frac{1}{12} (d_2 + s_F)\, s_F^2 + \frac{1}{12} (d_a - d_2 - 2\, d_L')\, h_F^2$$

$W = 19.6 \cdot 10^3$ mm^3;

the inverse resilience with Equation (38) and $h_A = 72$ mm (Figure 38) becomes

$$\gamma = \frac{d_a + d_2}{4\, \pi\, E\, h_A\, W} = 0.157 \cdot 10^{-9}\ 1/\text{Nmm}$$

and where $a_K = \frac{k - d_2 - s}{2} = 56.85$ mm, the resilience for 20° C becomes

$$\delta_1 = \gamma\, a_D^2 = 0.393 \cdot 10^{-6}\ \text{mm/N}$$

$$\delta_2 = \gamma\, a_D\, a_K = 0.447 \cdot 10^{-6}\ \text{mm/N}$$

$$\delta_3 = \gamma\, (a_K - a_D)\, a_D = 0.054 \cdot 10^{-6}\ \text{mm/N}$$

and for 300° C correspondingly

$$\delta_1 = 0.458 \cdot 10^{-6}\ \text{mm/N}$$

$$\delta_2 = 0.521 \cdot 10^{-6}\ \text{mm/N}$$

$$\delta_3 = 0.063 \cdot 10^{-6}\ \text{mm/N}.$$

The resilience of the seal is determined with Equation (31), whereby the elastic deformation (shortening) of the flange plates is neglected. Young's modulus of It-material is approximated in the area of interest as the secant modulus as

$E_D = 1300$ N/mm^2 for 20° C and

$E_D = 2200$ N/mm^2 for 300°.

The following equations are thus obtained:

$$\delta_P = \frac{h_D}{E_D \pi \; d_D \; b_D} = 0.111 \cdot 10^{-6} \text{ mm/N for } 20° \text{ C}$$

and

$$\delta_P = 0.111 \cdot 10^{-6} \cdot \frac{1.3}{2.2} = 0.066 \cdot 10^{-6} \text{ mm/N for } 300° \text{ C}$$

5.6.3. Determination of the Force Ratio and of the Force Loss due to Embedding

According to Equation (106) the following are determined for 20° C

$$\Phi_{P1} = \frac{\delta_P - 2\,\delta_3}{\delta_S/\varkappa + \delta_P + 2\,\delta_2 - 2\,\delta_3} = 0.003 \text{ and}$$

$$1 - \Phi_{P1} = 1 - 0.003 = 0.997$$

as well as for 300° C

$$\Phi_{P1} = -0.055 \text{ and } 1 - \Phi_{P1} = 1.055.$$

If, for operation at 20°, according to Equation (47), instead of $\delta_S + \delta_P$ in the demoninator we put in

$$\delta_S/\varkappa + 2\,\delta_1 + \delta_P = 0.989 \cdot 10^{-6} \text{ mm/N},$$

then we can determine the force loss due to embedding as

$$F_Z = \frac{f_Z}{\delta_S/\varkappa + 2\,\delta_1 + \delta_P} = \frac{0.1 \text{ mm}}{0.989 \cdot 10^{-6} \text{ mm/N}} = 101 \cdot 10^3 \text{ N}$$

Since the resiliencies change at 300°, the graphic determination is simpler (see Sec. 5.6.4., Conditions c).

5.6.4. Determination of the Maximum Bolt Preload

For the conditions a) the following is obtained according to Equation (9)

$$F_{M\,max} = \alpha_A\,[F_{D\,min} + (1 - \Phi_{P1})\,F_A + F_Z] = 570 \cdot 10^3 \text{ N}.$$

We arrive at the same result if we draw the joint diagram according to Figure 40. From Point P onward, the increase of the seal characteristic is plotted with $\delta_P = 0.111 \cdot 10^{-6}$ mm/N. Point H lies in the level of $F_{D\ min} = 83 \cdot 10^3$; vertically over it, in the distance $F_A = 152 \cdot 10^3$ N, lies Point K. For any force F_V' (Point V')—but here taken logically at $200 \cdot 10^3$—we calculate for complete unloading of the seal Point M' with $F_A' = F_V'/(1 - \Phi_{P1}) = 201 \cdot 10^3$ N. If we draw the parallels to Point V'M' through Point K then we get Point V of the diagram as a section with the seal characteristic. The rise of line SV is produced from the resiliencies of the clamping parts $\delta_m/m + 2\ \delta_1$ $= 0.878 \cdot 10^{-6}$ mm/M, and thus Point S.

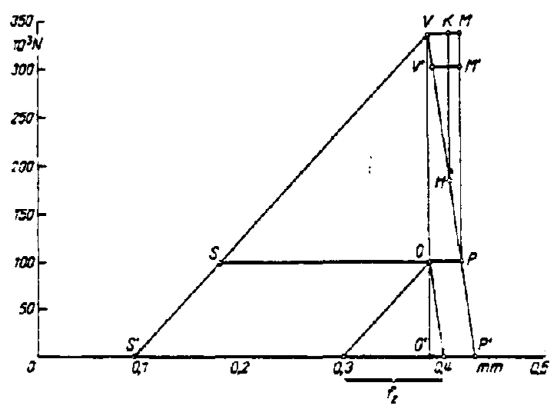

Figure 40: Joint diagram for conditions a).

For consideration of the embedding amount parallels are drawn through Point O to SV and PV which include the line $f_z = 0.1$ mm on the new base line S'V' of the clamping diagram. With this we can read the minimum preload $F_{M\ min} \approx 335 \cdot 10^3$ N (Line O'V'). From this follows, as calculated

$$F_{M\ max} = \alpha_A\ F_{M\ min} = 1.7 \cdot 335 \cdot 10^3 = 570 \cdot 10^3 \text{ N (as above).}$$

In the case of twelve bolts, each bolt is loaded with $570 \cdot 10^3/12 = 48 \cdot 10^3$ N.
According to Table 2 we get a clamping force of $F_{sp} = 159 \cdot 10^3$ for a reduced shank bolt M 27 – 8.8. The bolt size is therefore sufficient.

For the conditions b) the following is produced

$F_{M\ max} = \alpha_A\ [F_{D\ min} + (1 - \Phi_{P1})\ (F_A + F_L) + F_Z]$

$= 1.7 \cdot 10^3\ [83 + 0.997\ (152 + 500) + 101]$ N

$F_{M\ max} = 1418 \cdot 10^3$ N.

If we plot the joint diagram in the same way as for conditions a), Figure 41, we reach the same result. The load per bolt at $1418 \cdot 10^3/12 = 118 \cdot 10^3$ N lies beneath the dependable limit of $143 \cdot 10^3$ N for the quality 8.8.

The calculation of the value $F_{M\ max}$ in the case of conditions c) is made difficult due to the various resiliencies for 20° C and 300° C so that a graphic determination is simpler. The joint diagram, Figure 42, is designed with the resiliencies for 300° C in the same way as Figures 40 and 41 to Point S'. Corresponding to the higher embedding amount as a result of the creepage of the seal, Point S' lies rather far to the left of S (Note: Depending upon seal condition, there can be even essentially higher embedding amounts, e.g., 0.5 mm.) If we put in lines through S' and P' with rises corresponding to the resiliencies for 20° C, then we get Point V" from which the minimum preload $F_{V\ min} = 470 \cdot 10^3$ N is produced. In operation it falls to $440 \cdot 10^3$ N (Point K) and climbs in the cold state (pressureless) again to the value $F_{V\ min} = 470 \cdot 10^3$ N (Point V"). In the case of each additional loading the bolt strength alternates between Points K and V", thus with an amplitude of $30 \cdot 10^3/2 = 15 \cdot 10^3$ N/mm². The maximum loading per bolt is produced at $1.7 \cdot 470 \cdot 10^3/12 = 67 \cdot 10^3$ N.

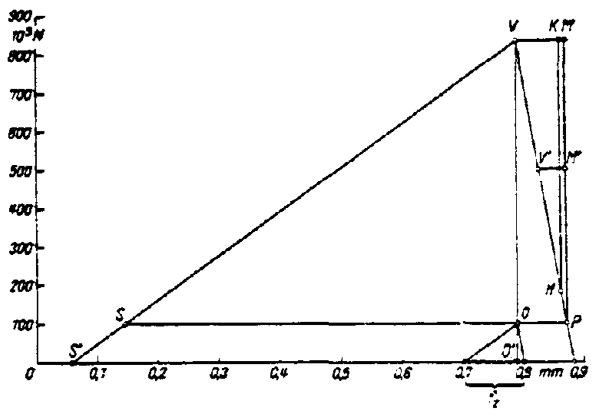

Figure 41: Joint diagram for the conditions b.

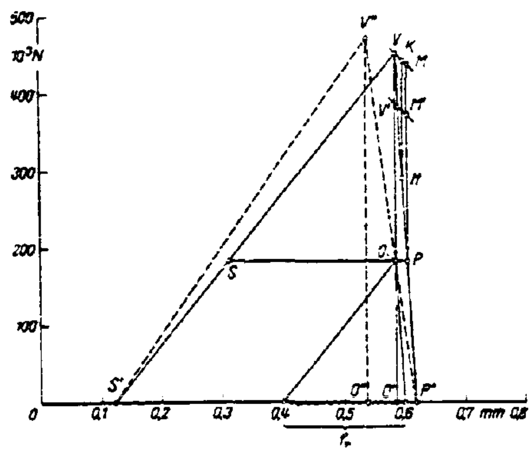

Figure 42: Joint diagram for the conditions c.

5.6.5. Fatigue Strength Testing

While under the conditions a) and b) the oscillation range (the difference of the forces at Points K and V in the Figures calculated as

$F_{SA} = \Phi_{F1}\ F_A$ or $F_{SA} = \Phi_{F1}\ (F_A + F_L)$

at 460 N or 1960 N) is slight, and the fatigue strength is not considered, this range is higher in the case of conditions c) with 30 · 10^3. The amplitude of the nominal tension is obtained as

$\sigma_a = F_{SA}/2 \cdot A_Y = 30 \cdot 10^3/2 \cdot 12 \cdot 347 = 3.6\ N/mm^2$.

Generally even this will cause no difficulties as long as no additional forces occur. The bending tension of the bolts connected with the tilt of the flange is nevertheless hardly noticable in the oscillation amplitude since the tilt hardly changes with the pressure.

5.6.6. Calculation of the Seal Characteristic

The force $F_{V\ min} = 207 \cdot 10^3$ N (a and b) or $F_{V\ min} = 435 \cdot 10^3$ N necessary for the deformation of the seal is produced in all cases by the minimum preload forces.

Additionally, the strength of the flanges must be checked since these would cause stronger embedding due to plastic deformation in the case of overloading. This occurs with the help of the relation

$\sigma_b = M/W' \approx F_{M\ max}\ a_D/(2\ \pi\ 1.5\ H) =$

$= F_{M\ max} \cdot 0.27 \cdot 10^3\ N/mm^2$.

The greatest value is obtained for the conditions b) as

$\sigma_b = 1418 \cdot 10^3\ N \cdot 0.27 \cdot 10^{-3}\ 1/mm^2 = 383\ N/mm^2$

so that a flange material with an elastic limit of 1.5 · 383 N/mm^2 = 574 N/mm^2 is necessary.

References

[1] *Junker, G.* and *D. Blume*: New Methods for a Systematic Calculation of Bolted Joints (German) Düsseldorf: Triltsch-Verlag, 1965.

[2] *Illgner, K.-H.*: Design of Bolted Joints for Dynamic Stress. (German) Masch.-Markt 70 (1964) No. 78.

[3] *Boenick, U*: Investigations of Bolted Joints. (German) Doctoral Dissertation, TU Berlin 1966.

[4] *Weber, H.*: Static and Dynamic Investigations of Eccentrically Loaded Joints. (German) Doctoral Dissertation, Berlin 1966.

[5] *Wiegang, H., K.-H. Illgner* and *K. H. Beelich*: Concerning the Reduction of the Preload in Bolted Joints due to Embedding Procedures. (German) Werkst. u. Betr. 98 (1965) pp. 823-27.

[6] *Junker, G.*: Mass Examination Concerning Tightening in Bolted Joints with Motorized Wrenches. (German) Beilage Draht-Welt 56 (1970) Heft 3.

[7] *Junker, G.*: Contact Pressure under Bolt Heads. (German) Masch.-Markt (1961) No. 38, pp. 29-39.

[8] *Birger, J. A.*: The Shortening of Bolted Plates or Flanges. (Russian) Russian Engng. J. (1961) No. 5, pp. 35-38. Summary in: Konstruktion 15 (1963) No. 4.

[9] *Fritsche, G.*: Principles of a More Accurate Calculation of Statically and Dynamically Loaded Bolted Joints. (German) Doctoral Dissertation, TU Berlin 1962.

[10] *Rydschenko, V. M.* and *V. A. Tkachenko*: The Maximum Bolt Force in a Prestressed Joint. (Russian) Russian Engng. J. (1962) No. 8, pp. 11-13. Summary in: Konstruktion 15 (1963) No. 11, p. 466.

[11] *Vitkup, E. B.*: The Deformation of Bolted Plates. (Russian) Russian Engng. J. (1961) No. 5, pp. 39-40. Summary in: Konstruktion 15 (1963) No. 4, p. 161.

[12] *Weiss, H.* and *F. Wallner*: The High-strength Structural Steel Bolt under Tension Loading. (German) Stahlbau-Rundschau (1963) No. 24, pp. 15-22.

[13] *Fernlund, J.*: Pressure Distribution Between the Sealing Faces of Bolted Flanges. (German) Konstruktion 22 (1970) Heft 6, pp. 218 ff.

[14] *Agatonovic, P.*: Behavior of Bolted Joints under Combined Working Loads. (German) Doctoral Dissertation, TU Berlin 1973.

[15] *Dreger, H.*: Simplified Calculation of Preloaded Bolts. (German) Konstruktion (1965) Heft 8, pp. 320-25.

[16] *Dreger, H.*: Embedding Amounts and their Consideration in the Case of Simplified Calculation of Preloaded Bolts. (German) Konstruktion (1955) Heft 5, pp. 209-12.

[17] *Benz, W.*: High-strength Bolts and Bolted Joints in the Construction of Motors. (German) Konstruktion (1955) Heft 5, pp. 175-84.

[18] Beyer, Statics in Construction with Reinforced Concrete. (German) Berlin/Heidelberg: Springer-Verlag 1956, pp. 654-55.

[19] *Lang, O. R.*: Transmissions in High-speed Internal Combustion Engines. (German) Konstruktionsbücher No. 22, Berlin/Heidelberg: Springer-Verlag 1966.

[20] The Calcula* on of the Force Fit of Plain Bearing Races. (German) MTZ 22 (1921) Heft 2 and 4.

[21] *Junker, G.*: Friction, Disturbance Factor in the Case of Bolt Assembly. (German) Verbindungstechnik 6 (1974) Heft 11.

[22] *Dreger, H.:* Determination of the Basic Quantities for the Calculation of High-duty Bolted Joints According to the Guideline VDI 2230. (German) Drahtwelt 62 (1976) Heft 7, pp. 291-94.

[23] *Dreger, H.:* Commentaries for VDI-Guideline 2230 and for the Determination of the Basic Quantities for the Calculation of High-duty Bolted Joints. (German) Drahtwelt 62 (1976) Hefts 8, 9, 10, pp. 331-36; 391-95; 433-35.

[24] *Dreger, H.:* Statics of Multi-bolted Joints. (German) VDI-Bericht 220. Düsseldorf: VDI-Verlag 1974, pp. 55-67.

CALCULATION TABLES

(Translator's Note: The following pages represent keys to the tables found in this guideline and should be used with them. All commas between numerals are to be read as decimals points, e.g., 14,56 = 14.56.)

Table 1: Clamping Forces F_{sp} and Tightening Torque M_{sp} for Full Shank Bolts

with Standard Metric Thread According to DIN 13, p. 13.

Column 1 = Diameter

" 2 = Class

" 3 = Clamping forces F_{sp} in N for μ_G

" 4 = Tightening torque M_{sp} in Nm for μ_K

Table 2: Clamping Forces F_{sp} and Tightening Torque M_{sp} for Reduced Shank

Bolts with Standard Metric Thread According to DIN 13, p. 13.

Column 1 = Diameter

" 2 = Class

" 3 = Clamping forces F_{sp} in N for μ_G

" 4 = Tightening torque M_{sp} in Nm for μ_K

Table 3: Clamping Forces F_{sp} and Tightening Torque for Full Shank Bolts with

Fine Metric Thread According to DIN 13, p. 13.

Column 1 = Diameter

" 2 = Class

" 3 = Clamping forces F_{sp} in N for μ_G

" 4 = Tightening torque M_{sp} in Nm for μ_K

Table 4: Clamping Forces F_{sp} and Tightening Torque M_{sp} for Reduced Shank

Bolts with Fine Metric Thread According to DIN 13, p. 13.

Column 1 = Diameter

" 2 = Class

" 3 = Clamping forces F_{sp} in N for μ_G

" 4 = Tightening torque M_{sp} in Nm for μ_K

<u>Table 5</u>: Friction Coefficients for Various Surface and Lubricant Conditions.*

[Main column I]

Surface I -- a) μ_K: bolt head or nut

b) μ_G: bolt thread

[Minor columns 1-3]

Steel, darkened or zinc phosphated

Column 1 = pressed, rolled

" 2 = turned, cut

" 3 = ground

[Minor columns 4-5]

Column 4 = Steel, cadmium-plated 6 μm

" 5 = " , zinc-plated 6 μm

[Words running vertically in left margin]

leicht geölt = lightly oiled

trocken = dry

mit Kleber = [illegible] adhesi[illegible]

[Major column II]

Surface II -- toward material

toward nut thread

[Levels in descending order]

Level 1 = Steel, rolled

planed, milled, turned, cut

ground

Level 2 = Gray cast iron, planed, milled, turned, cut

Black malleable cast iron, ground

Level 3 = Steel, cadmium-plated 6 μm

" " internal thread

zinc-plated 6 μm

" " internal thread

(ground, rolled), phosphated

(machined), phosphated

Level 4 = Al-Mg alloys

Level 5 = Steel, cadmium-plated 6 μm

" " internal thread

zinc-plated 6 μm

" " internal thread

Level 6 = Steel, gray cast iron, black malleable case iron

cut

---

* The friction coefficient $\mu_{K\ min}$ for the determination of the appropriate clamping moment M_{sp} ($M_A \approx 0.9\ M_{sp}$) and the friction coefficient $\mu_{G\ min}$ for the determination of the clamping force F_{sp} can be found in Tables 1 to 4 (or $\mu_{ges\ min}$ if $\mu = \mu_K$).

** for synthetic lubricants and micro-encapsulated adhesives

Table 6: Estimation of the Diameter Range of Bolts.

[Boxed chart in upper left]

Column 1 = Force in N

Columns 2-4 = Nominal diameter in mm

Strength class

[Directly below boxed chart]

Example:

A joint is dynamically and eccentrically loaded by the axial force F_A = 8500 N. The bolt with the strength class 12.9 should be installed with a torque wrench.

A 10,000 N is the next-greatest force to F_A in column 1.

B Two steps for an "eccentric and dynamic axial force" lead to $F_{M\ min}$ = 25,000 N.

C One step for "tightening with a torque wrench" leads to $F_{M\ max}$ = 40,000

D For $F_{M\ max}$ = 40,000 N we find in column 2 (Strength class 12.9): M 10.

[Top right]

A From column 1 choose the next-greatest force to the working load F_A being applied on the joint.

B The required minimum preload $F_{M\ min}$ is produced by proceeding further from this number at:

Four steps for static or dynamic transverse force

or

Two steps for dynamically and eccentrically acting axial force

or

One step for dynamically and concentrically or statically and eccentrically acting working load

or

No steps for statically and concentrically acting force

C The required <u>maximum preload</u> $F_{M\ max}$ is produced by proceeding from the force $F_{M\ min}$ at:

Two steps for tightening the bolt with a simple wrench which is set over the tightening torque--or

One step for tightening with a torque wrench or precision wrench which is set and determined by means of dynamic torque measuring or length measuring--or

No steps for tightening over angle control into the elastic area or by means of elastic limit-controlled tightening directed by computer.

D The required bolt dimension in mm for the selected strength class is in columns 1 to 4 next to the number located.

<u>Table 7</u>: Optimum Values for the Embedding Amount per Interface for Temporally Alternating Working Loads. (For restrictions see Sec. 4.4.).

The thread counts as an interface!

[Top left]

Number of interfaces (including thread)

[Top right]

Embedding amount in μm for the clamping length l_K/d =

Table 8: Force Ratio Φ_K.

[Top left]

Full shank bolts

[Top right]

Reduced shank bolts

[Vertical in left margin]

Force ratio Φ

[Vertical in chart]

M12 with l_K = 42 mm (see Example 5.1, S 4)

[Vertical under chart]

Al-Lg = Aluminum alloy

GG = Gray cast iron

Stahl = Steel

Werkstoff der verspannten Teile = Material of clamped parts

[Centered under chart]

Clamping length ratio l_K/d [arrow]

Presented function derived from Equations 25, 27, 29, 30, 31, 53:

$$\log\left(\frac{1}{\Phi_K} - 1\right) + \log\frac{E_S}{E_P} - \underbrace{\log\ 1.8}_{\text{(only for reduced shank bolts)}} =$$

$$\log\left\{\left[1.2 + \frac{C}{2}\left(0.31\frac{l_K}{d} + \frac{l_K^2}{100}\right)\right]\left(1 + 1.25\frac{d}{l_K}\right)\right\}$$

with $C = \left(\frac{D_A}{d_K} - 1\right)$ and the mean values in the dimension area M4 to M30

(standard thread) by d_{Km} = 1.56 d; D_{Bm} = 1.11 d; d_{2m} = 0.19 d; d_{3m} = 0.83 d; and 1.0 free thread length.

Table 9: Resilience of Clamped Parts.

[Vertical in left margin]

Resilience δ_P in 10^{-3} $\mu m/N$.

[Diagonal in chart]

Thread diameter d = 30 mm

(s.Beispiel 5.1 R4) = (see Example 5.1. S 4)

[Vertical in right margin]

Clamping ratio l_K / d

[Vertical below chart]

Al-Lg = Aluminum alloy

GG = Gray cast iron

Stahl = Steel

[Horizontal below chart]

Sleeve ⟶ Plate

Presented functions derived from Equations 29, 30, 31:

$$\log \delta_P = -(\log d + \log E_P + \log y) \text{ with}$$

$$y = \frac{\pi}{4}\left(1.2 \frac{d}{l_K} + C \frac{0.31}{2} + C \frac{l_K}{200\ d}\right) \text{ and } C = \frac{(D_A - 1)}{d_K}$$

and from mean values in the dimension area M4 to M30 by d_{Km} = 1.56 d and D_{Bm} = 1.11 d.

Table 10: Length Ratio for the Interface of the Eccentric, Clamped and Non-loaded Joint.

<u>Table 11</u>: Pitch, Tension Cross Section, Core Cross Section and Forces $F_{0.2}$ for Full Shank Bolts with Standard and Fine Metric Thread According to DIN 13, p. 13.

Column 1 = Diameter

" 2 = Pitch p mm

" 3 = Stress area A_s mm^2

" 4 = Core cross section A_3 mm^2

Columns 5-7 = Force at the minimum elastic limit $F_{0.2} = \sigma_{0.2}\ A_s$ with strength class according to DIN/ISO 898.

Metrisches Regelgewinde = Standard metric thread

" Feingewinde = Fine " "

<u>Table 12</u>: Pitch, Reduced Shank Cross Section, Core Cross Section and Forces $F_{0.2}$ for Reduced Shank Bolts with Standard and Fine Metric Thread According to DIN 13, p. 13.

Column 1 = Diameter

" 2 = Pitch p mm

" 3 = Reduced shank diameter d_T h 13 $(0.9 \cdot d_3)$ mm

" 4 = Reduced shank cross section $A_{T\ min} = A_s$ mm^2

Columns 5-7 = Force of the minimum elastic limit $F_{0.2} = \sigma_{0.2}\ A_s$ with strength class according to DIN/ISO 898.

Metrisches Regelgewinde = Standard metric thread

" Feingewinde = Fine " "

<u>Table 13</u>: Optimum Values for the Fatigue Strength of Annealed Bolts of the Strength Classes 8.8, 10.9, 12.9 (Haigh Diagram).

[Vertical margin]

Fatigue strength $\pm \sigma_A$

[Horizontal below chart]

Relative mean tension $\frac{\sigma_m}{\sigma_{0.2}}$ 100

[In chart referring to dotted line on right]

Preload in the case of elastic limit or angle of rotation-controlled tightening procedures.

[In chart referring to dotted line on left]

Upper limit of preload for torque-controlled tightening

[On diagonal lines in descending order]

M4 to M8; M10 to M16; M18 to M30

[In box in lower left corner]

For rolled bolts we can calculate with appox. doubled values.

<u>Table 14</u>: Allowable Bearing Stress p_G in N/mm² for Compressed Parts of Various Materials.

Werkstoff	= Material
Anziehen	= Tightening (procedure)
motorisch/von Hand	= motorized/by hand
GG 25	= gray cast iron 25

<u>Table 15</u>: Factors which Influence the Fatigue Strength in the Positive Sense.

<u>1. Clamping Ratio</u>.

1.1. Expanding the lengthening and bending elasticity by:

reduced shank bolts,

long bolts,

high strength bolts,

through-bolts with nuts,

attaching a sleeve,

reducing Young's modulus.

1.2. Reinforcement of the clamped parts by:

design measures,

using materials with great elasticity as well as by separating bearing and sealing functions.

1.3. Avoiding bending by:

reducing the eccentricity,

raising the preload.

1.4 Maintaining the residual clamping force by:

avoiding embedding,

avoiding conditions which cause unbolting.

<u>2. Bolting Conditions</u>.

2.1. Equal distribution of tension by:

bolt material with low elasticity,

suited nut types,

suited thread profiles,

pitch differential between bolt and nut threads,

high preload,

elastic thread liner.

2.2. Thread tolerances

(sufficient play in thread).

3. Fatigue Strength of the Bolt.

3.1. Shape influences at the head and shaft caused by:

increasing the head tensile,

large radii,

threading in the bolt hole.

3.2. Shape influences in the thread caused by:

large radii,

heel thread,

soft end thread.

4. Materials and Production.

4.1. Materials:

great durability,

high strength,

avoiding de- and recarburization as well as scaling ,

uninterrupted thread flow.

4.2. Surface improvement by:

strain-hardening,

burnishing and polishing,

applying internal pressure,

avoiding electropolishing.

5. Chemical Surface Conditions.

5.1. Avoiding corrosion.

(However, unfavorable influence due to galvanized protective layers).

Table 16: Recommended Minimum Engagement Depths for Blind-hole Thread.

Schraubenfestigkeitsklasse = bolt strength class

Gewindefeinheit d/P = fineness of thread d/P

GG-22 = gray cast iron 22

Table 17: Optimum Values for the Tightening Factor α_A.

Anziehfaktor α_A = tightening factor α_A

Anziehverfahren = tightening procedures

Bemerkungen = comments

(1) Elastic limit-controlled tightening (powered).

(1) Angle of rotation-controlled tightening (powered or manual).

[Comments] The preload scattering is overwhelmingly determined by the scattering of the elastic limit in a given bolt lot. The bolts here are dimensioned for $F_{M\ min}$. The tightening factor α_A therefore drops out for these tightening methods. The values in the parentheses serve to compare the tightening precision with the following procedures.

1.2 Tightening with length measurements of the suited bolts.

[Comments] Complicated procedure; only applicable in very restricted cases.

1.4 to 1.6 Torque-controlled tightening with a torque wrench or a precision wrench with dynamic torque measuring. Experimental determination of the specified tightening torque on the original joint part, e.g., by lengthening measurement of the bolt.

[Specific comments for these methods]

Lower values for:

---great number of adjustment or checking attempts (e.g. 20).

---slight scattering of the given moment.

---electronic torque limitation during assembly in the case of precision wrenches.

1.6 to 1.8 Torque-controlled tightening with a torque wrench or a precision wrench with dynamic torque measuring.
Determination of the specified tightening torque by estimation of the friction coefficient (surface and lubricant conditions).

[Specific comments for these methods]

Lower values for:

---precise torque wrench (e.g., with a meter).

---uniform tightening.

---precision wrench.

Higher values for:

---torque wrenches with signal device or which bend.

1.7 to 2.5 Torque-controlled tightening with wrench.
Adjustment of the wrench with tightening torque which is formed from the specified tighening torque (for estimated friction coefficient) and from an extra allowance.

[Specific comments for this method]

Lower values for:

---great number of checking attempts (tightening torque).

---wrenches with disengagement devices.

2.5 to 4 Impulse-controlled tightening with impact wrenches.
Adjustment of the wrench over the tightening torque--as above.

[Specific comments on this method]

Lower values for:

---great number of adjustment attempts (tightening torque).

---on the horizontal branch of the wrench characteristic.

---impulse transmission which is free from play.

[General comments for all methods from 1.4 to 4]

Lower values for:

---slight angle of rotation, i.e., relatively stiff joint.

---relatively soft opposing plane.

---opposing planes which are not prone to binding, e.g., phosphated.

Higher values for:

---high angle of rotation, i.e., relatively resilient joints as well as fine thread.

---great hardness of opposing plane connected with a rough surface.

---deviations in shape.

Table 18: K Factors for the Quick Calculation of the Tightening Torque for μ_G and μ_K.

[Dircetly above numbers in chart]

Head friction coefficient μ_K.

[Vertical in left margin]

Thread friction coefficient μ_G.

[At bottom of chart]

Maximum tightening torque $M_{A\ max} = K \cdot F_M \cdot d$ in Nm.

[Below chart]

F_M in N is the desired preload if 90% utilization of the elastic limit is predicted. Insert F_{sp} from Tables 1 to 4.

d in m is the nominal diameter of the bolt.

R = standard thread, F = fine thread.

Tafel 1. Spannkräfte F_{sp} und Spannmomente M_{sp} für Schaftschrauben mit metrischem Regelgewinde nach DIN 13, Bl.13

Abm.	Klasse	Spannkräfte F_{sp} in N für μ_G =							Spannmomente M_{sp} in Nm für μ_K =						
		0,08	0,10	0,125	0,15	0,16	0,20	0,25	0,08	0,10	0,125	0,14	0,16	0,20	0,25
M 4	8.8	4400	4250	[illegible]	3900	3750	3450	3100	2,4	2,6	2,9	3,1	3,3	3,8	4,4
	10.9	6200	5900	5700	5500	5300	4850	4350	3,4	3,7	4,1	4,4	4,6	5,3	6,2
	12.9	7400	7100	6800	6600	6300	5800	5200	4,1	4,4	4,9	5,2	5,6	6,4	7,4
M 5	8.8	7200	6900	6600	6400	6100	5600	5100	4,8	5,3	5,9	6,2	6,7	7,6	8,7
	10.9	10100	9700	9300	9000	8600	7900	7100	6,7	7,5	8,3	8,7	9,4	10,7	12,2
	12.9	12100	11700	11100	10800	10300	9500	8600	8,1	8,9	10,0	10,5	11,3	13,0	14,5
M 6	8.8	10100	9700	9300	9000	8600	7900	7100	8,1	8,9	9,9	10,5	11,2	13,0	14,5
	10.9	14200	13700	13000	12700	12100	11200	10000	11,4	12,5	14,0	15,0	16,0	18,0	20,5
	12.9	17000	16400	15700	15200	14600	13400	12100	13,5	15,0	16,5	17,5	19,0	21,5	25,0
M 8	8.8	18600	17900	17000	16500	15900	14600	13100	19	21	24	25	27	31	36
	10.9	26000	25000	24000	23200	22300	20500	18500	28	30	34	36	38	44	50
	12.9	31500	30000	29000	28000	27000	24600	22200	33	36	40	43	46	52	60
M 10	8.8	29500	28500	27000	26500	25500	23200	20900	39	42	47	50	53	61	70
	10.9	41500	40000	38000	37000	35500	32500	29500	55	60	66	70	75	85	98
	12.9	50000	48000	46000	44500	42500	39000	35500	65	72	79	84	90	103	118
M 12	8.8	43000	41500	39500	38500	37000	34000	30500	67	74	82	86	93	105	121
	10.9	61000	58000	56000	54000	52000	47500	43000	95	104	115	121	130	150	170
	12.9	73000	70000	67000	65000	62000	57000	52000	114	124	140	145	155	180	205
M 14	8.8	59000	57000	54000	53000	50000	46500	42000	107	117	130	135	145	165	190
	10.9	83000	80000	76000	74000	71000	65000	59000	150	165	180	195	205	235	270
	12.9	99000	96000	91000	89000	85000	78000	71000	180	195	220	230	250	280	320
M 16	8.8	81000	78000	75000	73000	70000	64000	58000	165	180	200	215	230	260	300
	10.9	114000	110000	105000	102000	98000	90000	82000	235	260	280	300	320	370	420
	12.9	137000	132000	126000	123000	118000	108000	98000	280	310	340	360	390	440	510
M 18	8.8	98000	95000	91000	88000	84000	78000	70000	230	250	280	290	310	360	410
	10.9	138000	134000	127000	124000	119000	109000	98000	320	350	390	410	440	500	580
	12.9	166000	160000	153000	148000	142000	131000	118000	390	420	470	490	530	600	690
M 20	8.8	127000	122000	117000	113000	109000	100000	90000	320	350	390	410	440	510	580
	10.9	178000	172000	164000	160000	153000	141000	127000	450	500	550	580	630	710	820
	12.9	214000	207000	197000	192000	184000	169000	153000	550	600	660	700	750	850	980
M 22	8.8	158000	153000	146000	142000	136000	125000	113000	440	480	530	560	600	690	790
	10.9	222000	215000	205000	199000	191000	176000	159000	620	680	750	790	850	970	1110
	12.9	265000	260000	246000	239000	230000	211000	191000	740	810	900	950	1020	1160	1350
M 24	8.8	183000	176000	168000	164000	157000	145000	130000	560	610	670	710	770	870	1000
	10.9	255000	248000	237000	230000	221000	203000	183000	780	860	950	1000	1080	1220	1400
	12.9	310000	300000	285000	275000	265000	244000	220000	940	1030	1140	1200	1300	1450	1700
M 27	8.8	239000	232000	221000	215000	206000	190000	172000	820	890	990	1050	1130	1300	1450
	10.9	335000	325000	310000	300000	290000	265000	241000	1150	1250	1400	1450	1600	1800	2050
	12.9	405000	390000	375000	365000	350000	320000	290000	1400	1500	1650	1750	1900	2150	2500
M 30	8.8	290000	280000	270000	260000	250000	231000	209000	1110	1210	1350	1400	1550	1750	2000
	10.9	410000	395000	380000	370000	355000	325000	295000	1550	1700	1900	2000	2150	2450	2800
	12.9	490000	475000	455000	440000	425000	390000	350000	1850	2050	2250	2400	2600	2950	3400

Tafel 2. Spannkräfte F_{sp} und Spannmomente M_{sp} für Taillenschrauben mit metrischem Regelgewinde nach DIN 13, Bl. 13

Abm.	Klasse	Spannkräfte F_{sp} in N für μ_G =							Spannmomente M_{sp} in Nm für μ_K =						
		0,08	0,10	0,125	0,14	0,16	0,20	0,25	0,08	0,10	0,125	0,14	0,16	0,20	0,25
M 4	8.8	3050	2950	2800	2700	2600	2350	2100	1,65	1,8	2,0	2,15	2,3	2,6	3,0
	10.9	4300	4150	3900	3800	3650	3300	2950	2,35	2,6	2,8	3,0	3,2	3,7	4,2
	12.9	5200	4950	4700	4550	4350	4000	3550	2,8	3,1	3,4	3,6	3,9	4,4	5,1
M 5	8.8	5100	4900	4650	4500	4300	3950	3550	3,4	3,7	4,1	4,4	4,7	5,4	6,2
	10.9	7200	6900	6500	6300	6100	5500	4950	4,8	5,2	5,8	6,2	6,6	7,6	8,7
	12.9	8600	8300	7800	7600	7300	6700	6000	5,7	6,2	6,9	7,4	7,9	9,1	10,5
M 6	8.8	7200	6900	6600	6400	6100	5600	5000	5,8	6,3	7,0	7,4	8,0	9,1	10,4
	10.9	10100	9700	9200	9000	8600	7800	7000	8,2	8,9	9,8	10,4	11,2	13,0	14,5
	12.9	12200	11700	11100	10700	10300	9400	8400	9,8	10,6	11,8	12,5	13,5	15,5	17,5
M 8	8.8	13200	12700	12100	11700	11200	10200	9200	14,0	15,5	17,0	18,0	19,5	22,0	25,0
	10.9	18600	17900	17000	16400	15700	14400	12900	19,5	21,5	24,0	25,0	27,0	31,0	36,0
	12.9	22300	21500	20400	19700	18900	17300	15500	23,5	26,0	29,0	30,0	33,0	37,0	43,0
M 10	8.8	21000	20200	19200	18600	17800	16300	14600	27	30	33	35	38	43	49
	10.9	29500	28500	27000	26000	25000	22900	20600	39	42	47	50	53	60	70
	12.9	35500	34000	32500	31500	30000	27500	24700	46	51	56	60	64	73	84
M 12	8.8	31500	30000	28500	28000	26500	24400	21900	49	53	59	63	67	76	88
	10.9	44000	42500	40500	39000	37500	34500	31000	69	75	83	88	95	108	124
	12.9	53000	51000	48500	47000	45000	41000	37000	83	90	100	106	114	130	150
M 14	8.8	44000	42000	40000	39000	37000	34000	30500	79	87	96	101	109	124	140
	10.9	62000	59000	56000	55000	52000	48000	43000	111	122	135	145	155	175	200
	12.9	74000	71000	68000	66000	63000	58000	52000	135	145	160	170	185	210	240
M 16	8.8	58000	56000	53000	51000	49000	45000	40500	117	130	140	150	160	185	210
	10.9	81000	78000	74000	72000	69000	63000	57000	165	180	200	210	230	260	300
	12.9	98000	94000	89000	87000	83000	76000	68000	200	215	240	250	270	310	360
M 18	8.8	73000	70000	66000	64000	62000	56000	51000	165	185	205	215	230	260	300
	10.9	102000	98000	93000	91000	87000	79000	71000	235	260	280	300	320	370	420
	12.9	123000	118000	112000	109000	104000	95000	86000	280	310	340	360	390	440	510
M 20	8.8	91000	87000	83000	80000	77000	70000	63000	230	250	280	290	320	360	410
	10.9	127000	123000	117000	113000	108000	99000	89000	320	350	390	410	440	500	580
	12.9	153000	147000	140000	136000	130000	119000	107000	390	420	470	500	530	600	700
M 22	8.8	117000	113000	107000	104000	100000	92000	82000	320	350	390	420	450	510	580
	10.9	165000	159000	151000	147000	140000	129000	116000	450	500	550	580	630	710	820
	12.9	198000	191000	181000	176000	168000	154000	139000	550	600	660	700	750	860	990
M 24	8.8	138000	133000	127000	123000	118000	108000	97000	420	460	510	540	580	650	750
	10.9	194000	187000	178000	172000	165000	152000	136000	590	640	710	750	810	920	1060
	12.9	233000	224000	213000	207000	198000	182000	163000	710	770	860	910	970	1100	1250
M 27	8.8	179000	172000	164000	159000	153000	140000	126000	610	660	730	780	840	950	1090
	10.9	250000	243000	231000	224000	215000	197000	177000	850	930	1030	1090	1170	1350	1550
	12.9	300000	290000	275000	270000	255000	236000	212000	1020	1120	1240	1300	1400	1600	1850
M 30	8.8	214000	206000	196000	190000	182000	167000	150000	810	880	980	1040	1110	1250	1450
	10.9	300000	290000	275000	265000	255000	235000	210000	1140	1240	1400	1450	1550	1800	2050
	12.9	360000	345000	330000	320000	305000	280000	255000	1350	1500	1650	1750	1900	2150	2450

Tafel 3. Spannkräfte F_{sp} und Spannmomente M_{sp} für Schaftschrauben mit metrischem Feingewinde nach DIN 13, Bl. 13

Abm.	Klasse	Spannkräfte F_{sp} in N für μ_G = 0,08	0,10	0,125	0,14	0,16	0,20	0,25	Spannmomente M_{sp} in Nm für μ_K = 0,08	0,10	0,125	0,14	0,16	0,20	0,25
M8x1	8.8	20300	19600	18700	18200	17400	16100	14500	21	23	26	27	29	33	39
	10.9	28500	27500	26500	25500	24500	22500	20500	30	33	36	38	41	47	54
	12.9	34000	33000	31500	30500	29500	27000	24500	36	39	44	46	50	57	65
M10x1,25	8.8	31500	30500	29000	28500	27000	25000	22600	41	45	50	53	57	65	74
	10.9	44500	43000	41000	40000	38500	35000	32000	58	63	70	74	80	91	105
	12.9	53000	52000	49500	48000	46000	42500	38000	69	76	84	89	96	109	125
M12x1,25	8.8	48000	46500	44500	43500	41500	38500	34500	73	81	89	95	102	116	135
	10.9	68000	66000	63000	61000	59000	54000	48500	103	113	125	130	145	165	190
	12.9	81000	79000	75000	73000	70000	65000	58000	124	135	150	160	170	195	225
M12x1,5	8.8	45500	44000	42000	41000	39000	36000	32500	70	77	85	91	97	111	130
	10.9	64000	62000	59000	57000	55000	51000	45500	99	108	120	125	135	155	180
	12.9	77000	74000	71000	69000	66000	61000	55000	119	130	145	155	165	185	215
M14x1,5	8.8	65000	63000	60000	59000	56000	52000	47000	116	125	140	150	160	185	210
	10.9	92000	89000	85000	83000	79000	73000	66000	165	180	200	210	225	260	300
	12.9	110000	107000	102000	99000	95000	88000	79000	195	215	240	250	270	310	360
M16x1,5	8.8	88000	85000	81000	79000	76000	70000	63000	175	195	215	230	245	280	320
	10.9	124000	120000	115000	111000	107000	99000	89000	250	270	300	320	340	390	450
	12.9	148000	144000	137000	134000	128000	118000	107000	300	330	360	380	410	470	540
M18x1,5	8.8	114000	111000	106000	103000	99000	92000	83000	260	280	310	330	360	410	470
	10.9	161000	156000	149000	145000	140000	129000	116000	360	390	440	460	500	570	660
	12.9	193000	187000	179000	174000	157000	154000	139000	430	470	530	560	600	680	790
M20x1,5	8.8	145000	140000	134000	131000	126000	116000	105000	360	390	430	460	500	570	650
	10.9	203000	197000	189000	184000	177000	163000	147000	500	550	610	650	700	800	920
	12.9	244000	237000	227000	220000	212000	196000	177000	600	660	730	780	840	950	1100
M22x1,5	8.8	178000	172000	165000	161000	155000	143000	129000	480	530	590	620	670	760	880
	10.9	250000	242000	232000	226000	217000	201000	181000	670	740	820	870	940	1070	1240
	12.9	300000	290000	280000	270000	260000	241000	218000	810	890	990	1050	1130	1300	1500
M24x2	8.8	203000	197000	188000	183000	176000	162000	146000	600	660	730	780	830	950	1100
	10.9	285000	275000	265000	255000	247000	228000	206000	850	930	1030	1090	1170	1350	1550
	12.9	340000	330000	315000	310000	295000	275000	247000	1020	1110	1240	1300	1400	1600	1850
M27x2	8.8	265000	255000	245000	238000	229000	211000	191000	870	960	1070	1130	1220	1400	1600
	10.9	370000	360000	345000	335000	320000	295000	270000	1230	1350	1500	1600	1700	1950	2250
	12.9	445000	430000	415000	400000	385000	355000	320000	1500	1600	1800	1900	2050	2350	2700
M30x2	8.8	330000	320000	310000	300000	290000	265000	240000	1220	1350	1500	1600	1700	1950	2250
	10.9	465000	450000	435000	420000	405000	375000	340000	1700	1900	2100	2200	2400	2700	3150
	12.9	560000	540000	520000	505000	485000	450000	405000	2050	2250	2500	2650	2850	3250	3750

Tafel 4. Spannkräfte F_{sp} und Spannmomente M_{sp} für Taillenschrauben mit metrischem Feingewinde nach DIN 13, Bl. 13

Abm.	Klasse	Spannkräfte F_{sp} in N für μ_G =							Spannmomente M_{sp} in Nm für μ_K =						
		0,08	0,10	0,125	0,14	0,16	0,20	0,25	0,08	0,10	0,125	0,14	0,16	0,20	0,25
M8 x 1	8.8	15000	14400	13700	13300	12700	11700	10500	15,5	17,0	19,0	20,0	21,5	24,5	28,0
	10.9	21000	20300	19300	18700	17900	16400	14700	22,0	24,0	27,0	28,0	30,0	34,0	40,0
	12.9	25000	24300	23100	22400	21500	19700	17700	26,0	29,0	32,0	34,0	36,0	41,0	48,0
M10x1,25	8.8	23200	22400	21300	20600	19700	18100	16200	30	33	36	38	41	47	54
	10.9	32500	31500	30000	29000	28000	25500	22800	42	46	51	54	58	66	76
	12.9	39000	37500	36000	35000	33500	30500	27500	50	55	61	65	70	79	91
M12x1,25	8.8	36000	34500	33000	32000	31000	28000	25500	54	60	66	70	76	86	99
	10.9	51000	49000	46500	45000	43500	39500	35500	77	84	93	99	106	121	140
	12.9	61000	59000	56000	54000	52000	47500	42500	92	101	.12	119	130	145	170
M12x1,5	8.8	33500	32000	30500	29500	28500	26000	23300	51	56	62	66	71	80	93
	10.9	47000	45000	43000	41500	40000	36500	32500	72	79	87	92	99	113	130
	12.9	56000	54000	51000	50000	48000	44000	39500	86	[illegible]	105	111	119	135	155
M14x1,5	8.8	49000	47500	45000	44000	42000	38500	34500	87	95	106	112	120	135	160
	10.9	69000	67000	64000	62000	59000	54000	48500	122	135	150	155	170	195	220
	12.9	83000	80000	76000	74000	71000	65000	58000	145	160	180	190	205	230	270
M16x1,5	8.8	64000	62000	59000	57000	55000	50000	45000	130	140	155	165	175	200	235
	10.9	90000	87000	83000	80000	77000	71000	63000	180	195	220	230	250	280	330
	12.9	108000	104000	99000	96000	92000	85000	76000	220	235	260	280	300	340	390
M18x1,5	8.8	87000	84000	80000	77000	74000	68000	61000	190	210	235	250	270	300	350
	10.9	122000	118000	112000	109000	105000	96000	86000	270	300	330	350	380	430	490
	12.9	146000	141000	135000	131000	125000	115000	103000	320	360	400	420	450	510	590
M20x1,5	8.8	113000	109000	104000	101000	97000	89000	80000	280	300	340	360	390	440	510
	10.9	159000	154000	147000	142000	137000	126000	113000	390	430	480	500	540	620	710
	12.9	191000	184000	176000	171000	164000	151000	136000	470	510	570	600	650	740	860
M22x1,5	8.3	134000	130000	124000	121000	116000	106000	95000	360	400	440	470	500	570	660
	10.9	189000	183000	175000	169000	163000	149000	134000	510	560	620	660	700	800	930
	12.9	227000	219000	209000	203000	195000	179000	161000	610	670	740	790	850	970	1110
M24x2	8.8	157000	151000	144000	140000	134000	123000	111000	460	510	560	600	640	730	840
	10.9	220000	213000	203000	197000	189000	174000	156000	650	710	790	840	900	1030	1180
	12.9	265000	255000	244000	236000	227000	208000	187000	780	850	950	1010	1080	1230	1400
M27x2	8.8	201000	194000	185000	180000	172000	158000	142000	660	730	810	860	920	1050	1210
	10.9	280000	275000	260000	255000	240000	225000	200000	930	1020	1140	1200	1300	1500	1700
	12.9	340000	325000	[illegible]	305000	290000	265000	240000	1120	1230	1350	1450	1550	1750	2050
M30x2	8.8	260000	250000	241000	234000	224000	206000	185000	950	1050	1160	1230	1350	1500	1750
	10.9	365000	355000	340000	330000	315000	290000	260000	1350	1450	1650	1750	1850	2150	2450
	12.9	440000	425000	405000	395000	380000	350000	315000	1600	1750	1950	2100	2250	2550	2950

Tafel 5: Reibungszahlen für verschiedene Oberflächen- und Schmierzustände *)

	Oberfläche I a) μ_K: Schraubenkopf- und Mutter b) μ_G: Schraubengewinde					Oberfläche II gegen Werkstück gegen Muttergewinde
	Stahl, geschwärzt oder Zn-phosphatiert			Stahl verkadmet 6 µm	Stahl verzinkt 6 µm	
	gepreßt gerollt	gedreht geschnitten	geschliffen			
leicht geölt	0,13 bis 0,19	0,10 bis 0,18	0,16 bis 0,22	0,08 bis 0,16	0,10 bis 0,18	Stahl, gewalzt
	0,10 bis 0,18		0,10 bis 0,18	0,10 bis 0,16	0,10 bis 0,18	gehobelt, gefräst, gedreht, geschnitten
	0,16 bis 0,22	0,10 bis 0,18	0,16 bis 0,22	0,08 bis 0,16	0,10 bis 0,18	geschliffen
	0,10 bis 0,18		0,10 bis 0,18	0,08 bis 0,16	0,10 bis 0,18	GG, gehobelt, gefräst, gedreht, geschnitten
	0,16 bis 0,22	0,10 bis 0,18	0,16 bis 0,22	0,08 bis 0,16	0,10 bis 0,18	GTS, geschliffen
	0,08 bis 0,16	0,08 bis 0,15	0,08 bis 0,16	0,12 bis 0,20		Stahl, verkadmet 6 µm
				0,12 bis 0,16		verkadmet, Innengewinde
	0,10 bis 0,18	0,10 bis 0,16	0,10 bis 0,20		0,16 bis 0,20	verzinkt 6 µm
					0,10 bis 0,18	verzinkt, Innengewinde
	0,12 bis 0,20		0,10 bis 0,20			(geschliffen, gewalzt) phosphatiert
	0,10 bis 0,18					(spanend bearbeitet) phosphatiert
	0,08 bis 0,20		0,08 bis 0,20			Al-Mg-Legierungen
trocken	0,08 bis 0,16		0,08 bis 0,16	0,16 bis 0,24		Stahl, verkadmet 6 µm
	0,08 bis 0,14		0,08 bis 0,14	0,12 bis 0,16		verkadmet, Innengewinde
	0,10 bis 0,18		0,10 bis 0,18		0,20 bis 0,30	verzinkt 6 µm
	0,08 bis 0,16		0,08 bis 0,16		0,12 bis 0,20	verzinkt, Innengewinde
mit Kleber	0,18 bis 0,30 **)					Stahl, GG, GTS geschnitten

*) In den Tafeln 1 bis 4 sind für die Ermittlung der Spannkraft F_{sp} die Reibungszahl $\mu_{G\,min}$ und für die Ermittlung des zugehörigen Spannmomentes M_{sp} ($M_A \approx 0{,}9\,M_{sp}$) die Reibungszahl $\mu_{K\,min}$ zu Grunde zu legen (bzw. $\mu_{ges\,min}$ wenn $\mu = \mu_K$)

**) für Flüssigkunststoffe und mikroverkapselte Kleber

Tafel 6. Abschätzen des Durchmesserbereichs von Schrauben

1	2	3	4
Kraft in N	Nenndurchmesser*) in mm		
	Festigkeitsklasse		
	12.9	10.9	8.8
250			
400			
630			
1000			
1600	3	3	3
2500	3	3	4
4000	4	4	5
6300	4	5	5
10000	5	6	8
16000	6	8	8
25000	8	10	10
40000	10	12	14
63000	12	14	16
100000	16	16	20
160000	20	20	24
250000	24	27	30
400000	30	36	
630000	36		

Beispiel:

Eine Verbindung wird dynamisch und exzentrisch durch die Axialkraft F_A = 8500 N belastet. Die Schraube mit der Festigkeitsklasse 12.9 soll mit Drehmomentschlüssel montiert werden.

- **A** 10000 N ist die nächst größere Kraft zu F_A in Spalte 1
- **B** 2 Schritte für „exzentrische und dynamische Axialkraft" führen zu $F_{M\,min}$ = = 25000 N
- **C** 1 Schritt für „Anziehen mit Drehmomentschlüssel" führt zu $F_{M\,max}$ = 40000 N
- **D** Für $F_{M\,max}$ = 40000 N findet man in Spalte 2 (Festigkeitsklasse 12.9): M 10

A Wähle in Spalte 1 die nächst größere Kraft zu der an den Verschraubungen angreifenden Betriebskraft F_A.

B Die erforderliche Mindestvorspannkraft $F_{M\,min}$ ergibt sich, indem man von dieser Zahl weitergeht um:

4 Schritte für statische oder dynamische Querkraft

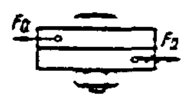

oder

2 Schritte für dynamisch und exzentrisch angreifende Axialkraft

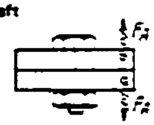

oder

1 Schritt für dynamisch und zentrisch oder statisch und exzentrisch angreifende Betriebskraft

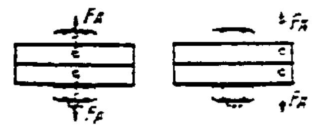

oder

0 Schritte für statisch und zentrisch angreifende Axialkraft

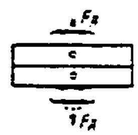

C Die erforderliche maximale Vorspannkraft $F_{M\,max}$ ergibt sich, indem man von dieser Kraft $F_{M\,min}$ weitergeht um:

2 Schritte für Anziehen der Schraube mit einfachem Drehschrauber, der über Nachziehmoment eingestellt wird — oder

1 Schritt für Anziehen mit Drehmomentschlüssel oder Präzisionsschrauber, der mittels dynamischer Drehmomentmessung oder Längungsmessung der Schraube eingestellt und kontrolliert wird — oder

0 Schritte für Anziehen über Winkelkontrolle in den überelastischen Bereich oder mittels Streckgrenzkontrolle durch Computersteuerung.

D Neben der gefundenen Zahl steht in Spalte 1 bis 4 die erforderliche Schraubenabmessung in mm für die gewählte Festigkeitsklasse der Schraube.

Tafel 7. Richtwerte für den Setzbetrag pro Trennfuge für zeitlich veränderliche Betriebskräfte (Einschränkungen s. Abschn. 4.4). Das Gewinde zählt als Trennfuge!

Anzahl der Trennfugen (einschließlich Gewinde)	Setzbetrag in µm für Klemmlänge l_K/d =			
	1	2,5	5	10
2 bis 3	1	1,5	2	2,5
4 bis 5	0,75	1	1,25	1,5
6 bis 7	0,5	0,7	0,9	1,1

Tafel 8. Kraftverhältnis Φ_K

Schaftschrauben | Taillenschrauben

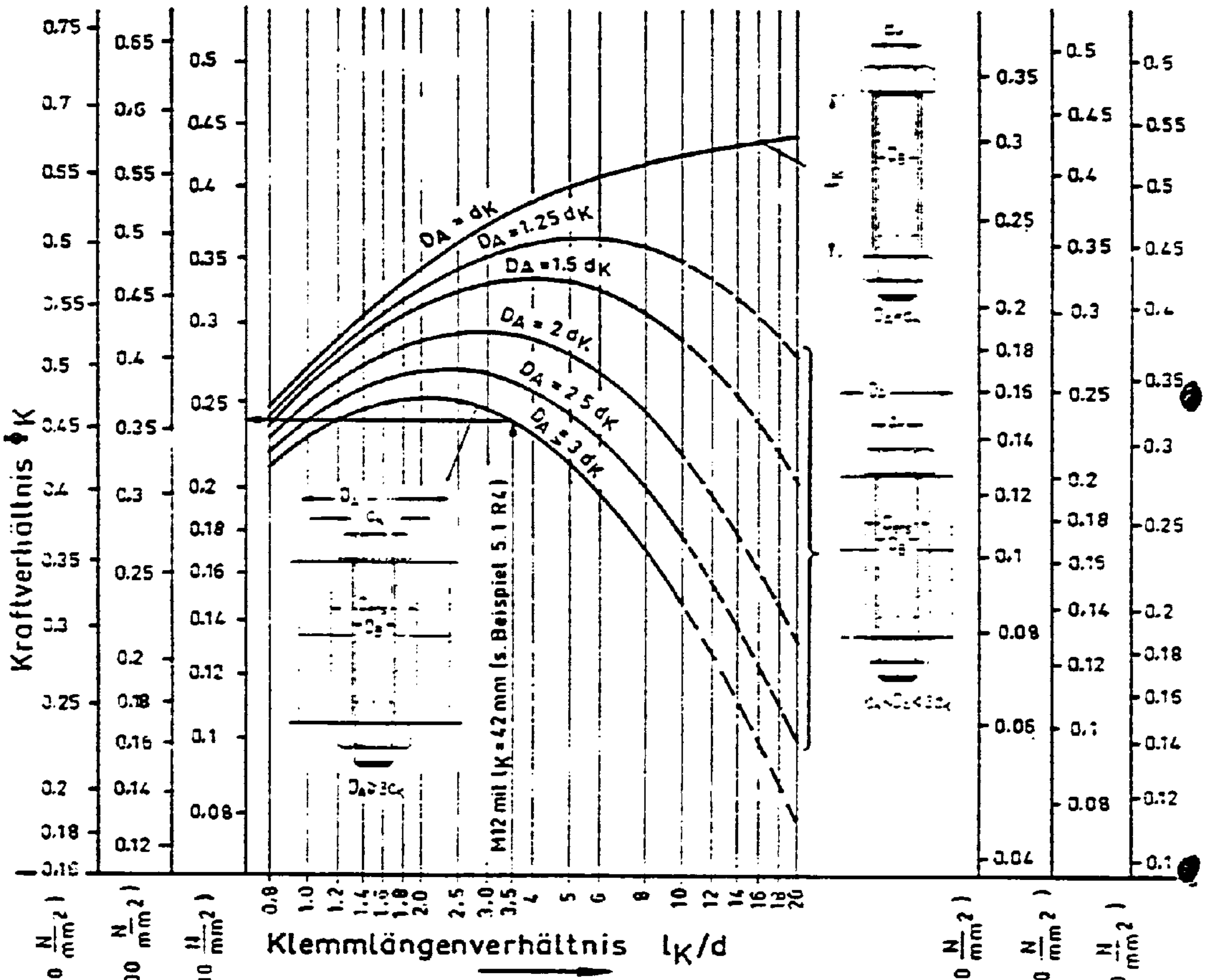

Al-Lg ($E = 69000\ \frac{N}{mm^2}$) | GG ($E = 118000\ \frac{N}{mm^2}$) | Stahl ($E = 205000\ \frac{N}{mm^2}$)

Werkstoff der verspannten Teile

Dargestellte Funktionen, abgeleitet aus den Gleichungen 25, 27, 29, 30, 31, 53:

$$\log\left(\frac{1}{\Phi_K}-1\right)+\log\frac{E_S}{E_P}\underbrace{-\log 1.8}_{\text{nur für Taillenschr.}}=\log\left\{\left[1.2+\frac{C}{2}\left(0.31\frac{l_K}{d}+\frac{l_K^2}{100}\right)\right]\left(1+1.25\frac{d}{l_K}\right)\right\}$$

mit $C = \left(\frac{D_A}{d_K}-1\right)$ und den mittleren Werten im Abmessungsbereich M4 bis M30 (Regelgewinde) von $d_{Km} = 1.56\,d$; $D_{Bm} = 1.11\,d$; $d_{2m} = 0.91\,d$; $d_{3m} = 0.83\,d$; und 1.0 d freie Gewindelänge

Stahl ($E = 205000\ \frac{N}{mm^2}$) | GG ($E = 118000\ \frac{N}{mm^2}$) | Al-Lg ($E = 69000\ \frac{N}{mm^2}$)

Werkstoff der verspannten Teile

Tafel 9. Nachgiebigkeit der verspannten Teile

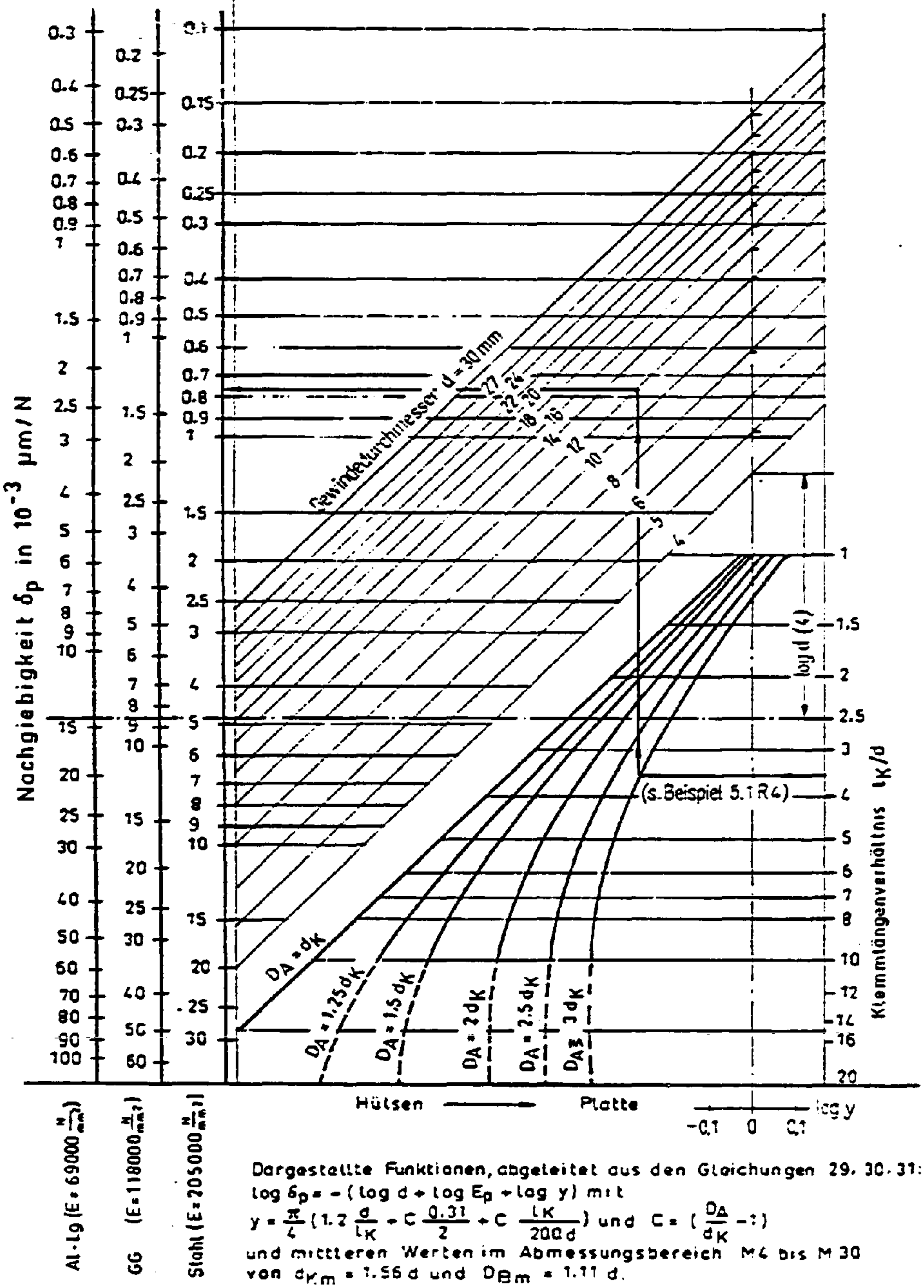

Dargestellte Funktionen, abgeleitet aus den Gleichungen 29, 30, 31:

$\log \delta_p = -(\log d + \log E_p + \log y)$ mit

$$y = \frac{\pi}{4}\left(1.2\,\frac{d}{l_K} + C\,\frac{0.31}{2} + C\,\frac{l_K}{200\,d}\right) \text{ und } C = \left(\frac{D_A}{d_K} - 1\right)$$

und mittleren Werten im Abmessungsbereich M 4 bis M 30 von $d_{Km} = 1.56\,d$ und $D_{Bm} = 1.11\,d$.

Tafel 10. Längenverhältnis für die Trennfuge der exzentrischen vorgespannten und nicht belasteten Verbindung

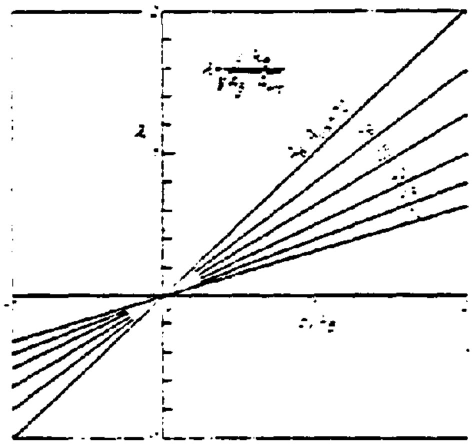

Tafel 11. Steigung, Spannungsquerschnitt, Kernquerschnitt und Kräfte $F_{0,2}$ für Schaftschrauben mit metrischem Regel- und Feingewinde nach DIN 13, Bl. 13

Abmessung	Steigung P mm	Spannungsquerschnitt A_S mm²	Kernquerschnitt A_3 mm²	Kraft an der Mindest-Streckgrenze $F_{0,2} = \sigma_{0,2} A_S$ bei Festigkeitsklasse nach DIN/ISO 898: 8.8 N	10.9 N	12.9 N
Metrisches Regelgewinde						
M 4	0,7	8,78	7,75	5600	7900	9500
M 5	0,8	14,2	12,7	9100	12800	15300
M 6	1,0	20,1	17,9	12900	18100	21700
(M 7)	1,0	28,9	26,2	18500	26000	31000
M 8	1,25	36,6	32,8	23400	33000	39500
M 10	1,5	58,0	52,3	37000	52000	63000
M 12	1,75	84,3	76,2	54000	76000	91000
M 14	2,0	115	105	74000	103000	124000
M 16	2,0	157	144	100000	141000	170000
M 18	2,5	193	175	122000	174000	208000
M 20	2,5	245	225	157000	220000	265000
M 22	2,5	303	282	194000	275000	325000
M 24	3,0	353	324	226000	320000	380000
M 27	3,0	459	421	295000	415000	495000
M 30	3,5	561	519	360000	505000	605000
Metrisches Feingewinde						
M 8	1,0	39,2	36,0	25000	35500	42500
M 10	1,25	61,2	56,3	39000	55000	66000
M 12	1,25	92,1	86,0	59000	83000	99000
M 12	1,5	88,1	81,1	56000	79000	95000
M 14	1,5	125	116	80000	112000	135000
M 16	1,5	167	157	107000	150000	180000
M 18	1,5	216	205	138000	194000	233000
M 20	1,5	272	259	174000	245000	295000
M 22	1,5	333	319	213000	300000	360000
M 24	2,0	384	365	246000	345000	415000
M 27	2,0	496	473	315000	445000	535000
M 30	2,0	621	596	395000	560000	670000

Tafel 12. Steigung, Taillenquerschnitt, Kernquerschnitt und Kräfte $F_{0,2}$ für Taillenschrauben mit metrischem Regel- und Feingewinde nach DIN 13, Bl. 13

Abmessung	Steigung P mm	Taillendurchmesser d_T h13 $(0{,}9 \cdot d_3)$ mm	Taillenquerschnitt $A_{T\,min} = A_S$ mm²	Kraft an der Mindest-Streckgrenze $F_{0,2} = \sigma_{0,2} A_S$ bei Festigkeitsklasse nach DIN/ISO 898: 8.8 N	10.9 N	12.9 N
Metrisches Regelgewinde						
M 4	0,7	2,8	6,2	3950	5600	6700
M 5	0,8	3,6	10,2	6500	9200	11000
M 6	1,0	4,3	14,5	9300	13000	15700
(M 7)	1,0	5,2	21,2	13600	19100	22900
M 8	1,25	5,8	26,4	16900	23800	28500
M 10	1,5	7,3	41,8	27000	37500	45000
M 12	1,75	8,9	62,2	40000	56000	67000
M 14	2,0	10,5	86,5	55500	78000	93000
M 16	2,0	12,0	113	72000	102000	122000
M 18	2,5	13,5	143	92000	129000	154000
M 20	2,5	15	177	113000	159000	191000
M 22	2,5	17	227	145000	204000	245000
M 24	3,0	18,5	269	172000	242000	290000
M 27	3,0	21	346	221000	310000	375000
M 30	3,5	23	415	265000	375000	450000
Metrisches Feingewinde						
M 8	1,0	6,1	29,2	18700	26500	31500
M 10	1,25	7,6	45,3	29000	41000	49000
M 12	1,25	9,4	69,4	44500	62000	75000
M 12	1,5	9,1	65,0	41500	58000	70000
M 14	1,5	11,0	95,0	61000	85000	103000
M 16	1,5	12,5	123	79000	111000	133000
M 18	1,5	14,5	165	106000	148000	178000
M 20	1,5	16,5	214	137000	193000	231000
M 22	1,5	18,0	254	163000	229000	275000
M 24	2,0	19,5	298	191000	270000	320000
M 27	2,0	22,0	380	243000	340000	410000
M 30	2,0	25,0	491	315000	440000	500000

Tafel 13. Richtwerte für die Dauerhaltbarkeit von schlußvergüteten Schrauben der Festigkeitsklassen 8.8, 10.9, 12.9 (Haigh-Diagramm)

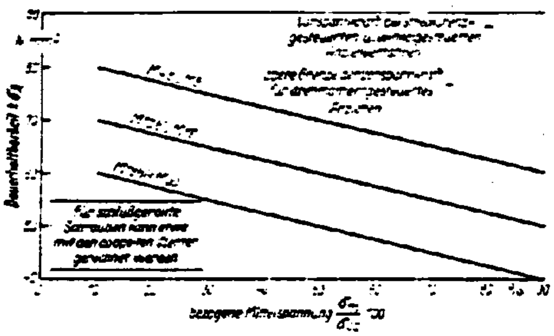

Tafel 14. Grenzflächenpressung p_G in N/mm^2 für gedrückte Teile verschiedener Werkstoffe

Werkstoff	Anziehen	
	motorisch	von Hand
St 37	200	300
St 50	330	500
C 45 V	600	900
GG-25	500	750
GD Mg Al 9	80	120
GK Mg Al 9	80	120
GK Al Si 6 Cu 4	120	180

Tafel 15. Faktoren, die die Dauerhaltbarkeit im positiven Sinne beeinflussen

1. Verspannungsverhältnis

1.1. Vergrößern der Längs- und Biege-Elastizität durch
- Dehnschrauben
- lange Schrauben
- hochfeste Schrauben
- Durchsteckschrauben mit Muttern
- Aufsetzen einer Hülse
- Vermindern des E-Moduls

1.2. Versteifen der verspannten Teile durch
- konstruktive Maßnahmen
- Verwenden von Werkstoffen mit großem E-Modul sowie durch Trennung von Trag- und Dicht-Funktionen

1.3. Vermeiden von Biegung durch
- Vermindern der Exzentrizität
- Erhöhen der Vorspannkraft

1.4. Erhalten der Restklemmkraft durch
- Vermeiden von Setzen
- Vermeiden von Losdrehvorgängen

2. Einschraubbedingungen

2.1. Gleichmäßige Spannungsverteilung durch
- Schraubenwerkstoffe mit kleinem E-Modul
- geeignete Mutterformen
- geeignete Gewindeprofile
- Steigungsdifferenz zwischen Schrauben- und Muttern-gewinde
- hohe Vorspannkraft
- elastische Gewindeeinsätze

2.2. Gewindetoleranzen
(ausreichendes Gewindespiel)

3. Dauerhaltbarkeit der Schraube

3.1. Formeinflüsse an Kopf und Schaft durch
- Vergrößern der Kopfsteifigkeit
- große Radien
- Fasen am Durchgangsloch

3.2. Formeinflüsse am Gewinde durch
- große Radien
- am Fuß tragende Gewindezähne
- weichen Gewindeauslauf

4. Werkstoffe und Herstellung

4.1. Werkstoffe
- große Zähigkeit
- hohe Festigkeit
- Vermeiden von Ent- und Aufkohlungen sowie Verzunderungen
- ununterbrochener Faserverlauf

4.2. Oberflächenverbesserung durch
- Kaltverfestigung
- Glätten und Polieren
- Aufbringen von Eigenspannungen
- Vermeiden von Elektropolieren

5. Chemische Oberflächeneinflüsse

5.1. Vermeiden von Korrosion
(jedoch ungünstiger Einfluß von galvanischen Schutzschichten)

Tafel 16. Empfohlene Mindest-Einschraubtiefen für Sacklochgewinde

Schraubenfestigkeitsklasse	8.8	8.8	10.9	10.9
Gewindefeinheit d/P	<9	≥9	<9	≥9
AlCuMg1F40	1,1 d	1,4 d		–
GG-22	1,0 d	1,2 d		1,4 d
St 37	1,0 d	1,25 d		1,4 d
St 50	0,9 d	1,0 d		1,2 d
C45V	0,8 d	0,9 d		1,0 d

Tafel 17. Richtwerte für den Anziehfaktor α_A

Anziehfaktor α_A	Anziehverfahren	Bemerkungen	
(1)	Streckgrenzgesteuertes Anziehen motorisch	Die Vorspannkraftstreuung wird überwiegend bestimmt durch die Streuung der Streckgrenze im verbauten Schraubenlos. Die Schrauben werden hier für $F_{M\,min}$ dimensioniert; der Anziehfaktor α_A entfällt deshalb für diese Anziehmethoden; die eingeklammerten Werte dienen dem Vergleich der Anziehgenauigkeit mit den folgenden Verfahren.	
(1)	Drehwinkelgesteuertes Anziehen motorisch oder manuell		
1,2	Anziehen mit Längungsmessung der gereckten Schraube	Aufwendiges Verfahren, nur sehr begrenzt anwendbar.	
1,4 bis 1,6	Drehmomentgesteuertes Anziehen mit Drehmomentschlüssel oder Präzisions-Drehschrauber mit dynamischer Drehmomentmessung. Versuchsmäßige Bestimmung der Sollanziehmomente am Original-Verschraubungsteil, z.B. durch Längungsmessung der Schraube	Niedrigere Werte für: große Zahl von Einstell- bzw. Kontrollversuchen (z.B. 20). Geringe Streuung des abgegebenen Momentes. Elektronische Drehmomentbegrenzung während der Montage bei Präzisions-Drehschraubern.	Niedrigere Werte für: • kleine Drehwinkel, d.h. relativ steife Verbindungen • relativ weiche Gegenlage • Gegenlagen, die nicht zum Fressen neigen, z.B. phosphatiert Höhere Werte für (bei): • große Drehwinkel, d.h. relativ nachgiebige Verbindungen sowie Feingewinde • große Härte der Gegenlage, verbunden mit rauher Oberfläche • Formabweichungen
1,6 bis 1,8	Drehmomentgesteuertes Anziehen mit Drehmomentschlüssel oder Präzisionsdrehschrauber mit dynamischer Drehmomentmessung. Bestimmung des Sollanziehmomentes durch Schätzen der Reibungszahl (Oberflächen- und Schmierverhältnisse).	Niedrigere Werte für: • genaue Drehmomentschlüssel (z.B. mit Meßuhr) • gleichmäßiges Anziehen • Präzisionsdrehschrauber Höhere Werte für: signalgebende oder ausknickende Drehmomentschlüssel	
1,7 bis 2,5	Drehmomentgesteuertes Anziehen mit Drehschrauber. Einstellen des Schraubers mit Nachziehmoment, das aus Sollanziehmoment (für geschätzte Reibungszahl) und einem Zuschlag gebildet wird.	Niedrigere Werte für: • große Zahl von Kontrollversuchen (Nachziehmoment) • Schrauber mit Abschaltkupplungen	
2,5 bis 4	Impulsgesteuertes Anziehen mit Schlagschrauber. Einstellen des Schraubers über Nachziehmoment – wie oben	Niedrigere Werte für: • große Zahl von Einstellversuchen (Nachziehmoment) • auf horizontalem Ast der Schraubercharakteristik • spielfreie Impulsübertragung	

Tafel 18. *K*-Faktoren für die schnelle Berechnung des Anziehmomentes für μ_G und μ_K

Faktor $K = \left(0,16\,P + 0,58\,d_2 \cdot \mu_G + \frac{D_m}{2}\,\mu_K\right)/d$

Gewindereibungszahl μ_G		Kopfreibungszahl μ_K: 0,08	0,10	0,125	0,14	0,16	0,20	0,25
0,08	R	0,118	0,131	0,148	0,158	0,171	0,198	0,231
	F	0,112	0,125	0,142	0,152	0,166	0,192	0,226
0,10	R	0,128	0,142	0,159	0,169	0,182	0,209	0,242
	F	0,123	0,136	0,153	0,163	0,176	0,203	0,237
0,125	R	0,142	0,155	0,172	0,182	0,195	0,222	0,255
	F	0,137	0,150	0,167	0,177	0,190	0,217	0,250
0,14	R	0,150	0,163	0,180	0,190	0,203	0,230	0,263
	F	0,145	0,158	0,175	0,185	0,198	0,225	0,258
0,16	R	0,160	0,173	0,190	0,200	0,214	0,240	0,274
	F	0,156	0,169	0,186	0,196	0,209	0,234	0,269
0,20	R	0,181	0,195	0,211	0,221	0,235	0,261	0,295
	F	0,177	0,191	0,208	0,218	0,231	0,258	0,291
0,25	R	0,208	0,221	0,238	0,248	0,261	0,288	0,231
	F	0,205	0,218	0,235	0,245	0,258	0,285	0,318

Maximales Anziehdrehmoment $M_{A\,max} = K \cdot F_M \cdot d$ in Nm

F_M in N gewünschte Vorspannkraft, wenn 90 %ige Streckgrenzenausnutzung vorgesehen ist.
F_{90} aus Tafeln 1 bis 4 einsetzen.

d in m Nenndurchmesser der Schraube

R = Regelgewinde, F = Feingewinde

Symbols and Terminology.

A Cross sectional area, general.

A_B Cross section, cross sectional area of bolted prismatic parts when they fulfill the conditions of a "bending body" in the case of eccentric clamping and loading.

A_{ers} Substitutional area, cross sectional area of a hollow cylinder with the same elastic resilience as that of the clamped parts.

A_i Cross sectional area of a cylindrical element of a bolt.

A_N Nominal cross section.

A_P Bolt head or nut bearing area.

A_S Stress area of the bolt thread according to DIN 13:

$$A_S = \frac{\pi}{4} \cdot \left(\frac{d_2 + d_3}{2}\right)^2$$

A_T Cross section of reduced shank area in a bolt.

A_0 Smallest cross section of a bolt shaft.

A_3 Cross sectional area at minor diameter of bolt thread.

C Spring Constant.

D_a External diameter of a clamped sleeve.

D_B Hole diameter of the clamped parts = internal diameter of the substitutional cylinder.

D_{km} Effective friction diameter of the bolt head or nut bearing area.

E Young's modulus.

E_P Young's modulus of clamped parts.

E_S Young's modulus of bolt materials.

F Force, general.

F_A Axial force, axial working load or axial component of the working load F_B.

F_{Aab} Eccentric axial force at the lift-off limit.

F_{Ao} Upper limit value of an alternating axial force F_A.

F_{Au} Lower limit value of an alternating axial force F_A.

F_B Working load in any direction.

F_K Clamping force.

F_{Kab} Clamping force at the lift-off limit.

F_{Kerf} Clamping force which is necessary for sealing functions, friction contact and prevention of one-sided lift-off in the interface.

F_{KR} Residual clamping force in the interface in the case of unloading due to F_{PA} and embedding during operation.

F_M Initial preload.

$F_{M\,max}$ Initial preload for which a bolt must be designed so that in spite of imprecision in the tightening procedure or expected embedding the required clamping force is achieved and maintained in the joint.

$F_{M\,min}$ Smallest initial preload which adjusts itself in the case of $F_{M\,max}$ as a result of imprecision in the tightening procedure.

F_{PA} Portion of the axial force which unloads the clamped parts.

F_Q Transverse force, working force directed transversely to the bolt axis or the transverse component of a working load F_B directed in any direction.

F_S Bolt force.

F_{SA} Portion of the axial force F_A which additionally loads the bolt.

F_{SAa} Alternating loading of the bolt by the additional force F_{SA}.

F_{Sm} Mean value of the bolt force in the case of alternating working load.

F_{sp} Axial clamping force of the bolt with 90% utilization of the elastic limit by σ_{red} [90% yield load].

F_V Preload, general.

F_{Vab} Preload at the lift-off limit.

F_{Verf} Least preload which is necessary for sealing functions, friction contact and the prevention of one-sided lift-off in the interface under observation of unloading by the working force.

F_{Vm} Mean preload.

F_Z Preload loss as a result of embedding in operation.

$F_{0.2}$ Bolt force at the minimum elastic limit.

I_B Moment of inertia of the area A_B.

I_i Moment of inertia of any area.

I_3 Moment of inertia of the core cross section of the bolt thread.

M_A Tightening torque for assembly.

M_B Effective bending moment at the bolting position.

M_b Bending moment at the bolting position from the eccentrically acting axial force F_A.

M_{GA} Effective part of the tightening torque in the thread.

M_K Friction moment in the bolt head bearing area.

M_{Pb} Portion of M_B which is taken up by the clamped parts.

M_{Sb} Portion of M_b which is taken up by the bolt.

M_{sp} Tightening torque to produce preloading of a bolt equal to 90% of yield (F_{sp}).

M_T Effective torque at the bolting position in the interface.

P Pitch of the bolt thread.

U Location for $\sigma = 0$.

W_P Polar resistance moment for the surface A_0.

W_3 Resistance moment of the core cross section of the bolt thread.

a Distance of the force line of application from the axis of rotation for the area A_B.

b Expanse of the interface.

d Bolt diameter = external thread diameter.

d_K External diameter of bolt head or nut bearing area.

d_G Diameter for the clamping cross section A_G.

d_T Shaft diameter in the case of reduced shank bolts.

d_0 Diameter at the smallest cross section of the bolt shaft.

d_2 Pitch diameter of the bolt thread.

f Length change under a force F.

f_i Length change of any part i.

f_{PA} Length change of the clamped parts by F_{PA}.

f_{PAn} Length change of the clamped parts due to load introduction over the clamped parts.

f_{PM} Shortening of the clamped parts due to F_M.

f_{SA} Lengthening of the bolt due to F_{SA}.

f_{SAn} Lengthening of the bolt due to F_{SA} in the case of load introduction over the clamped parts.

f_{SM} Lengthening of the bolt due to F_M.

f_Z Plastic deformation due to embedding, embedding amount.

h_{min} Plate thickness (see Figures 6, 19 and 20).

k_B Radius of gyration for the area A_B.

l Length, general.

l_{ers} Substitutional length for a bolt with threading over the entire length with the same β_S as any bolt.

l_i Length of a cylindrical individual element of the bolt.

l_K Clamping length.

m Number of bolts in a flange joint.

n Factor, which when multiplied with the clamping length l_K, gives the thickness of the areas of the clamped parts unloaded by the axial force F_A.

p Bearing stress.

p_G Allowable bearing stress under the bolt head.

s Distance of the bolt axis for the axis of gyration for the area A_B.

t Configuration of the bolts in the case of a multi-bolted joint.

u Perimeter distance in clamped prisms from the axis of rotation for the area A_B (in the direction A-A).

v Perimeter distance in clamped prisms from the axis of rotation for the area A_B (opposite the direction A-A).

α Angle of pressure of the bolt thread.

α_A Tightening factor $F_{V\,max}$ / $F_{V\,min}$.

β Elastic bending resilience.

β_i Elastic bending resilience of any part of the bolt.

β_G Elastic bending resilience of the screwed-in thread.

β_K Elastic bending resilience of the bolt head.

β_P Elastic bending resilience of the clamped parts.

β_S Elastic bending resilience of the bolt.

γ Tilt or angle of inclination of clamped parts as a result of eccentric loading.

γ_P Angle of inclination of the clamped prisms.

γ_S Angular deformation of the bolt.

δ Elastic resilience.

δ_G Elastic resilience of the screwed-in thread.

δ_i Elastic resilience of any part i.

δ_K Elastic resilience of the bolt head.

δ_P Elastic resilience of the clamped parts in the case of concentric clamping and concentric loading.

δ_P^* Elastic resilience of clamped parts in the case of eccentric clamping.

δ_P^{**} Elastic resilience of the clamped parts in the case of eccentric clamping and eccentric loading.

δ_S Elastic resilience of the bolt.

ϑ Angle of rotation in the case of tightening of a bolt.

$$\lambda = \frac{s / k_D}{A_D / A_{ers}}$$

Length ratio for the interface of the eccentrically clamped and non-loaded joint.

μ_G Friction coefficient in the thread.

μ' Friction coefficient in the V-thread increased opposed to μ.

μ_{ges} Mean friction coefficient for thread and head bearing area.

ρ' Friction angle to μ'.

σ_A Stress amplitude of fatigue strength.

σ_a Fatigue loading [alternating or cycling stress] of the bolt.

σ_B Tensile strength of the bolt, minimum value according to DIN 276, p. [Blatt] 3.

$\sigma_{B\,max}$ Tensile strength of the bolt, maximum value according to DIN 276, p. [Blatt] 3.

σ_D Fatigue strength or durability.

σ_M Normal tension in the thread as a result of F_M.

σ_m Mean tension.

σ_{red} Combined tension and torsional stress.

σ_{SA} Tension caused by the portion F_{SA} of the axial force in the core cross section of the bolt.

σ_{SAb} Tension in the bending traction thread of the bolt thread caused by the axial force portion F_{SA} and the bending moment M_b in the case of eccentric load application.

σ_{SAd} Like σ_{SAb}, but on the bending-compressive side of the bolt.

$\sigma(x)$ Tension at position x.

$\sigma_{0.2}$ 0.2% off-set yield strength (minimum value according to DIN 267, p. [Blatt] 3).

τ Torsional stress in the thread as a result of M_{GA}.

Φ Force ratio F_{SA} / F_A.

Φ_e Force ratio in the case of eccentric application of the axial force F_A.

Φ_{eK} Force ratio Φ_e for load introduction under the bolt head and nut areas.

Φ_{en} Force ratio Φ_e for load introduction inside the clamped parts.

Φ_{F1} Force ratio in the case of flange-like joints.

Φ_K Force ratio for concentric load introduction under the bolt head and nut areas.

Φ_m Force ratio in the case of pure moment loading by M_B.

Φ_n Force ratio for concentric introduction of the axial force F_A inside the clamped parts in levels at the distance $n\ l_K$.

φ Pitch angle of the bolt thread.

Inverse resilience in the case of flanges and flange-like parts.

For geometric quantities in the case of flange joints see Figures 9 and 10.